UNIVERSITY OF AMSTERDAM

UvA-DARE (Digital Academic Repository)

Search for long-lived particles in final states with displaced dimuon vertices in pp collisions at √s = 13 TeV with the ATLAS detector

Aaboud, M.; ATLAS Collaboration

DOI
10.1103/PhysRevD.99.012001

Publication date
2019

Document Version
Final published version

Published in
Physical Review D. Particles and Fields

License
CC BY

Link to publication

Citation for published version (APA):
Aaboud, M., & ATLAS Collaboration (2019). Search for long-lived particles in final states with displaced dimuon vertices in *pp* collisions at √s = 13 TeV with the ATLAS detector. *Physical Review D. Particles and Fields*, *99*(1), Article 012001. https://doi.org/10.1103/PhysRevD.99.012001

General rights
It is not permitted to download or to forward/distribute the text or part of it without the consent of the author(s) and/or copyright holder(s), other than for strictly personal, individual use, unless the work is under an open content license (like Creative Commons).

Disclaimer/Complaints regulations
If you believe that digital publication of certain material infringes any of your rights or (privacy) interests, please let the Library know, stating your reasons. In case of a legitimate complaint, the Library will make the material inaccessible and/or remove it from the website. Please Ask the Library: https://uba.uva.nl/en/contact, or a letter to: Library of the University of Amsterdam, Secretariat, P.O. Box 19185, 1000 GD Amsterdam, The Netherlands. You will be contacted as soon as possible.

UvA-DARE is a service provided by the library of the University of Amsterdam (https://dare.uva.nl)

Download date:11 Oct 2026

Search for long-lived particles in final states with displaced dimuon vertices in pp collisions at $\sqrt{s} = 13$ TeV with the ATLAS detector

M. Aaboud *et al.*[*]
(ATLAS Collaboration)

(Received 10 August 2018; published 3 January 2019; corrected 13 November 2019)

A search is performed for a long-lived particle decaying into a final state that includes a pair of muons of opposite-sign electric charge, using proton-proton collision data collected at $\sqrt{s} = 13$ TeV by the ATLAS detector at the Large Hadron Collider corresponding to an integrated luminosity of 32.9 fb^{-1}. No significant excess over the Standard Model expectation is observed. Limits at 95% confidence level on the lifetime of the long-lived particle are presented in models of new phenomena including gauge-mediated supersymmetry or decay of the Higgs boson, H, to a pair of dark photons, Z_D. Lifetimes in the range $c\tau = 1$–2400 cm are excluded, depending on the parameters of the model. In the supersymmetric model, the lightest neutralino is the next-to-lightest supersymmetric particle, with a relatively long lifetime due to its weak coupling to the gravitino, the lightest supersymmetric particle. The lifetime limits are determined for very light gravitino mass and various assumptions for the neutralino mass in the range 300–1000 GeV. In the dark photon model, the lifetime limits are interpreted as exclusion contours in the plane of the coupling between the Z_D and the Standard Model Z boson versus the Z_D mass (in the range 20–60 GeV), for various assumptions for the $H \to Z_D Z_D$ branching fraction.

DOI: 10.1103/PhysRevD.99.012001

I. INTRODUCTION

The ATLAS and CMS experiments at the Large Hadron Collider (LHC) were conceived to address a variety of questions not fully explained within the Standard Model (SM) of particle physics. The data collected by the LHC experiments have not yet revealed evidence of physics beyond the Standard Model (BSM). As a result, there is an increased emphasis on the exploration of unusual final-state signatures that would elude the searches based on experimental methods aimed at prompt signatures. In many models of BSM physics there are free parameters that influence the lifetimes of the new particle states, with no strong motivation for assuming that all the particles decay promptly[1] and thus give final states investigated with standard analysis techniques. Nor are there any strong demands that these are stable on the detector scale and only weakly interacting, leading to missing transverse momentum signatures. Particle lifetimes in the SM, for instance, span roughly 28 orders of magnitude [1], from the strong decay to the scale of the neutron lifetime. There are a number of BSM models where long-lived particles (LLPs) arise naturally [2,3]. Supersymmetry (SUSY) [4–9] with R-parity violation [10,11], general gauge-mediated (GGM) supersymmetry breaking [12–14], and split supersymmetry [15,16] are examples where small couplings, mass scales associated with the BSM physics, or heavy mediator particles, respectively, lead to high-mass (greater than a few hundred GeV) LLPs. Scenarios with low-mass LLPs include hidden-valley models [17], stealth supersymmetry [18], and dark-sector gauge bosons [3,19].

Events with long-lived particles may feature vertices that are significantly displaced from the proton-proton (pp) interaction point (IP). This article presents the results of a search for displaced vertices (DVs) formed by a pair of muons of opposite-sign electric charge, denoted "OS" muons. The search is designed to be sensitive to decays of LLPs with masses between 20 and 1100 GeV and DVs at distances ranging from a few centimeters to a few meters from the IP. The data sample consists of pp collisions at $\sqrt{s} = 13$ TeV and an integrated luminosity of 32.9 fb^{-1} collected with the ATLAS detector at the LHC.

Although SM decay products typically consist primarily of hadrons, due to the relatively large number of color degrees of freedom for quarks, there are notable advantages to searching for DVs using only tracks of identified muons: the design of the ATLAS muon spectrometer allows detection of dimuon DVs within an unusually large decay volume, free from backgrounds associated with

[*]Full author list given at the end of the article.

[1]For the purposes of this analysis, a promptly decaying particle is one with a lifetime no larger than a few tens of picoseconds.

Published by the American Physical Society under the terms of the Creative Commons Attribution 4.0 International license. Further distribution of this work must maintain attribution to the author(s) and the published article's title, journal citation, and DOI. Funded by SCOAP[3].

 © 2019 CERN, for the ATLAS Collaboration

vertices produced in interactions of hadrons with detector material [20,21].

Previous searches by the ATLAS Collaboration for high-mass LLPs that decay within the inner detector to give displaced dilepton vertices excluded LLP lifetimes of $c\tau = 0.1$–100 cm [22]. ATLAS has also searched for very low mass LLPs (< 10 GeV) by considering pairs of highly collimated leptons [23], with sensitivity to LLP lifetimes of $c\tau = 0.1$–20 cm. Several other LLP searches targeting a wide range of lifetimes and signatures have been conducted by the ATLAS [24–33], CMS [34–40], LHCb [41–44], CDF [45], D0 [46,47], *BABAR* [48], Belle [49], and ALEPH [50] collaborations.

II. ATLAS DETECTOR

The ATLAS detector [51,52] at the LHC covers nearly the entire solid angle around the collision point.[2] It consists of an inner tracking detector surrounded by a thin superconducting solenoid, electromagnetic and hadronic calorimeters, and a muon spectrometer incorporating superconducting toroidal magnets.

The inner detector (ID) is immersed in a 2 T axial magnetic field and provides charged-particle tracking in the range $|\eta| < 2.5$. A high-granularity silicon pixel detector covers the vertex region and typically provides four measurements per track, the first hit being normally in the innermost layer. It is followed by a silicon microstrip tracker, which usually provides four two-dimensional measurement points per track. These silicon detectors are complemented by a transition radiation tracker, which enables radially extended track reconstruction up to $|\eta| = 2.0$. The transition radiation tracker also provides electron identification information based on the fraction of hits (typically 30 in total) above a higher energy-deposit threshold corresponding to transition radiation.

The calorimeter system covers the pseudorapidity range $|\eta| < 4.9$. Within the region $|\eta| < 3.2$, electromagnetic calorimetry is provided by barrel and end cap high-granularity lead/liquid-argon (LAr) sampling calorimeters, with an additional thin LAr presampler covering $|\eta| < 1.8$ to correct for energy loss in material upstream of the calorimeters. Hadronic calorimetry is provided by a steel/scintillator-tile calorimeter, segmented into three barrel structures within $|\eta| < 1.7$, and two copper/LAr hadronic end cap calorimeters. The solid-angle coverage is completed with forward copper/LAr and tungsten/LAr calorimeter modules optimized for electromagnetic and hadronic measurements respectively.

The muon spectrometer (MS) comprises separate trigger and high-precision tracking chambers measuring the deflection of muons in a magnetic field generated by three superconducting air-core toroidal magnets, each with eight coils. The field integral of the toroids ranges between 2.0 and 6.0 T m across most of the detector. The MS is designed to detect muons in the region $|\eta| < 2.7$ and to provide momentum measurements with a relative resolution better than 3% over a wide transverse momentum (p_{T}) range and up to 10% at $p_{\mathrm{T}} \sim 1$ TeV. It consists of a barrel ($|\eta| < 1.05$), with an inner radius of about 500 cm, and two end cap sections ($1.05 < |\eta| < 2.7$).

Resistive-plate chambers in the barrel and thin-gap chambers in the end cap regions provide triggering capability to the detector as well as (η, ϕ) position measurements with a typical spatial resolution of 5–10 mm. A precise momentum measurement is provided by three layers of monitored drift-tube chambers (MDT), with each chamber providing six to eight η measurements along the muon trajectory. For $|\eta| > 2$, the inner layer is instrumented with a quadruplet of cathode-strip chambers (CSC) instead of MDTs. The single-hit resolution in the bending plane for the MDT and the CSC is about 80 and 60 μm, respectively. The muon chambers are aligned with a precision between 30 and 60 μm. The material between the IP and the MS ranges from approximately 100 to 190 radiation lengths, depending on η, and consists mostly of the calorimeters.

Online event selection is performed with a two-level trigger system [53]. A hardware-based level-1 trigger which uses information from the MS trigger chambers and the calorimeters is followed by a software-based trigger.

III. DATA AND SIMULATED SAMPLES

Proton-proton collision data, collected at the LHC during 2016, with a center-of-mass energy $\sqrt{s} = 13$ TeV, are analyzed. After application of detector and data-quality requirements, the integrated luminosity of the data sample is 32.9 fb^{-1}.

Samples of Monte Carlo (MC) simulated events are used for studies of both the LLP signal and background processes. The detector response was simulated with GEANT4 [54,55], and the events were processed with the same reconstruction software as used for the data. The distribution of the number of additional pp collisions in the same or neighboring bunch crossings ("pileup") is accounted for by overlaying minimum-bias events simulated with PYTHIA8 [56] using the A2 set of tuned parameters (tune) [57] and MSTW2008LO parton distribution function (PDF) set [58]. The pileup profile in the MC samples is reweighted to match the distribution observed in the data.

[2]ATLAS uses a right-handed coordinate system with its origin at the nominal interaction point in the center of the detector and the z axis along the beam pipe. The x axis points from the IP to the center of the LHC ring, and the y axis points upwards. Cylindrical coordinates (r, ϕ) are used in the transverse plane, ϕ being the azimuthal angle around the z axis. The pseudorapidity is defined in terms of the polar angle θ as $\eta = -\ln\tan(\theta/2)$. Angular distances are measured in units of $\Delta R \equiv \sqrt{(\Delta\eta)^2 + (\Delta\phi)^2}$.

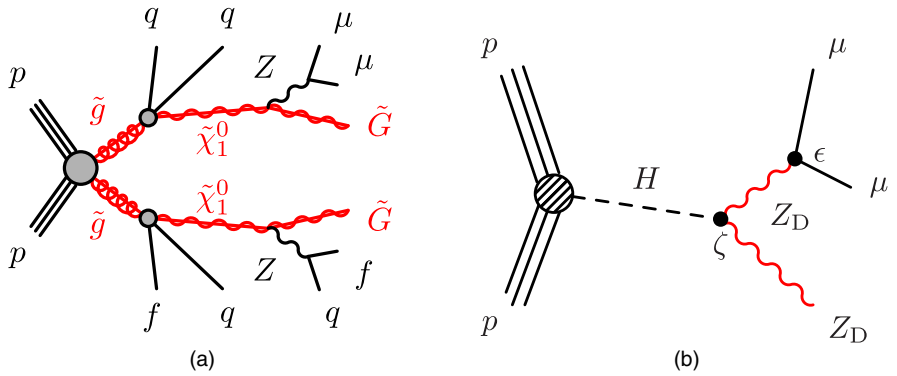

FIG. 1. Diagrams representing BSM processes considered signals in this article: (a) long-lived neutralino $\tilde{\chi}_1^0$ decay in a GGM scenario, and (b) long-lived dark photons Z_D produced from Higgs boson decay. The quarks, q, may have different flavors (excluding the top quark). The symbol f represents fermions lighter than half the mass of the Z boson.

A. BSM signal samples

Monte Carlo simulated samples from two different BSM physics models are used to tune selection criteria and to evaluate signal efficiencies for use in converting signal yields into cross sections. The chosen models, a general gauge-mediated supersymmetry and dark-sector gauge boson model, represent a variety of BSM physics possibilities, as well as final-state topologies and kinematics, to which the analysis may be sensitive. The two processes are illustrated in Fig. 1. Samples for both models were generated with MadGraph5_aMC@NLO [59] using the NNPDF23LO PDF set [60] and Pythia8 for parton showering and hadronization. The matrix elements were calculated to next-to-leading order in the strong coupling constant. The EvtGen generator [61] was used for weak decays of heavy-flavor hadrons. The hadronization and underlying-event parameters were set according to the A14 tune [57].

In R-parity-conserving (RPC) SUSY models where gauge interactions mediate the breaking of the supersymmetry, the gravitino $\tilde{G}$ acquires its mass from a "super-Higgs" mechanism and may be very light: $m_{\tilde{G}} = \mathcal{O}(\text{keV})$. The mass is given by

$$m_{\tilde{G}} = \frac{F_0}{\sqrt{3}M_{\text{Pl}}} = \left(\frac{\sqrt{F_0}}{100\ \text{TeV}}\right)^2 \times 2.4\ \text{eV}, \qquad (1)$$

where $\sqrt{F_0}$ is the fundamental scale of supersymmetry breaking, typically $\gtrsim$100 TeV, and M_{Pl} is the Planck scale. Hence, the gravitino is the lightest supersymmetric particle (LSP). All heavier supersymmetric particles decay promptly through cascades leading to the next-to-lightest supersymmetric particle (NLSP), which then decays into the LSP gravitino via an interaction with a $1/F_0$ suppression. The NLSP, depending on model choices, is either the lightest slepton or lightest neutralino, $\tilde{\chi}_1^0$. For the latter case, chosen for this search and described in Ref. [62], if $\tilde{\chi}_1^0$ has a significant wino or higgsino component the branching fraction for the decay $\tilde{\chi}_1^0 \to Z\tilde{G}$ can be $\mathcal{O}(1)$. The lifetime of the $\tilde{\chi}_1^0$ is determined by F_0 [or, alternatively, by $m_{\tilde{G}}$, according to Eq. (1)] and its mass $m_{\tilde{\chi}_1^0}$,

$$c\tau_{\tilde{\chi}_1^0} \propto \frac{16\pi F_0^2}{m_{\tilde{\chi}_1^0}^5} \approx \left(\frac{100\ \text{GeV}}{m_{\tilde{\chi}_1^0}}\right)^5 \left(\frac{\sqrt{F_0}}{300\ \text{TeV}}\right)^4 \times 1\ \text{cm},$$

and hence $\tilde{\chi}_1^0$ is long-lived (i.e., nonprompt) for $\sqrt{F_0} = 10^3$ TeV to 10^4 TeV.

In the GGM model, a pp interaction creates a pair of gluinos, followed by a cascade of decays leading to $\tilde{\chi}_1^0 \to Z\tilde{G}$. A simplified model is used whereby the cascade of decays of SUSY particles is reduced to a single vertex: $\tilde{g} \to qq\tilde{\chi}_1^0$, where q represents any of the quarks lighter than the top quark, with equal probability for each. Six signal samples were generated with $m_{\tilde{g}} = 1.1$ TeV and $\tilde{\chi}_1^0$ masses and lifetimes given in Table I. The value of 1.1 TeV for the gluino mass was chosen to be consistent with the value used in Ref. [22], the previous search for DVs with a GGM interpretation. The signal cross sections are calculated to next-to-leading order in the strong coupling constant, adding the resummation of soft gluon emission at next-to-leading-logarithm accuracy (NLO + NLL) [63–67]. The nominal cross sections and their uncertainties are taken

TABLE I. MC signal samples for the GGM SUSY interpretation. For a given $m_{\tilde{\chi}_1^0}$, the gravitino mass is chosen to give the desired lifetime. For all samples, $m_{\tilde{g}} = 1100$ GeV, $\sigma(pp \to \tilde{g}\tilde{g}) = 163.5$ fb, $B(\tilde{\chi}_1^0 \to Z\tilde{G}) = 1.0$, and $B(Z \to \mu^+\mu^-) = 0.03366$.

$m_{\tilde{\chi}_1^0}$ [GeV]	$c\tau_{\tilde{\chi}_1^0}$ [cm]
300	100
300	500
700	100
700	500
1000	100
1000	500

from an envelope of cross-section predictions using different PDF sets and factorization and renormalization scales, as described in Ref. [68].

A number of BSM theories feature a "hidden" or "dark" sector of matter that does not interact directly with SM particles but may nevertheless interact weakly with SM matter via coupling to the Higgs field. These are "Higgs portal" models that address the dark-matter problem and electroweak baryogenesis. The model considered for this search is one in which there exists a $U(1)_{\mathrm{D}}$ symmetry in the dark sector, and the dark vector gauge boson Z_{D}, often called a "dark photon," is given mass via a singlet scalar field H_{D} that breaks the symmetry and is analogous to the Higgs field H in the visible SM sector [3,69].

The BSM terms in the Lagrangian density include both a hypercharge portal and a Higgs portal, providing kinetic Z-Z_{D} mixing [i.e., mixing between $U(1)_Y$ and $U(1)_{\mathrm{D}}$] and H-H_{D} mixing, regulated by the small coupling parameters ϵ and ζ, respectively. There are two vector-boson mass eigenstates, one that is mostly Z_{D} and another that is mostly SM Z, as well as two scalar mass eigenstates, one that is mostly H_{D} and another that is mostly H. For simplicity, the physical (mass) states are denoted by H, H_{D}, Z, and Z_{D}.

In the scenario where the singlet scalar H_{D} is heavier than the SM H boson, which means that the process $H \to H_{\mathrm{D}}H_{\mathrm{D}}$ is kinematically forbidden, and Z_{D} is lighter than half the H mass, events with a displaced dimuon vertex signature would be observable in experiments at the LHC. The Z_{D} bosons are produced on-shell in Higgs boson decays and decay to SM fermions due to their induced couplings to the electroweak current. A small value of ϵ ($\lesssim 10^{-5}$) results in a long-lived Z_{D} state: $c\tau_{Z_{\mathrm{D}}} \propto 1/\epsilon^2$. The branching fraction for $H \to Z_{\mathrm{D}}Z_{\mathrm{D}}$ is determined by the value of ζ and the masses of the scalar singlets:

$$B(H \to Z_{\mathrm{D}}Z_{\mathrm{D}}) \propto \zeta \frac{m_H^2}{|m_{H_{\mathrm{D}}}^2 - m_H^2|},$$

where values as large as 25% have not yet been ruled out by constraints from Higgs coupling fits [70,71]. For $\epsilon \ll 1$, the Z_{D} branching fraction to muons, $B(Z_{\mathrm{D}} \to \mu^+\mu^-)$, is independent of ϵ but varies with $m_{Z_{\mathrm{D}}}$ [69]: from a value of 0.1475 for $m_{Z_{\mathrm{D}}} = 20$ GeV to a value of 0.1066 for $m_{Z_{\mathrm{D}}} = 60$ GeV. Five signal samples were generated with Z_{D} masses and lifetimes given in Table II. The Higgs boson is produced via the gluon-gluon fusion process, assuming a cross section of 44.1 pb, calculated at next-to-next-to-leading order in the strong coupling constant, adding the resummation of soft gluon emission at next-to-next-to-leading-logarithmic accuracy [72]. The inclusion of other production processes was found to have a negligible impact on the analysis.

The signal samples were generated with values of the LLP lifetime that were chosen to provide sufficiently large number of DVs across the full fiducial decay volume of the search: approximately $0 < r_{\mathrm{vtx}} < 400$ cm. To obtain distributions corresponding to a different lifetime, $c\tau_{\mathrm{new}}$, each event is given a weight. The weight w_i assigned to each LLP i is computed as

$$w_i(t_i) = \frac{\tau_{\mathrm{gen}}}{\mathrm{e}^{-t_i/\tau_{\mathrm{gen}}}} \cdot \frac{\mathrm{e}^{-t_i/\tau_{\mathrm{new}}}}{\tau_{\mathrm{new}}},$$

where the first factor reweights the exponential decay to a constant distribution and the second factor reweights to the desired lifetime. The quantity t_i is the proper decay time of the LLP and $c\tau_{\mathrm{gen}}$ is the lifetime assumed in generating the sample. The event-level weight is the product of the weights for the two LLPs in each event. The event-level signal efficiency is then the sum of weights for all events for which at least one reconstructed dimuon vertex satisfies the selection criteria, divided by the total number of events generated. This scheme ensures that any dependence of the efficiency on the decay time of both LLPs in the event, and not just the one decaying to a dimuon final state, is properly taken into account for each choice of $c\tau_{\mathrm{new}}$.

The lifetime reweighting technique is validated by using a signal sample of a given $c\tau_{\mathrm{gen}}$ to predict the efficiency for a different lifetime and comparing with the value directly obtained from a sample generated with that lifetime.

TABLE II. MC signal samples for the dark-sector interpretation. For all samples, $m_H = 125$ GeV, $m_{H_{\mathrm{D}}} = 300$ GeV, $\sigma(pp \to H) = 44.1$ pb (via the gluon-gluon fusion production process) and $B(H \to Z_{\mathrm{D}}Z_{\mathrm{D}}) = 0.10$.

$m_{Z_{\mathrm{D}}}$ [GeV]	$c\tau_{Z_{\mathrm{D}}}$ [cm]	$B(Z_{\mathrm{D}} \to \mu^+\mu^-)$
20	50	0.1475
40	50	0.1370
40	500	0.1370
60	50	0.1066
60	500	0.1066

B. SM background samples

The MC simulations of background processes are used only as a guide for some of the selection criteria and for categorization of the types of background, while the background yield itself is predicted from techniques that use solely the data. The MC generators, hadronization, and showering software packages, underlying-event simulation and choice of parton distribution functions are summarized in Table III. Further details about the generator settings used for these processes can also be found in Refs. [73–77].

Each of the simulated background samples is scaled to correspond to an integrated luminosity of 32.9 fb^{-1}, the size of the data sample.

TABLE III. The MC generators, hadronization, and showering software package, underlying-event simulation and PDF sets used for the simulated background events. The mass range of the low-mass Drell-Yan sample is restricted to $6 < m_{\mu\mu} < 60$ GeV.

Sample	MC generator	Hard-process PDF	Hadronization and showering	Nonperturbative tune and parton-shower PDF
Z + jets	POWHEG [78,79]	CT10 [80]	PYTHIA8 [56]+EVTGEN [61]	AZNLO+CTEQ6L1 [81]
Low-mass Drell-Yan	POWHEG		PYTHIA8+EVTGEN	AZNLO+CTEQ6L1
$t\bar{t}$	POWHEG	CT10	PYTHIA6 [82]+EVTGEN	P2012 [83]+CTEQ6L1
W + jets	POWHEG	CT10	PYTHIA8	AZNLO+CTEQ6L1
ZZ	POWHEG-BOX v2 [84]	CT10nlo	PYTHIA8	AZNLO+CTEQ6L1
WW	POWHEG-BOX v2	CT10nlo	PYTHIA8	AZNLO+CTEQ6L1
WZ	POWHEG-BOX v2	CT10nlo	PYTHIA8	AZNLO+CTEQ6L1
Single top	POWHEG [85,86]	CT10	PYTHIA6	P2012+CTEQ6L1

IV. EVENT SELECTION, SIGNAL EFFICIENCIES, AND BACKGROUND ESTIMATE

Candidate signal events are selected by identifying $\mu^+\mu^-$ pairs consistent with having been produced in a vertex displaced at least several centimeters from the IP.[3] The selection criteria are designed to strongly suppress background from SM processes that produce muons near the IP while efficiently accepting signal events over a wide range of LLP masses, lifetimes and velocities. To retain the greatest possible model independence, minimal requirements are placed on other aspects of the event.

The initial event selection is performed with a combination of triggers that require either the presence of a muon candidate or large missing transverse momentum, whose magnitude is denoted $E_{\mathrm{T}}^{\mathrm{miss}}$. Next, offline selection criteria are used to first identify suitable muon candidates, and then pairs of muons of opposite charge consistent with a DV. The backgrounds from all SM beam-collision and non-beam-collision processes (cosmic-ray muons or beam-halo particles) are estimated directly from the data. Finally, the number of vertices expected from background processes is compared with the observed number of vertices in data in two signal regions, distinguished by the dimuon invariant mass.

A. Trigger requirements

Events must satisfy the requirements of at least one of four different triggers in order to achieve the best possible efficiency for a wide variety of signal topologies and kinematics. The triggers used and their descriptions are given in Table IV. The first two triggers are highly efficient for signals with high-mass states that feature muons with large transverse momentum and large transverse impact parameters, d_0, such as the GGM model, while the final two allow efficient selection of signals featuring low-mass states, and therefore lower-p_{T} muons (e.g., the dark-sector model). All three of the muon triggers use only measurements in the MS to identify muons.

The thresholds for the $E_{\mathrm{T}}^{\mathrm{miss}}$ and collimated-dimuon triggers changed during the course of 2016 data taking. To account for these changes, the highest available threshold for each trigger is used and offline requirements are imposed corresponding to the thresholds listed in the table. Moreover, additional stricter requirements are imposed on the corresponding offline quantity in order to ensure that the trigger efficiency falls on the efficiency plateau.

For signal events with displaced dimuon vertices, the single-muon trigger efficiency falls off approximately linearly with $|d_0|$, from a maximum of about 70% at 0 cm to approximately 10% at the fiducial limit of 400 cm, due to requirements that favor muon candidates that originate close to the IP. The calorimeter-based $E_{\mathrm{T}}^{\mathrm{miss}}$ trigger is employed to recover some signal efficiency. As muons leave little energy in the calorimeter and the $E_{\mathrm{T}}^{\mathrm{miss}}$ at the trigger level is computed only using the calorimeter signals, the $E_{\mathrm{T}}^{\mathrm{miss}}$ trigger is an effective muon trigger.

The collimated-dimuon trigger is based on reconstruction of muon tracks with low p_{T} thresholds. The large rates associated with the low p_{T} thresholds are offset by requiring two muons in the MS that are within a cone of size $\Delta R = 0.5$. The efficiency of this trigger for a given signal model is strongly dependent on the magnitude of the boost of the particle decaying to the dimuon final state, as this determines the likelihood of the two muons being found within a cone of size $\Delta R = 0.5$. The trimuon trigger increases the efficiency for selecting events with particles that have a relatively large branching fraction to muons, as is the case of the Z_{D} in the signal model explored in this article.

B. Offline reconstruction and preselection

Interaction vertices from the pp collisions are reconstructed from at least two tracks with p_{T} larger than 400 MeV that are consistent with originating from the beam-collision region in the x-y plane. Selected events are required to have at least one reconstructed interaction vertex.

[3]The RMS spread of the z distribution of the pp interaction vertices is 47.7 mm and the spreads in the x and y directions are less than 0.01 mm.

TABLE IV. Description of triggers used to select events. The quantity $\Delta R_{\mu\mu}$ is the angular distance between the two muons in the collimated-dimuon trigger.

Signal type	Trigger	Description	Thresholds
High mass	$E_{\mathrm{T}}^{\mathrm{miss}}$	Missing transverse momentum	$E_{\mathrm{T}}^{\mathrm{miss}} > 110$ GeV
	Single muon	Single muon restricted to the barrel region	Muon $\lvert\eta\rvert < 1.05$ and $p_{\mathrm{T}} > 60$ GeV
Low mass	Collimated dimuon	Two muons with small angular separation	p_{T} of muons > 15 and 20 GeV and $\Delta R_{\mu\mu} < 0.5$
	Trimuon	Three muons	$p_{\mathrm{T}} > 6$ GeV for all three muons

Jet candidates are reconstructed from topological clusters [87], built from energy deposits in the calorimeters calibrated to the electromagnetic scale, using the anti-k_t algorithm [88] with radius parameter $R = 0.4$. The reconstructed jets are calibrated to the hadronic energy scale by scaling their four-momenta to the particle level [89]. The jets are required to have $p_{\mathrm{T}} > 20$ GeV and $|\eta| < 4.4$. If a jet in an event fails the "loose" jet-quality requirements of Ref. [90], the event is vetoed in order to suppress detector noise and noncollision backgrounds [90,91]. To reduce the contamination due to jets originating from pileup interactions, an additional requirement on the jet vertex tagger [92] output is made for jets with $p_{\mathrm{T}} < 60$ GeV and $|\eta| < 2.4$.

The muon reconstruction algorithm [93] starts by finding tracks in the MS, denoted MS tracks, and extrapolating their trajectories towards the IP. All MS track parameters are expressed at the point of closest approach to the IP and their uncertainties reflect the effects of multiple Coulomb scattering in the detector material. Although the highest track reconstruction efficiency is obtained for muons originating near the IP, appreciable efficiency is obtained for muons with transverse impact parameters as large as 200 cm. In order to optimize the resolution of the track parameters, the following criteria are imposed. The MS tracks are required to have transverse momentum greater than 10 GeV, $|\eta| < 2.5$, measurements in each of the three layers of both the precision and trigger chambers, an uncertainty in the d_0 measurement less than 20 cm and to not traverse regions of the MS that are poorly aligned.

Interactions between beam protons and beam collimators upstream of the IP are a source of high-momentum muons, denoted beam-induced-background (BIB) muons, that can enter the ATLAS detector nearly parallel to the beam axis. Most MS tracks generated by this process are identified and rejected with the method described in Ref. [91] and results in a negligible reduction in signal efficiency.

Track reconstruction is performed independently in the ID, and an attempt is made to match each MS track with an ID track. The two matched tracks are then used as input to a combined fit that takes into account all of the ID and MS measurements, the energy loss in the calorimeter and multiple-scattering effects. During the fit, additional MS measurements may be added to or removed from the track to improve the fit quality. The ID track is required to be within the ID acceptance, $|\eta| < 2.5$, to have transverse momentum greater than 400 MeV, to have a minimum number of hits in each ID subsystem and to have $|d_0| < 1$ cm. Hence, these combined-muon candidates correspond to muons produced within ~1 cm of the x-y position of the IP.

To suppress background from misidentified jets as well as from hadron decays to muons inside jets, all muon candidates are required to have at least a minimum angular separation from all jets (muon-jet overlap removal) and to satisfy track-based isolation criteria. Muon-jet overlap removal is accomplished by requiring that $\Delta R_{\mu-\mathrm{jet}} > \min(0.4, 0.04 + 10\ \mathrm{GeV}/p_{\mathrm{T}}^{\mu})$ for all jets in the event, where $\Delta R_{\mu-\mathrm{jet}}$ is the angular separation between the muon candidate and the jet in consideration. The track-based isolation quantity $I_{\Delta R=0.4}^{\mathrm{ID}}$ is defined as the ratio of the scalar sum of p_{T} of all ID tracks matched to the primary vertex, and with $p_{\mathrm{T}} > 0.5$ GeV within a cone of size $\Delta R = 0.4$ around the muon candidate, to the muon p_{T}. To remove the contribution of the ID track forming the muon candidate (if it exists), the ID track that is nearest to and within $\Delta R = 0.1$ of the muon candidate and has a p_{T} within 10% of the MS-track p_{T} is not used in the sum. Muon candidates are required to have $I_{\Delta R=0.4}^{\mathrm{ID}} < 0.05$. The muon-jet overlap and isolation requirements are removed in defining control regions used to study backgrounds described in Sec. IV F.

Muon candidates that trigger in a small set of resistive-plate chambers that can have timing jitter are rejected. This amounts to no more than 0.3% of selected muon candidates, which has a negligible effect on the signal acceptance.

To distinguish between muon candidates that originate from prompt and nonprompt decays, the following classification of MS tracks is used. Those for which a successful ID-MS combination has been made, defined by the requirement that the angular distance between the MS track and nearest combined-muon track is less than 0.1, are referred to as "MScomb" muon candidates and the rest are referred to as "MSonly" muon candidates, as summarized in Table V. The large majority of MS tracks are MScomb, which reflects the fact that most muons are produced very close to the IP.

C. Selection of dimuon vertices

The selection criteria described below are used to define a sample of dimuon vertices (preselection) to which

TABLE V. Definition of categories of muon candidates. Tracks in the ID are reconstructed with maximum $|d_0|$ of 1 cm.

Muon candidate	Definition
MScomb	Successful ID-MS combination
MSonly	Standalone MS (no match with ID track)

additional criteria are applied to form signal regions (SRs) in which data are compared to background estimates, and control regions (CRs) which are used to provide those background estimates.

Within each event, all possible pairs of muon candidates, both MScomb and MSonly, are formed. For each pair, the muon candidate with the largest p_{T} is designated the "leading" muon, while the other is designated the "subleading" muon. An algorithm which assumes a straight-line extrapolation of the muon trajectory from the MS inner surface towards the IP is used to determine whether or not the two muons are consistent with originating from a common vertex. The midpoint between the points of closest approach along the trajectories of the two muon candidates is taken to be the three-dimensional location of the vertex. This simple approach is sufficient for the purposes of this analysis, as the location of the putative dimuon vertex is only used in defining the geometrical acceptance of the analysis. The decay length L_{vtx} and projections onto the x-y plane and z axis, r_{vtx} and z_{vtx} respectively, are measured relative to the IP. It is convenient to sign the vertex radius r_{vtx} according to the following definition. If the angle between the projections in the x-y plane of the vertex momentum vector (the dimuon momentum vector) and the "flight direction" (the vector connecting the IP with the displaced dimuon vertex) is less than $\pi/2$ then it is assigned a positive value, otherwise it is assigned a negative value. When the LLP decays exclusively into a pair of muons or there is a small mass difference between the LLP and the dimuon state, the two vectors are typically closely aligned and the signed r_{vtx} more often has a positive value. Examples are the dark-sector model and the GGM model for cases where there is a relatively small mass difference between the $\tilde{\chi}_1^0$ and the Z boson. In all cases, LLPs are distinguished by relatively large values of the magnitude of signed r_{vtx}.

Vertices are selected as follows. To reduce combinatorial background from random track crossings, the distance of closest approach between the two straight-line extrapolations is required to be less than 20 cm. As the vertex position is poorly measured for tracks that are nearly parallel to each other, vertices for which the opening angle of the muon pair is less than 0.1 are rejected. Vertices are required to be within the cylindrical fiducial volume $|r_{\mathrm{vtx}}| < 400$ cm and $|z_{\mathrm{vtx}}| < 600$ cm. Background from muons with relatively low momentum in multijet events, as well as Υ decays to dimuons, is reduced by requiring that the dimuon invariant mass, $m_{\mu\mu}$, be larger than 15 GeV. The ability to determine the spatial location of the vertex varies with the p_{T} of the muons in the vertex and the opening angle between them. The average resolutions of r_{vtx} and z_{vtx} are in the range of 2–3 cm. Cosmic-ray muons that pass through the detector in time with a pp collision are sometimes reconstructed as two separate MS tracks that have an opening angle of π: $\Delta\phi = \pi$ and $\Sigma\eta = 0$, where $\Delta\phi$ is the difference in ϕ between the two MS tracks and $\Sigma\eta$ is the sum of their η values. Vertices formed by such MS tracks are effectively eliminated by requiring $\sqrt{(\Sigma\eta)^2 + (\pi - \Delta\phi)^2} > 0.1$.

Backgrounds that contribute to the preselection sample include SM proton-proton collision processes as well as events with muons that are not associated with the pp collision (e.g., cosmic-ray muons). The dominant contributions to the former are low-mass Drell-Yan and Z + jets processes, collectively referred to simply as DY. At small values of $m_{\mu\mu}$, dimuon vertices from multijet processes are also substantial. Dimuon vertices reconstructed in $t\bar{t}$ and single-top events make small contributions, while W + jets and diboson processes are found to be negligibly small backgrounds.

Distributions of $m_{\mu\mu}$ and signed r_{vtx} for opposite-charge and same-charge (SS) dimuon vertices satisfying the preselection criteria are shown in Fig. 2. Also shown are the expected contributions from the background processes discussed above. Due to the limited number of simulated multijet events, this source of background is not included in the MC distributions. Its relative contribution is expected to be dominant for SS pairs and most pronounced for OS ones at small values of $m_{\mu\mu}$, as determined from studies of events where the muon-jet overlap and muon isolation requirements are inverted, and this is the dominant source of difference between the data and MC distributions in those regions of Fig. 2. The fraction of events in the data with multiple dimuon vertices passing the preselection criteria is 0.065%.

The preselected dimuon vertices are divided into two regions to be used in searches for low- and high-mass signal models, which are summarized in Table VI. To further suppress the DY background in the high-mass region, where Z + jets production dominates, and improve the search sensitivity, the transverse boost of the dimuon pair, defined as the ratio of the transverse momentum of the dimuon system to its invariant mass, is required to be larger than 2. This reduces the DY background by approximately a factor of 20, with a small reduction in the signal efficiencies, where the decay of a heavy BSM particle produces the dimuon state (a Z boson in the GGM model) with a relatively large boost.

The next sections describe the SR and CR selection criteria based on the designation of muon candidates as MScomb or MSonly.

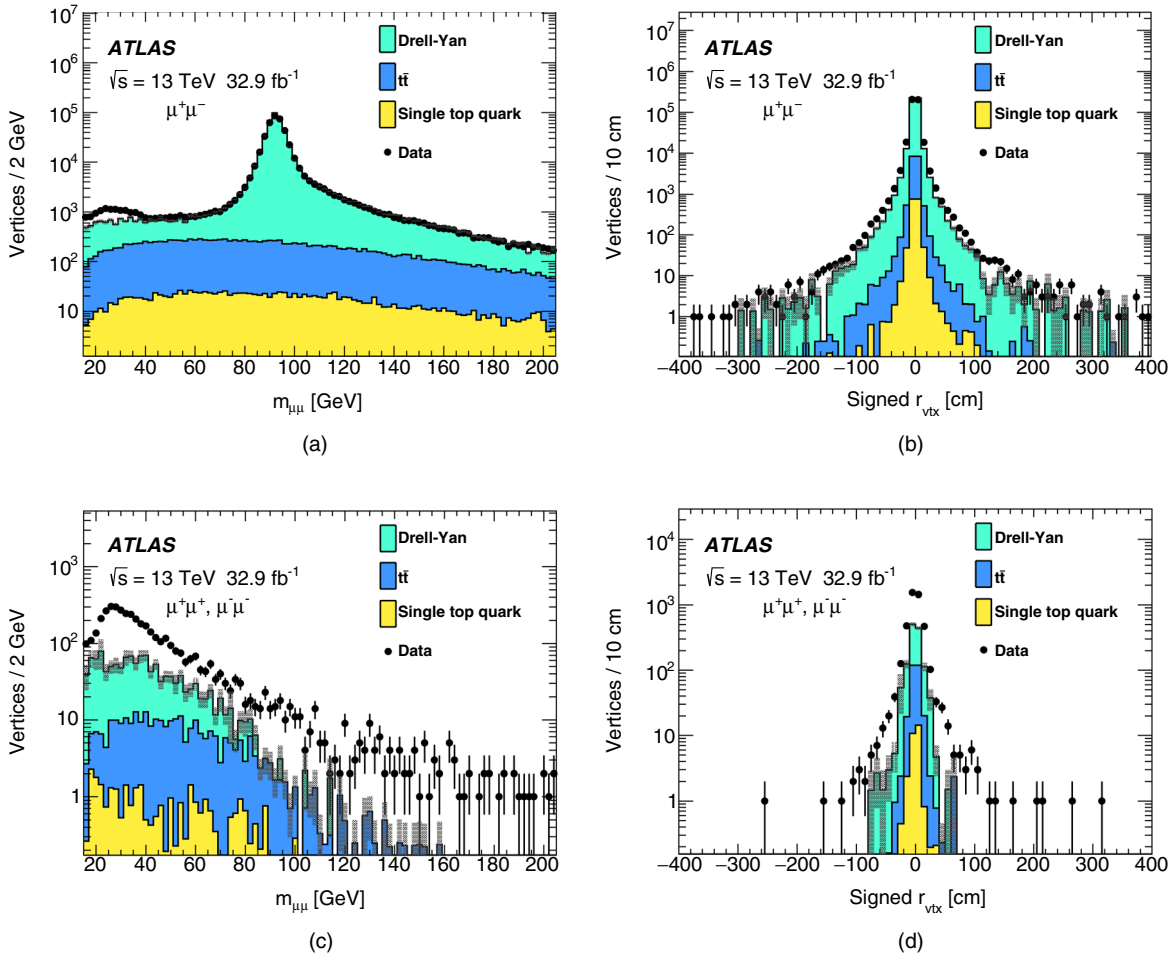

FIG. 2. Distributions of (a) dimuon invariant mass $m_{\mu\mu}$ and (b) signed vertex radius r_{vtx} for opposite-charge dimuon vertices satisfying the preselection requirements described in the text; (c) $m_{\mu\mu}$ and (d) signed r_{vtx} for same-charge dimuon vertices satisfying the preselection requirements described in the text. The stacked histograms represent the expected contributions from various SM background processes and are derived from MC simulations scaled to an integrated luminosity of 32.9 fb^{-1}. Multijet processes are not included in the background due to the limited number of simulated events. The contributions from these processes are most substantial at small values of $m_{\mu\mu}$. The shaded bands represent the statistical uncertainties in the simulated background. The observed distributions for data are given by the points with error bars.

TABLE VI. Selection criteria for low- and high-mass regions, in addition to the preselection requirements described in the text. The definitions of the low- and high-mass signal regions are also given.

Selection	Low mass	High mass
p_{T}^{μ} [GeV]	> 10	> 20
$m_{\mu\mu}$ [GeV]	15–60	> 60
Dimuon transverse boost	⋯	> 2
	$\mathrm{SR_{low}}$	$\mathrm{SR_{high}}$
Muon candidates	Both MSonly	Both MSonly
Muon candidate charge	Opposite charge	Opposite charge

D. Signal regions and signal efficiency

Signal is characterized by vertices where both muon candidates are MSonly. This requirement unavoidably leads to a reduction in efficiency for decays close to the IP. Displaced-vertex analyses that make use of ID tracks [22] effectively recover such signal events. Two orthogonal signal regions are used to increase the sensitivity to low- and high-mass signal models, $\mathrm{SR_{low}}$ and $\mathrm{SR_{high}}$, respectively. The two regions are summarized in Table VI. For both SRs, the muons are required to have opposite charge.

The product of acceptance and reconstruction efficiency determined from simulated signal events is shown in Fig. 3 as a function of generated L_{vtx} and leading muon d_0, for the GGM model and for the dark-sector model. The lower efficiency observed for small L_{vtx} or small $|d_0|$ (more apparent in the Z_{D} models) is due to the veto on MScomb

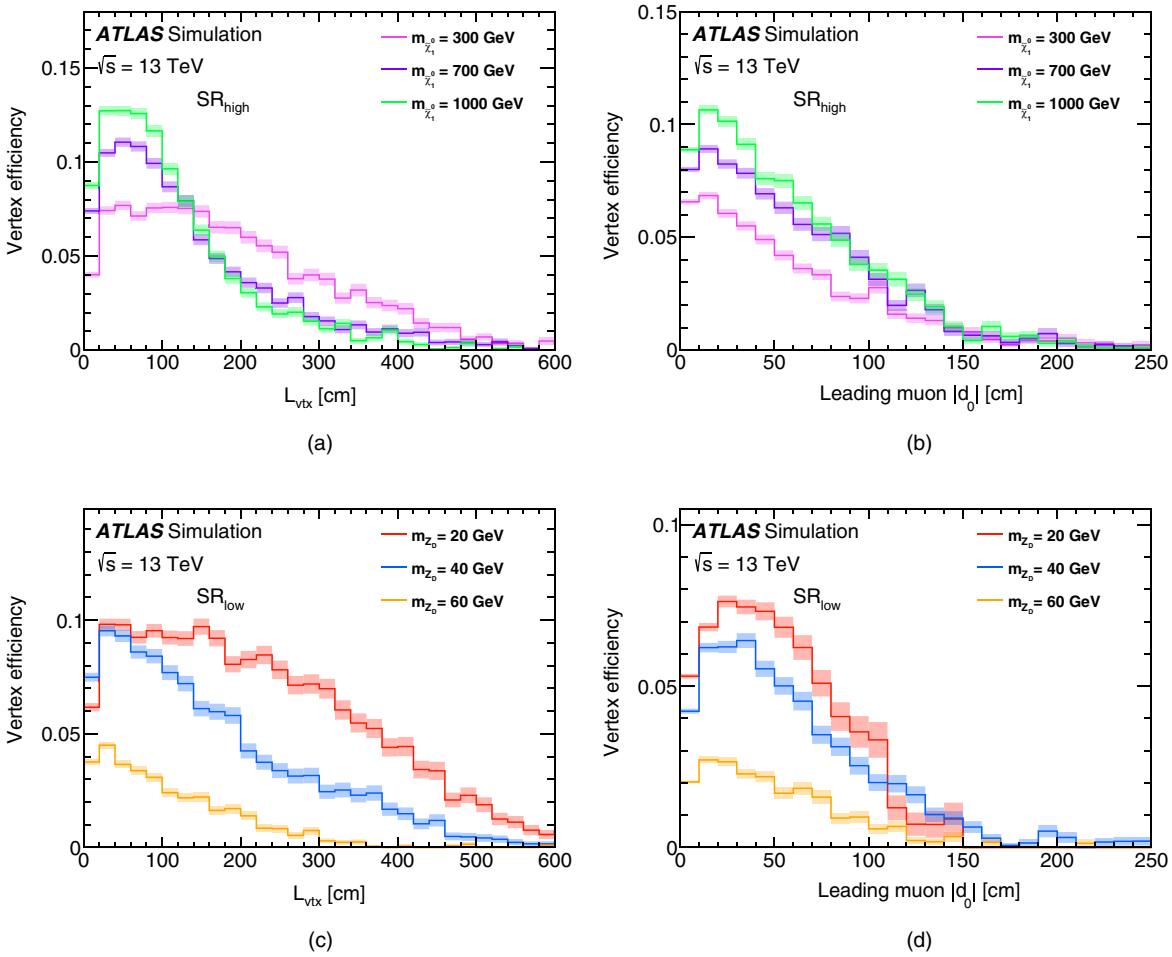

FIG. 3. The efficiency for selecting a displaced dimuon vertex that satisfies the requirements of $\mathrm{SR_{high}}$ and $\mathrm{SR_{low}}$ as function of (a) and (c) generated decay length L_{vtx}, and (b) and (d) generated transverse impact parameter d_0 of the leading muon. These efficiencies are calculated relative to all generated signal vertices and include geometrical acceptance and reconstruction effects. The distributions in (a) and (b) are derived from signal events with a long-lived neutralino, $\tilde{\chi}_1^0$, decaying to a Z boson (with $Z \to \mu^+\mu^-$) and a gravitino. The distributions in (c) and (d) are derived from signal events with a long-lived dark photon, Z_{D}, that decays to $\mu^+\mu^-$. The shaded bands represent the statistical uncertainties in the efficiencies.

muons, while the loss at large values reflects the lower MS reconstruction efficiency for tracks with trajectories that do not extrapolate back to a region close to the IP. The value of L_{vtx} where maximum efficiency is achieved is different for each choice of Z_{D} mass due to the large differences in boost.

The total event-level efficiencies, including trigger and offline selection criteria, as functions of the lifetime of the LLP, are shown in Fig. 4 and maximum values are in the $c\tau$ region 20–50 cm. The reweighted samples, as described in Sec. III, are used to estimate the efficiencies for values of the lifetime which were not used in generating the simulated samples. This event-level efficiency is defined as the fraction of generated events that are selected and have at least one dimuon DV.

Distributions of $m_{\mu\mu}$ and signed r_{vtx} for signal vertices in simulated events, for both $\mathrm{SR_{high}}$ and $\mathrm{SR_{low}}$, are displayed in Fig. 5. The vertex properties are computed using the parameters of the reconstructed MS tracks and the distributions are normalized to the expected yields in the signal regions.

E. Control regions and background estimation

Dimuon vertices are categorized as described in Table VII. The observed yields of same-charge dimuon vertices in all four regions A, B, C, and D are used to estimate the background yields in the SRs due to muons produced more than about a centimeter from the IP, referred to as nonprompt muons. The observed yields in the opposite-charge B, C, and D CRs are used to predict the background yield from SM processes that produce prompt muons (those produced within about a centimeter of the IP) in the SRs (opposite-charge dimuon vertices in region A). Muons from decays of hadrons containing b and c quarks are, within the context of this analysis, considered to be prompt muons.

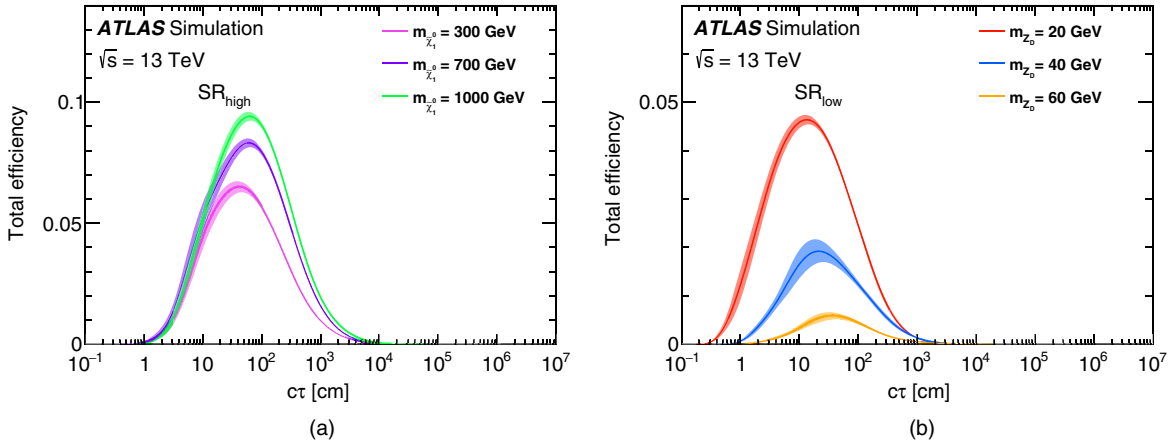

FIG. 4. Overall event-level efficiencies after the signal-region selections (combining trigger and offline selection), as a function of the lifetime of the long-lived BSM particle, for (a) the GGM model and (b) the dark-sector model. The shaded bands represent the statistical uncertainties only.

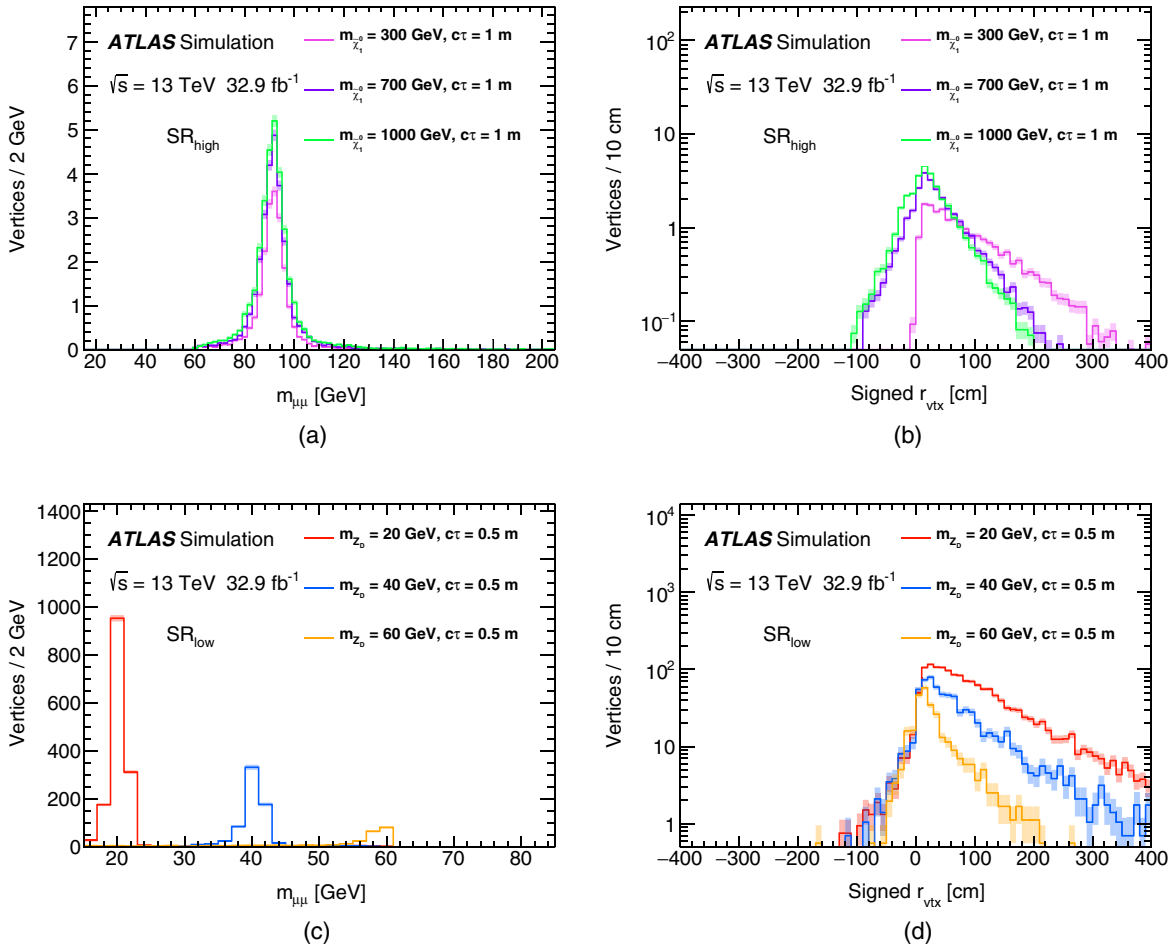

FIG. 5. Distributions derived from MC simulations of (a) dimuon invariant mass $m_{\mu\mu}$ and (b) vertex radius r_{vtx} for signal vertices in SR_{high} with a long-lived neutralino, $\tilde{\chi}_1^0$ ($m_{\tilde{\chi}_1^0} = 300$, 700, and 1000 GeV and $c\tau_{\tilde{\chi}_1^0} = 100$ cm) decaying to a Z boson (with $Z \to \mu^+\mu^-$) and a gravitino; (c) $m_{\mu\mu}$ and (d) r_{vtx} for signal vertices in SR_{low} with a long-lived dark photon, Z_{D} ($m_{Z_{\text{D}}} = 20$, 40, and 60 GeV; and $c\tau_{Z_{\text{D}}} = 50$ cm), that decays to $\mu^+\mu^-$. The shaded bands represent the statistical uncertainties. The distributions are normalized to the expected yields in the signal regions for $m_{\tilde{g}} = 1100$ GeV, $\sigma(pp \to \tilde{g}\,\tilde{g}) = 0.1635$ pb, $B(\tilde{\chi}_1^0 \to Z\tilde{G}) = 1.0$, and $B(Z \to \mu^+\mu^-) = 0.03366$; and $m_H = 125$ GeV, $m_{H_{\text{D}}} = 300$ GeV, $\sigma(pp \to H) = 44.1$ pb, $B(H \to Z_{\text{D}}Z_{\text{D}}) = 100\%$, and the value of $B(Z_{\text{D}} \to \mu^+\mu^-)$ varying between 0.1475 and 0.1066 for the range $m_{Z_{\text{D}}} = 20$–60 GeV.

TABLE VII. Description of four regions used in estimating background yields. The ordering of the muon candidates in the description of the dimuon vertex is leading muon first, then subleading muon.

Region name	Muon candidates in vertex
A	MSonly-MSonly
B	MSonly-MScomb
C	MScomb-MSonly
D	MScomb-MScomb

F. Nonprompt muon vertices

Nonprompt muons are those for which no matching ID track is expected. Examples of such sources of background nonprompt muons are cosmic-ray muons, BIB muons, fake MS tracks generated from random hit combinations, and those arising from pion or kaon decay.

Cosmic-ray and BIB muons will usually not produce ID tracks, as they rarely pass close enough to the IP to produce an ID track that satisfies the track reconstruction criteria, in particular the $|d_0| < 1$ cm requirement. As a result, they produce mostly MSonly muon candidates. As described in Sec. IV B, dimuon vertices reconstructed from a single cosmic-ray or BIB muon that generates two MS tracks are effectively eliminated in the preselection by taking advantage of the fact that the angle between the two tracks will be nearly 180°. On the other hand, vertices formed when a single MS track from a cosmic-ray or BIB muon is paired with an unrelated muon candidate produced from the pp collision will satisfy these selection criteria and more readily contribute to the background.

Pions and kaons have relatively large lifetimes and feature large branching fractions to final states with one muon. Such decays often result in either no ID track being reconstructed, due to the requirement of at least a minimum number of ID hits, or the ID track of the pion/kaon failing to be matched to the muon MS track. In both of these two cases, a MSonly muon candidate will be produced.

Vertices that contain one or more nonprompt muons are referred to as "nonprompt vertices." If the vertex contains a cosmic-ray or BIB muon paired with an unrelated muon candidate, the charges of the two MS tracks will be largely uncorrelated. However, some charge correlation is expected in vertices containing muons from pion/kaon decay, because the pion/kaon is produced from the same pp collision that produces the other muon in the vertex. For the latter, the charge correlation is studied by measuring the ratio of OS to SS dimuon vertices, $R_q^{\pi/K}$, in the data. As muons from pion/kaon decay are not expected to be isolated from jets, the quantity $R_q^{\pi/K}$ is measured in a sample of dimuon vertices where the selection criteria are those of the preselection, except that the jet-muon overlap and isolation requirements are removed for both muons. The value ranges from 1.39 ± 0.09 to 1.55 ± 0.03, depending on the region (A, B, C, or D). As no statistical difference in $R_q^{\pi/K}$ is observed for the low- and high-mass regions, a single value is used for both regions. For dimuon vertices composed of BIB or cosmic-ray muons, the muon charges are assumed to be entirely uncorrelated: $R_q^{\cos/\mathrm{BIB}} = 1.0$.

TABLE VIII. Observed number of SS vertices N^{SS}, charge ratio $R_{q,\mathrm{SR}}$ and predicted yields of nonprompt dimuon vertices $N_{\mathrm{SR}}^{\mathrm{nonprompt}}$ in each signal region. The uncertainty in $N_{\mathrm{SR}}^{\mathrm{nonprompt}}$ combines in quadrature the statistical uncertainty, derived from the observed number of SS vertices, and the uncertainty in the charge ratio. The statistical uncertainty on N^{SS} for the case where the central value is measured to be zero is taken to be the 68% one-sided Poisson confidence-level interval: +1.14.

Region	N^{SS}	$R_{q,\mathrm{SR}}$	$N_{\mathrm{SR}}^{\mathrm{nonprompt}}$
$\mathrm{SR}_{\mathrm{low}}$	11	1.24 ± 0.24	13.6 ± 4.9
$\mathrm{SR}_{\mathrm{high}}$	0	1.24 ± 0.24	$0.0^{+1.4}_{-0.0}$

Since the relative composition of the nonprompt dimuon background is unknown, the average of $R_q^{\pi/K}$ and $R_q^{\cos/\mathrm{BIB}}$ is assumed as the nominal value, R_q, with an uncertainty that is half the difference between the two values; this is shown in Table VIII ($R_q = 1.24 \pm 0.24$ for the SRs).

The numbers of OS nonprompt vertices in the regions A, B, C, and D are predicted using the number of SS vertices in each region and the appropriate R_q, as described above: $N_i^{\mathrm{nonprompt}} = R_{q,i} N_i^{\mathrm{SS}}$, where N_i^{SS} is the number of SS vertices observed in region i ($i =$ A, B, C, or D) and $R_{q,i}$ is the charge ratio for region i.

The predicted yields of nonprompt dimuon vertices for both SRs are given in Table VIII, where the uncertainty in R_q is treated as a systematic uncertainty added in quadrature to the statistical uncertainties.

G. Prompt muon vertices

The number of dimuon vertices in each of the SRs arising from prompt muon processes is estimated from the observed yields in the OS low-mass and high-mass B, C, and D control regions. Sources of such background in the SRs include SM processes that produce prompt muons that are reconstructed as MSonly due to detector or reconstruction effects, such as ID inefficiencies, or poorly reconstructed combined muons, collectively described as failed combined muon reconstruction.

To avoid double-counting of dimuons from nonprompt processes, the estimated number of nonprompt OS vertices in each region is subtracted:

$$N_i^{\mathrm{prompt}} = N_i^{\mathrm{OS}} - N_i^{\mathrm{nonprompt}}, \qquad i = \mathrm{B}, \mathrm{C}, \mathrm{D},$$

where N_i^{OS} is the number of OS vertices in region i, $N_i^{\mathrm{nonprompt}}$ is the number of OS nonprompt vertices in region

i (described in Sec. IV F) and N_i^{prompt} is the estimated number of opposite-charge vertices from prompt processes in region i. The quantity $N_{\text{B}}^{\text{prompt}}$ ($N_{\text{C}}^{\text{prompt}}$) is the estimated number of OS vertices from prompt processes with leading (subleading) muons that fail the combined reconstruction and are identified as MSonly, while the other muon candidate is identified as being MScomb. The quantity $N_{\text{D}}^{\text{prompt}}$ is the estimated number of OS vertices from prompt processes with muon candidates that pass the combined reconstruction and are both identified as being MScomb. With these definitions, the leading and subleading "transfer factors" are defined as follows:

$$f_{\text{L}} = N_{\text{B}}^{\text{prompt}}/N_{\text{D}}^{\text{prompt}},$$
$$f_{\text{S}} = N_{\text{C}}^{\text{prompt}}/N_{\text{D}}^{\text{prompt}}.$$

The leading transfer factor multiplied by $N_{\text{C}}^{\text{prompt}}$, or, alternatively, the subleading transfer factor multiplied by $N_{\text{B}}^{\text{prompt}}$, thus gives for prompt muon processes the predicted number of OS vertices in region A, the SRs in this case:

$$N_{\text{A}}^{\text{prompt}} = f_{\text{L}} \cdot N_{\text{C}}^{\text{prompt}} = f_{\text{S}} \cdot N_{\text{B}}^{\text{prompt}}.$$

The yields in the various regions are summarized in Table IX. The vertices in all CRs are used to verify that the designation of one of the MS tracks in the vertex as MScomb or MSonly is independent of the designation of the other as MScomb or MSonly (the measured correlation is negligibly small, < 0.0015). The predicted number of vertices from prompt background processes in the low- and high-mass SRs are 0.14 ± 0.22 and 0.504 ± 0.070, respectively, where the uncertainties are statistical only.

As a cross-check, the B, C, and D control regions are subdivided into bins of either muon p_{T} or muon η and ϕ, and the transfer factors and predictions of N^{prompt} in the SRs are recomputed. For both the low-mass and high-mass selection, the sum over the predicted prompt background yields in each bin is consistent with the nominal value.

TABLE IX. The number of opposite-charge vertices, N^{OS}, the number of same-charge vertices, N^{SS}, the estimated ratio of opposite-charge to same-charge nonprompt dimuon vertices, R_q and the estimated number of prompt dimuon vertices N^{prompt} in each of the control regions B, C, and D. The values of N^{prompt} are obtained by subtracting the product of N^{SS} and R_q from N^{OS}. The quoted uncertainties in N^{prompt} include the statistical component and the systematic uncertainty in R_q.

Region	N^{OS}	N^{SS}	R_q	N^{prompt}
Low-mass region				
B	124	63	1.28 ± 0.28	43 ± 23
C	451	335	1.20 ± 0.20	49^{+74}_{-49}
D	19599	3220	1.20 ± 0.20	15700 ± 660
High-mass region				
B	120	0	1.28 ± 0.28	120 ± 11
C	92	0	1.20 ± 0.20	92 ± 10
D	21940	24	1.20 ± 0.20	21900 ± 150

H. Total background

The predicted number of nonprompt muon vertices is summed with the predicted number of prompt muon vertices from SM background processes to give the predicted total number of background vertices in each of the SRs: 13.8 ± 4.9 and $0.50^{+1.41}_{-0.07}$ for SR_{low} and SR_{high}, respectively, where the uncertainties include the statistical components and the systematic uncertainty in R_q.

The reliability of the background estimation method is validated by applying it to both the sum of the simulated background samples and to a high-mass validation region in the data. The predicted number of dimuon vertices in the simulated sample agrees with the number of observed vertices, to within the statistical precision, in both the low- and high-mass signal regions. As the simulated samples do not include multijet processes or cosmic muon backgrounds, this is primarily a validation of the technique to estimate the background from prompt dimuon vertices. The validation region in data comprises dimuon vertices that satisfy all of the selection criteria of the high-mass region, with the exception that the requirement on the transverse boost of the dimuon system is inverted: it is required to have a value less than two, which ensures that there is negligible contribution from signal processes. The results are given in Table X. These two studies validate the method within the statistical precision.

V. SYSTEMATIC UNCERTAINTIES

The systematic uncertainties are described in detail below. They include those in the integrated luminosity, used in converting signal yields to cross sections; the background estimate, derived entirely from the data; and the signal efficiency, determined from MC simulations. All systematic uncertainties are treated as uncorrelated.

TABLE X. Predicted nonprompt $N_{\text{VR}}^{\text{nonprompt}}$, prompt $N_{\text{VR}}^{\text{prompt}}$, and total $N_{\text{VR}}^{\text{bkgd}}$ background yields and number of observed vertices $N_{\text{VR}}^{\text{obs}}$ in data in the high-mass validation region. The uncertainty in $N_{\text{VR}}^{\text{prompt}}$ includes the statistical component and the systematic uncertainty in R_q.

Yield	High-mass validation region
$N_{\text{VR}}^{\text{nonprompt}}$	$2.5^{+2.3}_{-1.6}$
$N_{\text{VR}}^{\text{prompt}}$	7.20 ± 0.25
$N_{\text{VR}}^{\text{bkgd}}$	$9.7^{+2.3}_{-1.6}$
$N_{\text{VR}}^{\text{obs}}$	13

The uncertainty in the 2016 integrated luminosity is 2.2%. It is derived, following a methodology similar to that detailed in Ref. [94], and using the LUCID-2 detector for the baseline luminosity measurements [95], from calibration of the luminosity scale using x-y beam-separation scans.

Sources of systematic uncertainties in the signal efficiencies include possible mismodeling of the trigger and MS efficiencies and pileup effects in the MC simulation. For the high-mass SR, the uncertainty associated with trigger and MS track reconstruction efficiency is determined by comparing the observed yields in the data with MC simulation of $Z+\text{jets}$ events, using the selection criteria of the OS B, C, and D control regions and the additional requirement $70 < m_{\mu\mu} < 110$ GeV. The difference between the yields in data and the simulated background samples is used to assign a systematic uncertainty of 1% to the combined trigger and MS track-reconstruction efficiency. For the low-mass SR, the efficiency of the trigger and MS track reconstruction is compared between MC simulation and data for $J/\psi \to \mu\mu$ events, using a tag-and-probe technique. The efficiency is measured as a function of the angular separation between the two muons, and a maximum deviation of 6% is observed. This difference is taken as an uncertainty in the signal efficiency. The agreement between data and MC simulation for the reconstruction efficiency for MS tracks with large impact parameters was studied by comparing a cosmic-ray muon simulation to cosmic-ray muon candidates in data [22]. Comparing the ratio of the muon candidate d_0 distributions in the two samples yields a d_0-dependent efficiency correction that is between 1% and 2.5%, with an average value of 1.5%. The systematic uncertainty on MS track reconstruction associated with this procedure is taken from the statistical uncertainty, and is 2% per track in the vertices.

The systematic uncertainty from pileup effects is determined by varying the pileup reweighting of simulated signal events in a manner that spans the expected uncertainty. This results in a systematic uncertainty of 0.2% in the signal efficiency.

The methods used to estimate the background are entirely data-driven, with statistical uncertainties arising from the numbers of events in the CRs. The nonprompt-vertex background estimate for both signal regions has a systematic uncertainty of 19% associated with knowledge of the charge correlation R_q, as described in Sec. IV F. Systematic uncertainties in the estimate of the prompt background are determined by varying the quantity that distinguishes MScomb from MSonly muons, the angular distance between the MS track and nearest combined-muon track, by ±50% and repeating the ABCD technique described in Sec. IV G. A 9% difference in the prompt background estimate is observed, and this is taken as a systematic uncertainty.

TABLE XI. Predicted nonprompt $N^{\text{nonprompt}}$, prompt N^{prompt}, and total N^{bkgd} background yields and number of observed vertices N^{obs} in data in SR_{low} and SR_{high}. The uncertainties in the predicted background yields are statistical uncertainties and systematic uncertainties added in quadrature.

Yield	SR_{low}	SR_{high}
$N^{\text{nonprompt}}$	13.6 ± 4.9	$0.0^{+1.4}_{-0.0}$
N^{prompt}	$0.1^{+0.2}_{-0.1}$	0.50 ± 0.07
N^{bkgd}	13.8 ± 4.9	$0.50^{+1.42}_{-0.07}$
N^{obs}	15	2

VI. RESULTS

The predicted number of nonprompt muon vertices is summed with the predicted number of prompt muon vertices from SM background processes to give the predicted total number of background vertices, N^{bkgd}, in each SR. The predicted background yields, along with the number of observed vertices in the data, are summarized in Table XI. The distributions of $m_{\mu\mu}$ and r_{vtx} are shown in Fig. 6 for the observed vertices in the two signal regions. Each dimuon vertex is in a separate event, and therefore the number of events observed is equivalent to the number of vertices. The dimuon vertex with the highest mass has $m_{\mu\mu} = 381$ GeV, $r_{\text{vtx}} = -220$ cm, and $z_{\text{vtx}} = 99$ cm. Close inspection of the event reveals characteristics of being cosmic in origin. The observation of one such dimuon vertex in SR_{high} is consistent, within the uncertainties, with the nonprompt background estimate of $N^{\text{nonprompt}} = 0.0^{+1.4}_{-0.0}$. The other vertex in SR_{high} has a mass compatible with the decay of the SM Z. The dimuon vertex with the largest value of r_{vtx} is in SR_{low} and has $m_{\mu\mu} = 46$ GeV, $r_{\text{vtx}} = 223$ cm, and $z_{\text{vtx}} = 56$ cm. The vertex is formed by an MS track passing through the top of the detector combined with another MS track passing through the bottom of the detector, with an angle of nearly 180° between them. This vertex is likely a cosmic-ray muon that narrowly survived the cosmic-ray veto criteria described in Sec. IV C.

As no significant excess of vertices over the SM background expectation is observed, 95% confidence-level (C.L.) upper limits on the signal event yields and production cross sections are calculated for various values of the proper decay distance $c\tau$ of the long-lived particle in each of the two BSM scenarios considered.[4] The limits are calculated using the CL_{S} prescription [96] with a Poisson likelihood used as the test statistic. Uncertainties in the signal efficiency and background expectation are included

[4]For events that are selected exclusively by the trimuon trigger the observed signal yield will have a quadratic dependence on $B(Z_{\text{D}} \to \mu^+\mu^-)$. The collimated-dimuon trigger efficiency dominates over the trimuon trigger efficiency for the values of $m_{Z_{\text{D}}}$ considered in this paper.

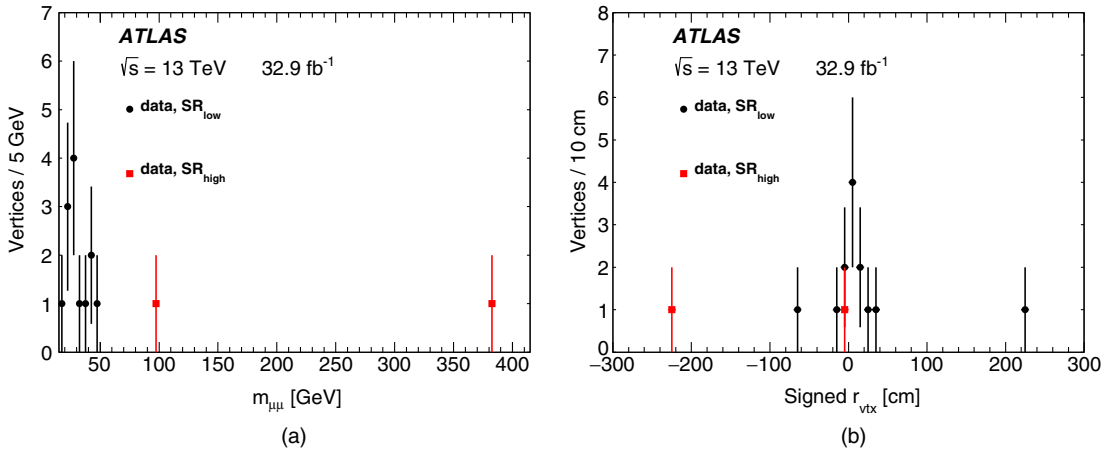

FIG. 6. Distributions of (a) dimuon invariant mass $m_{\mu\mu}$ and (b) vertex radius r_{vtx} for displaced dimuon vertices in the low-mass (black circles) and high-mass (red squares) signal regions.

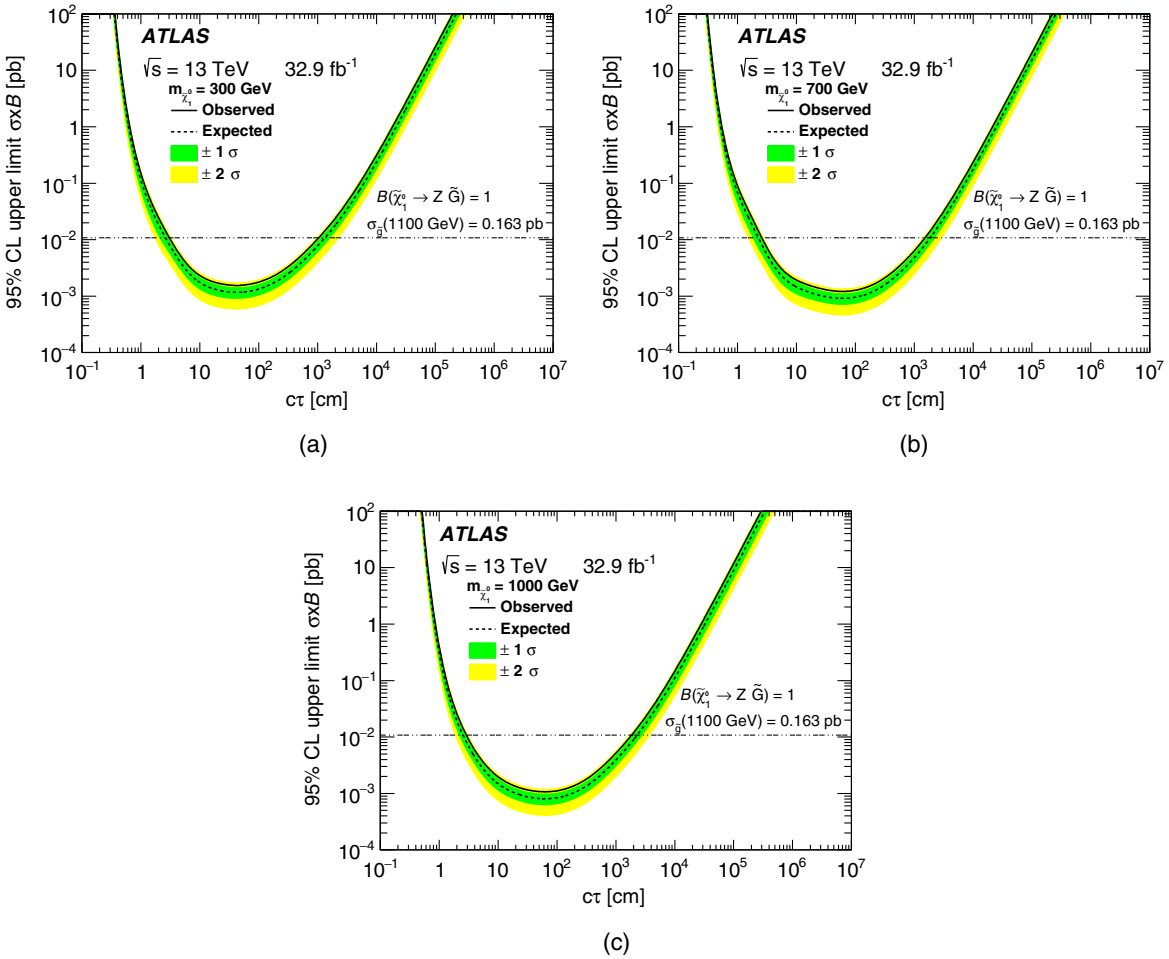

FIG. 7. The observed and expected 95% C.L. upper limits on the product of cross section and branching ratios for pair production of gluinos, leading to a final state of $\mu^+\mu^- + X$, in the GGM model, as a function of the $\tilde{\chi}_1^0$ lifetime, for $m_{\tilde{g}} = 1100$ GeV and three different choices of $m_{\tilde{\chi}_1^0}$: (a) 300 GeV, (b) 700 GeV, and (c) 1000 GeV. The shaded green (yellow) bands represent the 1σ (2σ) uncertainties in the expected limits. The dashed horizontal line represents the value of the cross section times branching fractions predicted from simulation, with $m_{\tilde{g}} = 1100$ GeV, $\sigma(pp \to \tilde{g}\tilde{g}) = 0.1635$ pb, $B(\tilde{\chi}_1^0 \to Z\tilde{G}) = 1.0$, and $B(Z \to \mu^+\mu^-) = 0.03366$.

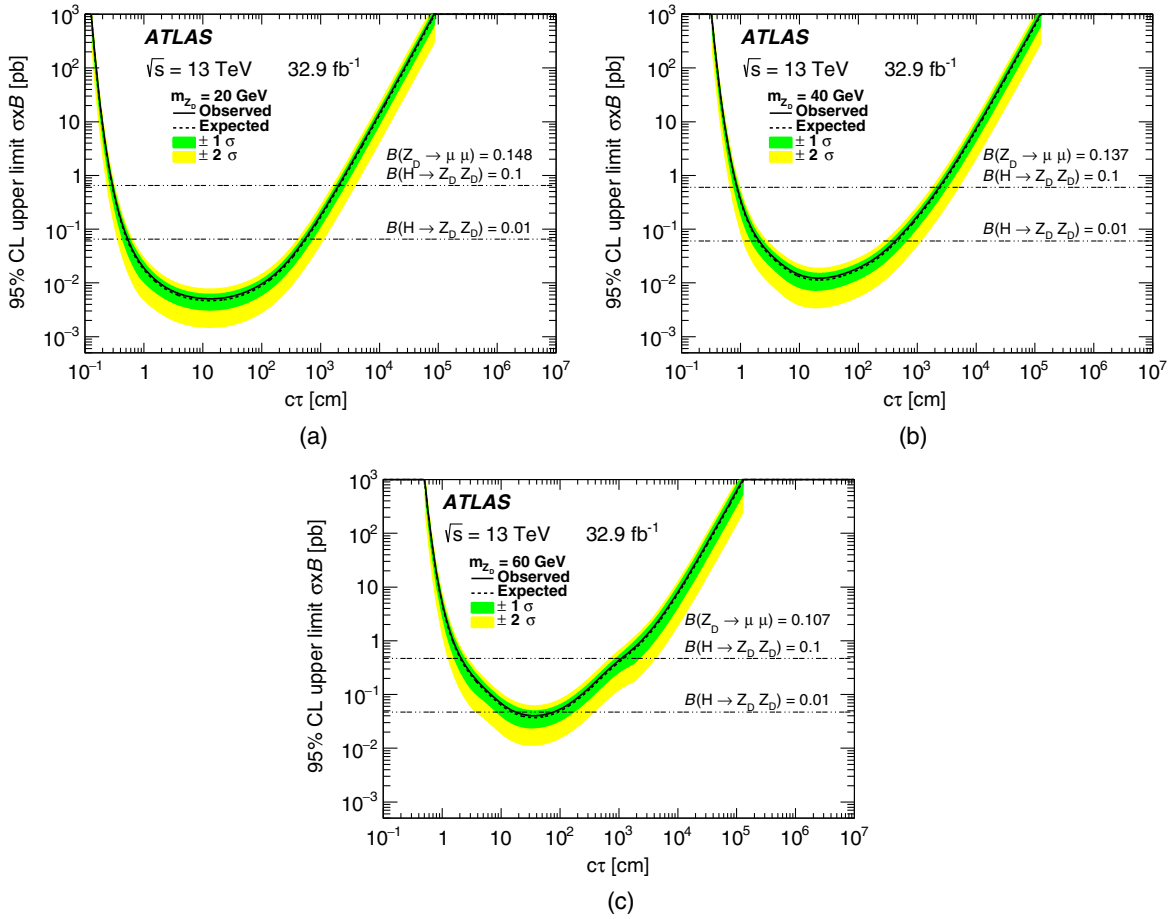

FIG. 8. The observed and expected 95% C.L. upper limits on the product of cross section and branching ratios, $\sigma \times B = \sigma(pp \to H) \times B(H \to Z_D Z_D) \times B(Z_D \to \mu^+\mu^-)$, in the dark-sector model, as a function of the Z_D lifetime, for three different choices of m_{Z_D}: (a) 20 GeV, (b) 40 GeV, and (c) 60 GeV. The shaded green (yellow) bands represent the 1σ (2σ) uncertainties in the expected limits. The dashed horizontal lines represent the values of the cross section times branching fractions predicted by simulation, with $m_H = 125$ GeV, $m_{H_D} = 300$ GeV, $\sigma(pp \to H) = 44.1$ pb and assuming $B(H \to Z_D Z_D) = 10\%$ or 1%. The value of $B(Z_D \to \mu^+\mu^-)$ varies between 0.1475 and 0.1066 for the range $m_{Z_D} = 20$–60 GeV.

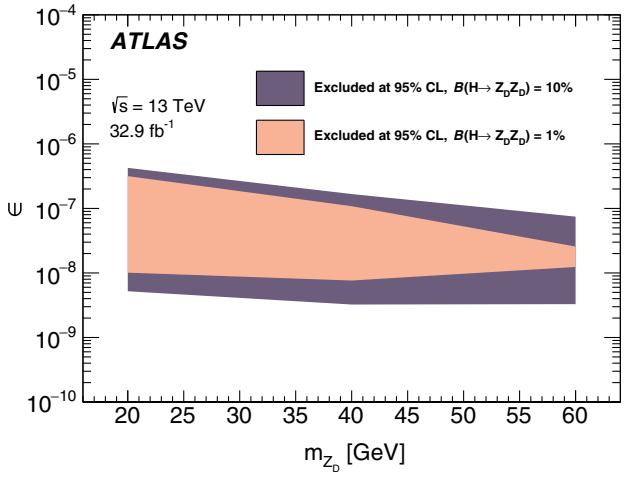

FIG. 9. The observed 95% C.L. excluded regions in the plane of Z_D-Z kinetic mixing parameter, ϵ, versus Z_D mass, for values of $B(H \to Z_D Z_D) = 1\%$ or 10%, and $m_{H_D} = 300$ GeV. The value of $B(Z_D \to \mu^+\mu^-)$ varies between 0.1475 and 0.1066 for the range $m_{Z_D} = 20$–60 GeV.

as nuisance parameters, and the CL_S values are calculated by generating ensembles of pseudoexperiments corresponding to the background-only and signal-plus-background hypotheses. Both the expected and observed limits are shown in Fig. 7 for the GGM model, and in Fig. 8 for the dark-sector model, where SR_{high} is used for the GGM model and SR_{low} is used for the dark-sector model. In the GGM model with a gluino mass of 1100 GeV and $\tilde{\chi}_1^0$ masses of 300, 700, and 1000 GeV, $c\tau_{\tilde{\chi}_1^0}$ values are excluded in the ranges 3.1–1000 cm, 2.6–1500 cm, and 2.9–1800 cm, respectively. The observed limits are about 1.5σ weaker than the expected limits because of the small excess of events observed in SR_{high}. In the dark-sector model with a dark-Higgs-boson mass of 300 GeV, $B(H \to Z_D Z_D) = 10\%$ and Z_D masses of 20, 40, and 60 GeV, $c\tau_{Z_D}$ values are excluded in the ranges 0.3–2000 cm, 0.9–2400 cm, and 2.1–1100 cm, respectively. These limits are translated into 95% exclusion contours in the plane of the Z_D-Z kinetic mixing parameter, ϵ, and the

Z_D mass, and are shown in Fig. 9. Values of ϵ of the order 10^{-8} are excluded for $20 < m_{Z_D} < 60$ GeV.

VII. CONCLUSION

This article reports on a search for BSM long-lived particles decaying into two muons of opposite-sign electric charge in a sample of pp collisions recorded by the ATLAS detector at the LHC with a center-of-mass energy of $\sqrt{s} =$ 13 TeV and an integrated luminosity of 32.9 fb^{-1}. The search is performed by identifying dimuon vertices with displacements from the pp interaction point in the range of 1–400 cm and having invariant mass $m_{\mu\mu}$ within one of two signal regions: 20–60 GeV or > 60 GeV. In neither signal region is a significant excess observed in the number of vertices relative to the predicted background. Hence upper limits at 95% confidence level on the product of cross section and branching fraction are calculated, as a function of lifetime, for production of long-lived particles in either a dark-sector model with dark-photon masses in the range 20–60 GeV, produced from decays of the Higgs boson, or in a general gauge-mediated supersymmetric model with a gluino mass of 1100 GeV and neutralino masses in the range 300–1000 GeV. For the models considered, the lower and upper lifetime limits are set from 1 to 2400 cm in $c\tau$, respectively, depending on the targeted model's parameters.

ACKNOWLEDGMENTS

We thank CERN for the very successful operation of the LHC, as well as the support staff from our institutions without whom ATLAS could not be operated efficiently. We acknowledge the support of ANPCyT, Argentina; YerPhI, Armenia; ARC, Australia; BMWFW and FWF, Austria; ANAS, Azerbaijan; SSTC, Belarus; CNPq and FAPESP, Brazil; NSERC, NRC and CFI, Canada; CERN; CONICYT, Chile; CAS, MOST and NSFC, China; COLCIENCIAS, Colombia; MSMT CR, MPO CR and VSC CR, Czech Republic; DNRF and DNSRC, Denmark; IN2P3-CNRS, CEA-DRF/IRFU, France; SRNSFG, Georgia; BMBF, HGF, and MPG, Germany; GSRT, Greece; RGC, Hong Kong SAR, China; ISF, I-CORE and Benoziyo Center, Israel; INFN, Italy; MEXT and JSPS, Japan; CNRST, Morocco; NWO, Netherlands; RCN, Norway; MNiSW and NCN, Poland; FCT, Portugal; MNE/IFA, Romania; MES of Russia and NRC KI, Russian Federation; JINR; MESTD, Serbia; MSSR, Slovakia; ARRS and MIZŠ, Slovenia; DST/NRF, South Africa; MINECO, Spain; SRC and Wallenberg Foundation, Sweden; SERI, SNSF and Cantons of Bern and Geneva, Switzerland; MOST, Taiwan; TAEK, Turkey; STFC, United Kingdom; DOE and NSF, United States of America. In addition, individual groups and members have received support from BCKDF, the Canada Council, CANARIE, CRC, Compute Canada, FQRNT, and the Ontario Innovation Trust, Canada; EPLANET, ERC, ERDF, FP7, Horizon 2020 and Marie Skłodowska-Curie Actions, European Union; Investissements d'Avenir Labex and Idex, ANR, Région Auvergne and Fondation Partager le Savoir, France; DFG and AvH Foundation, Germany; Herakleitos, Thales and Aristeia programmes co-financed by EU-ESF and the Greek NSRF; BSF, GIF and Minerva, Israel; BRF, Norway; CERCA Programme Generalitat de Catalunya, Generalitat Valenciana, Spain; the Royal Society and Leverhulme Trust, United Kingdom. The crucial computing support from all WLCG partners is acknowledged gratefully, in particular from CERN, the ATLAS Tier-1 facilities at TRIUMF (Canada), NDGF (Denmark, Norway, Sweden), CC-IN2P3 (France), KIT/GridKA (Germany), INFN-CNAF (Italy), NL-T1 (Netherlands), PIC (Spain), ASGC (Taiwan), RAL (UK) and BNL (USA), the Tier-2 facilities worldwide and large non-WLCG resource providers. Major contributors of computing resources are listed in Ref. [97].

[1] C. Patrignani *et al.*, Review of particle physics, Chin. Phys. C **40**, 100001 (2016).
[2] M. Fairbairn, A. C. Kraan, D. A. Milstead, T. Sjöstrand, P. Skands, and T. Sloan, Stable massive particles at colliders, Phys. Rep. **438**, 1 (2007).
[3] D. Curtin *et al.*, Exotic decays of the 125 GeV Higgs Boson, Phys. Rev. D **90**, 075004 (2014).
[4] Yu. A. Golfand and E. P. Likhtman, Extension of the Algebra of Poincare group generators and violation of p invariance, Pisma Zh. Eksp. Teor. Fiz. **13**, 452 (1971) [JETP Lett. **13**, 323 (1971)].
[5] D. V. Volkov and V. P. Akulov, Is the neutrino a goldstone particle?, Phys. Lett. **46B**, 109 (1973).
[6] J. Wess and B. Zumino, Supergauge transformations in four dimensions, Nucl. Phys. **B70**, 39 (1974).
[7] J. Wess and B. Zumino, Supergauge invariant extension of quantum electrodynamics, Nucl. Phys. **B78**, 1 (1974).
[8] S. Ferrara and B. Zumino, Supergauge invariant Yang-Mills theories, Nucl. Phys. **B79**, 413 (1974).
[9] A. Salam and J. A. Strathdee, Supersymmetry and non-abelian gauges, Phys. Lett. **51B**, 353 (1974).
[10] R. Barbier *et al.*, R-parity violating supersymmetry, Phys. Rep. **420**, 1 (2005).
[11] B. C. Allanach, M. A. Bernhardt, H. K. Dreiner, C. H. Kom, and P. Richardson, Mass spectrum in R-parity violating

minimal supergravity and benchmark points, Phys. Rev. D **75**, 035002 (2007).
[12] S. Dimopoulos, M. Dine, S. Raby, and S. D. Thomas, Experimental Signatures of Low-Energy Gauge Mediated Supersymmetry Breaking, Phys. Rev. Lett. **76**, 3494 (1996).
[13] C. Cheung, A. L. Fitzpatrick, and D. Shih, (Extra)ordinary gauge mediation, J. High Energy Phys. 07 (2008) 054.
[14] P. Meade, N. Seiberg, and D. Shih, General gauge mediation, Prog. Theor. Phys. Suppl. **177**, 143 (2009).
[15] J. L. Hewett, B. Lillie, M. Masip, and T. G. Rizzo, Signatures of long-lived gluinos in split supersymmetry, J. High Energy Phys. 09 (2004) 070.
[16] A. Arvanitaki, N. Craig, S. Dimopoulos, and G. Villadoro, Mini-split, J. High Energy Phys. 02 (2013) 126.
[17] T. Han, Z. Si, K. M. Zurek, and M. J. Strassler, Phenomenology of hidden valleys at hadron colliders, J. High Energy Phys. 07 (2008) 008.
[18] J. Fan, M. Reece, and J. T. Ruderman, Stealth supersymmetry, J. High Energy Phys. 11 (2011) 012.
[19] P. Schuster, N. Toro, and I. Yavin, Terrestrial and solar limits on long-lived particles in a dark sector, Phys. Rev. D **81**, 016002 (2010).
[20] ATLAS Collaboration, A measurement of material in the ATLAS tracker using secondary hadronic interactions in 7 TeV pp collisions, J. Instrum. **11**, P11020 (2016).
[21] ATLAS Collaboration, Study of the material of the ATLAS inner detector for Run 2 of the LHC, J. Instrum. **12**, P12009 (2017).
[22] ATLAS Collaboration, Search for massive, long-lived particles using multitrack displaced vertices or displaced lepton pairs in pp collisions at $\sqrt{s} = 8$ TeV with the ATLAS detector, Phys. Rev. D **92**, 072004 (2015).
[23] ATLAS Collaboration, Search for long-lived neutral particles decaying into lepton jets in proton-proton collisions at $\sqrt{s} = 8$ TeV with the ATLAS detector, J. High Energy Phys. 11 (2014) 088.
[24] ATLAS Collaboration, Search for displaced muonic lepton jets from light Higgs boson decay in proton-proton collisions at $\sqrt{s} = 7$ TeV with the ATLAS detector, Phys. Lett. B **721**, 32 (2013).
[25] ATLAS Collaboration, Search for displaced vertices arising from decays of new heavy particles in 7 TeV pp collisions at ATLAS, Phys. Lett. B **707**, 478 (2012).
[26] ATLAS Collaboration, Search for long-lived, heavy particles in final states with a muon and multitrack displaced vertex in proton-proton collisions at $\sqrt{s} = 7$ TeV with the ATLAS detector, Phys. Lett. B **719**, 280 (2013).
[27] ATLAS Collaboration, Search for nonpointing photons in the diphoton and $E_{\mathrm{T}}^{\mathrm{miss}}$ final state in $\sqrt{s} = 7$ TeV proton-proton collisions using the ATLAS detector, Phys. Rev. D **88**, 012001 (2013).
[28] ATLAS Collaboration, Search for pair-produced long-lived neutral particles decaying to jets in the ATLAS hadronic calorimeter in pp collisions at $\sqrt{s} = 8$ TeV, Phys. Lett. B **743**, 15 (2015).
[29] ATLAS Collaboration, Search for charginos nearly mass degenerate with the lightest neutralino based on a disappearing-track signature in pp collisions at $\sqrt{s} = 8$ TeV with the ATLAS detector, Phys. Rev. D **88**, 112006 (2013).
[30] ATLAS Collaboration, Search for nonpointing and delayed photons in the diphoton and missing transverse momentum final state in 8 TeV pp collisions at the LHC using the ATLAS detector, Phys. Rev. D **90**, 112005 (2014).
[31] ATLAS Collaboration, Search for long-lived, weakly interacting particles that decay to displaced hadronic jets in proton-proton collisions at $\sqrt{s} = 8$ TeV with the ATLAS detector, Phys. Rev. D **92**, 012010 (2015).
[32] ATLAS Collaboration, Search for heavy long-lived charged R-hadrons with the ATLAS detector in 3.2 fb^{-1} of proton-proton collision data at $\sqrt{s} = 13$ TeV, Phys. Lett. B **760**, 647 (2016).
[33] ATLAS Collaboration, Search for metastable heavy charged particles with large ionization energy loss in pp collisions at $\sqrt{s} = 13$ TeV using the ATLAS experiment, Phys. Rev. D **93**, 112015 (2016).
[34] CMS Collaboration, Search in leptonic channels for heavy resonances decaying to long-lived neutral particles, J. High Energy Phys. 02 (2013) 085.
[35] CMS Collaboration, Search for long-lived particles in events with photons and missing energy in proton-proton collisions at $\sqrt{s} = 7$ TeV, Phys. Lett. B **722**, 273 (2013).
[36] CMS Collaboration, Search for Displaced Supersymmetry in Events with an Electron and a Muon with Large Impact Parameters, Phys. Rev. Lett. **114**, 061801 (2015).
[37] CMS Collaboration, Search for long-lived particles that decay into final states containing two electrons or two muons in proton-proton collisions at $\sqrt{s} = 8$ TeV, Phys. Rev. D **91**, 052012 (2015).
[38] CMS Collaboration, Search for long-lived neutral particles decaying to quark-antiquark pairs in proton-proton collisions at $\sqrt{s} = 8$ TeV, Phys. Rev. D **91**, 012007 (2015).
[39] CMS Collaboration, Search for R-parity violating supersymmetry with displaced vertices in proton-proton collisions at $\sqrt{s} = 8$ TeV, Phys. Rev. D **95**, 012009 (2017).
[40] CMS Collaboration, Search for long-lived charged particles in proton-proton collisions at $\sqrt{s} = 13$ TeV, Phys. Rev. D **94**, 112004 (2016).
[41] LHCb Collaboration, Search for long-lived particles decaying to jet pairs, Eur. Phys. J. C **75**, 152 (2015).
[42] LHCb Collaboration, Search for Hidden-Sector Bosons in $B^0 \to K^{*0}\mu^+\mu^-$ Decays, Phys. Rev. Lett. **115**, 161802 (2015).
[43] LHCb Collaboration, Search for massive long-lived particles decaying semileptonically in the LHCb detector, Eur. Phys. J. C **77**, 224 (2017).
[44] LHCb Collaboration, Search for long-lived scalar particles in $B^+ \to K^+\chi(\mu^+\mu^-)$ decays, Phys. Rev. D **95**, 071101 (2017).
[45] CDF Collaboration, Search for long-lived parents of Z^0 bosons in $p\bar{p}$ collisions at $\sqrt{s} = 1.8$ TeV, Phys. Rev. D **58**, 051102 (1998).
[46] D0 Collaboration, Search for Neutral, Long-Lived Particles Decaying into Two Muons in $p\bar{p}$ Collisions at $\sqrt{s} = 1.96$ TeV, Phys. Rev. Lett. **97**, 161802 (2006).
[47] D0 Collaboration, Search for Resonant Pair Production of Neutral Long-Lived Particles Decaying to $b\bar{b}$ in $p\bar{p}$ Collisions at $\sqrt{s} = 1.96$ TeV, Phys. Rev. Lett. **103**, 071801 (2009).

[48] *BABAR* Collaboration, Search for Long-Lived Particles in e^+e^- Collisions, Phys. Rev. Lett. **114**, 171801 (2015).

[49] Belle Collaboration, Search for heavy neutrinos at Belle, Phys. Rev. D **87**, 071102 (2013).

[50] ALEPH Collaboration, Search for gauge mediated SUSY breaking topologies in e^+e^- collisions at centre-of-mass energies of up to 209 GeV, Eur. Phys. J. C **25**, 339 (2002).

[51] ATLAS Collaboration, The ATLAS Experiment at the CERN Large Hadron Collider, J. Instrum. **3**, S08003 (2008).

[52] ATLAS Collaboration, ATLAS insertable B-layer technical design report, CERN Report No. ATLAS-TDR-19, 2010, https://cds.cern.ch/record/1291633; ATLAS insertable B-layer technical design report Addendum, CERN Report No. ATLAS-TDR-19-ADD-1, 2012, https://cds.cern.ch/record/1451888.

[53] ATLAS Collaboration, Performance of the ATLAS trigger system in 2015, Eur. Phys. J. C **77**, 317 (2017).

[54] S. Agostinelli *et al.*, GEANT4: A simulation toolkit, Nucl. Instrum. Methods Phys. Res., Sect. A **506**, 250 (2003).

[55] ATLAS Collaboration, The ATLAS simulation infrastructure, Eur. Phys. J. C **70**, 823 (2010).

[56] T. Sjöstrand, S. Ask, J. R. Christiansen, R. Corke, N. Desai, P. Ilten, S. Mrenna, S. Prestel, C. O. Rasmussen, and P. Z. Skands, An introduction to PYTHIA 8.2, Comput. Phys. Commun. **191**, 159 (2015).

[57] ATLAS Collaboration, Further ATLAS tunes of Pythia 6 and Pythia 8, CERN Report No. ATL-PHYS-PUB-2011-014, 2011, https://cds.cern.ch/record/1400677.

[58] A. Sherstnev and R. S. Thorne, Parton distributions for LO generators, Eur. Phys. J. C **55**, 553 (2008).

[59] J. Alwall, R. Frederix, S. Frixione, V. Hirschi, F. Maltoni, O. Mattelaer, H.-S. Shao, T. Stelzer, P. Torrielli, and M. Zaro, The automated computation of tree-level and next-to-leading order differential cross sections, and their matching to parton shower simulations, J. High Energy Phys. 07 (2014) 079.

[60] A. D. Martin, W. J. Stirling, R. S. Thorne, and G. Watt, Parton distributions for the LHC, Eur. Phys. J. C **63**, 189 (2009).

[61] D. J. Lange, The EvtGen particle decay simulation package, Nucl. Instrum. Methods Phys. Res., Sect. A **462**, 152 (2001).

[62] P. Meade, M. Reece, and D. Shih, Long-lived neutralino NLSPs, J. High Energy Phys. 10 (2010) 067.

[63] W. Beenakker, R. Hopker, M. Spira, and P. M. Zerwas, Squark and gluino production at hadron colliders, Nucl. Phys. **B492**, 51 (1997).

[64] A. Kulesza and L. Motyka, Threshold Resummation for Squark-Antisquark and Gluino-Pair Production at the LHC, Phys. Rev. Lett. **102**, 111802 (2009).

[65] A. Kulesza and L. Motyka, Soft gluon resummation for the production of gluino-gluino and squark-antisquark pairs at the LHC, Phys. Rev. D **80**, 095004 (2009).

[66] W. Beenakker, S. Brensing, M. Krämer, A. Kulesza, E. Laenen, and I. Niessen, Soft-gluon resummation for squark and gluino hadroproduction, J. High Energy Phys. 12 (2009) 041.

[67] W. Beenakker, S. Brensing, M. Krämer, A. Kulesza, E. Laenen, L. Motyka, and I. Niessen, Squark and Gluino hadroproduction, Int. J. Mod. Phys. A **26**, 2637 (2011).

[68] C. Borschensky, M. Krämer, A. Kulesza, M. Mangano, S. Padhi, T. Plehn, and X. Portell, Squark and gluino production cross sections in pp collisions at $\sqrt{s} = 13$, 14, 33 and 100 TeV, Eur. Phys. J. C **74**, 3174 (2014).

[69] D. Curtin, R. Essig, S. Gori, and J. Shelton, Illuminating dark photons with high-energy colliders, J. High Energy Phys. 02 (2015) 157.

[70] ATLAS Collaboration, Constraints on new phenomena via Higgs boson couplings and invisible decays with the ATLAS detector, J. High Energy Phys. 11 (2015) 206.

[71] CMS Collaboration, Searches for invisible decays of the Higgs boson in pp collisions at $\sqrt{s} = 7$, 8, and 13 TeV, J. High Energy Phys. 02 (2017) 135.

[72] D. de Florian *et al.*, Handbook of LHC Higgs cross sections: 4. Deciphering the nature of the Higgs sector, arXiv:1610.07922, DOI: 10.23731/CYRM-2017-002.

[73] ATLAS Collaboration, Simulation of top-quark production for the ATLAS experiment at $\sqrt{s} = 13$ TeV, CERN Report No. ATL-PHYS-PUB-2016-004, 2016, https://cds.cern.ch/record/2120417.

[74] ATLAS Collaboration, ATLAS simulation of boson plus jets processes in Run 2, CERN Report No. ATL-PHYS-PUB-2017-006, 2017, https://cds.cern.ch/record/2261937.

[75] ATLAS Collaboration, Multi-boson simulation for 13 TeV ATLAS analyses, CERN Report No. ATL-PHYS-PUB-2016-002, 2016, https://cds.cern.ch/record/2119986.

[76] ATLAS Collaboration, Studies on top-quark Monte Carlo modelling with Sherpa and MG5_aMC@NLO, CERN Report No. ATL-PHYS-PUB-2017-007, 2017, https://cds.cern.ch/record/2261938.

[77] ATLAS Collaboration, Multi-boson simulation for 13 TeV ATLAS analyses, CERN Report No. ATL-PHYS-PUB-2017-005, 2017, https://cds.cern.ch/record/2261933.

[78] S. Alioli, P. Nason, C. Oleari, and E. Re, A general framework for implementing NLO calculations in shower Monte Carlo programs: the POWHEG BOX, J. High Energy Phys. 06 (2010) 043.

[79] S. Alioli, P. Nason, C. Oleari, and E. Re, NLO vector-boson production matched with shower in POWHEG, J. High Energy Phys. 07 (2008) 060.

[80] H.-L. Lai, M. Guzzi, J. Huston, Z. Li, P. M. Nadolsky, J. Pumplin, and C.-P. Yuan, New parton distributions for collider physics, Phys. Rev. D **82**, 074024 (2010).

[81] ATLAS Collaboration, Measurement of the Z/γ^* boson transverse momentum distribution in pp collisions at $\sqrt{s} =$ 7 TeV with the ATLAS detector, J. High Energy Phys. 09 (2014) 145.

[82] T. Sjostrand, P. Edén, C. Friberg, L. Lönnblad, G. Miu, S. Mrenna, and E. Norrbin, High-energy physics event generation with PYTHIA 6.1, Comput. Phys. Commun. **135**, 238 (2001).

[83] P. Z. Skands, Tuning Monte Carlo generators: The Perugia tunes, Phys. Rev. D **82**, 074018 (2010).

[84] P. Nason and G. Zanderighi, W^+W^-, WZ and ZZ production in the POWHEG-BOX-V2, Eur. Phys. J. C **74**, 2702 (2014).

[85] S. Alioli, P. Nason, C. Oleari, and E. Re, NLO single-top production matched with shower in POWHEG: s- and t-channel contributions, J. High Energy Phys. 09 (2009) 111; Erratum 02 (2010) 011.

[86] R. Frederix, E. Re, and P. Torrielli, Single-top t-channel hadroproduction in the four-flavour scheme with POWHEG and aMC@NLO, J. High Energy Phys. 09 (2012) 130.
[87] ATLAS Collaboration, Topological cell clustering in the ATLAS calorimeters and its performance in LHC Run 1, Eur. Phys. J. C **77**, 490 (2017).
[88] M. Cacciari, G. P. Salam, and G. Soyez, The anti-kt jet clustering algorithm, J. High Energy Phys. 04 (2008) 063.
[89] ATLAS Collaboration, Jet energy scale measurements and their systematic uncertainties in proton-proton collisions at $\sqrt{s} = 13$ TeV with the ATLAS detector, Phys. Rev. D **96**, 072002 (2017).
[90] ATLAS Collaboration, Selection of jets produced in 13 TeV proton-proton collisions with the ATLAS detector, CERN Report No. ATLAS-CONF-2015-029 (2015), https://cds.cern.ch/record/2037702.
[91] ATLAS Collaboration, Characterisation and mitigation of beam-induced backgrounds observed in the ATLAS detector during the 2011 proton-proton run, J. Instrum. **8**, P07004 (2013).
[92] ATLAS Collaboration, Performance of pile-up mitigation techniques for jets in pp collisions at $\sqrt{s} = 8$ TeV using the ATLAS detector, Eur. Phys. J. C **76**, 581 (2016).
[93] ATLAS Collaboration, Muon reconstruction performance of the ATLAS detector in proton-proton collision data at $\sqrt{s} = 13$ TeV, Eur. Phys. J. C **76**, 292 (2016).
[94] ATLAS Collaboration, Luminosity determination in pp collisions at $\sqrt{s} = 8$ TeV using the ATLAS detector at the LHC, Eur. Phys. J. C **76**, 653 (2016).
[95] G. Avoni *et al.*, The new LUCID-2 detector for luminosity measurement and monitoring in ATLAS, J. Instrum. **13**, P07017 (2018).
[96] A. L. Read, Presentation of search results: The CLs technique, J. Phys. G **28**, 2693 (2002).
[97] ATLAS Collaboration, ATLAS computing acknowledgements, CERN Report No. ATL-GEN-PUB-2016-002, https://cds.cern.ch/record/2202407.

Correction: The previously published rendition of Figure 9 contained an error and has been replaced.

M. Aaboud,[34d] G. Aad,[99] B. Abbott,[124] O. Abdinov,[13,a] B. Abeloos,[128] D. K. Abhayasinghe,[91] S. H. Abidi,[164] O. S. AbouZeid,[143] N. L. Abraham,[153] H. Abramowicz,[158] H. Abreu,[157] Y. Abulaiti,[6] B. S. Acharya,[64a,64b,b] S. Adachi,[160] L. Adamczyk,[81a] J. Adelman,[119] M. Adersberger,[112] A. Adiguzel,[12c,c] T. Adye,[141] A. A. Affolder,[143] Y. Afik,[157] C. Agheorghiesei,[27c] J. A. Aguilar-Saavedra,[136f,136a] F. Ahmadov,[77,d] G. Aielli,[71a,71b] S. Akatsuka,[83] T. P. A. Åkesson,[94] E. Akilli,[52] A. V. Akimov,[108] G. L. Alberghi,[23b,23a] J. Albert,[173] P. Albicocco,[49] M. J. Alconada Verzini,[86] S. Alderweireldt,[117] M. Aleksa,[35] I. N. Aleksandrov,[77] C. Alexa,[27b] T. Alexopoulos,[10] M. Alhroob,[124] B. Ali,[138] G. Alimonti,[66a] J. Alison,[36] S. P. Alkire,[145] C. Allaire,[128] B. M. M. Allbrooke,[153] B. W. Allen,[127] P. P. Allport,[21] A. Aloisio,[67a,67b] A. Alonso,[39] F. Alonso,[86] C. Alpigiani,[145] A. A. Alshehri,[55] M. I. Alstaty,[99] B. Alvarez Gonzalez,[35] D. Álvarez Piqueras,[171] M. G. Alviggi,[67a,67b] B. T. Amadio,[18] Y. Amaral Coutinho,[78b] L. Ambroz,[131] C. Amelung,[26] D. Amidei,[103] S. P. Amor Dos Santos,[136a,136c] S. Amoroso,[35] C. S. Amrouche,[52] C. Anastopoulos,[146] L. S. Ancu,[52] N. Andari,[21] T. Andeen,[11] C. F. Anders,[59b] J. K. Anders,[20] K. J. Anderson,[36] A. Andreazza,[66a,66b] V. Andrei,[59a] C. R. Anelli,[173] S. Angelidakis,[37] I. Angelozzi,[118] A. Angerami,[38] A. V. Anisenkov,[120b,120a] A. Annovi,[69a] C. Antel,[59a] M. T. Anthony,[146] M. Antonelli,[49] D. J. A. Antrim,[168] F. Anulli,[70a] M. Aoki,[79] L. Aperio Bella,[35] G. Arabidze,[104] Y. Arai,[79] J. P. Araque,[136a] V. Araujo Ferraz,[78b] R. Araujo Pereira,[78b] A. T. H. Arce,[47] R. E. Ardell,[91] F. A. Arduh,[86] J-F. Arguin,[107] S. Argyropoulos,[75] A. J. Armbruster,[35] L. J. Armitage,[90] A Armstrong,[168] O. Arnaez,[164] H. Arnold,[118] M. Arratia,[31] O. Arslan,[24] A. Artamonov,[109,a] G. Artoni,[131] S. Artz,[97] S. Asai,[160] N. Asbah,[44] A. Ashkenazi,[158] E. M. Asimakopoulou,[169] L. Asquith,[153] K. Assamagan,[29] R. Astalos,[28a] R. J. Atkin,[32a] M. Atkinson,[170] N. B. Atlay,[148] K. Augsten,[138] G. Avolio,[35] R. Avramidou,[58a] B. Axen,[18] M. K. Ayoub,[15a] G. Azuelos,[107,e] A. E. Baas,[59a] M. J. Baca,[21] H. Bachacou,[142] K. Bachas,[65a,65b] M. Backes,[131] P. Bagnaia,[70a,70b] M. Bahmani,[82] H. Bahrasemani,[149] A. J. Bailey,[171] J. T. Baines,[141] M. Bajic,[39] C. Bakalis,[10] O. K. Baker,[180] P. J. Bakker,[118] D. Bakshi Gupta,[93] E. M. Baldin,[120b,120a] P. Balek,[177] F. Balli,[142] W. K. Balunas,[133] J. Balz,[97] E. Banas,[82] A. Bandyopadhyay,[24] S. Banerjee,[178,f] A. A. E. Bannoura,[179] L. Barak,[158] W. M. Barbe,[37] E. L. Barberio,[102] D. Barberis,[53b,53a] M. Barbero,[99] T. Barillari,[113] M-S. Barisits,[35] J. Barkeloo,[127] T. Barklow,[150] N. Barlow,[31] R. Barnea,[157] S. L. Barnes,[58c] B. M. Barnett,[141] R. M. Barnett,[18] Z. Barnovska-Blenessy,[58a] A. Baroncelli,[72a] G. Barone,[26] A. J. Barr,[131] L. Barranco Navarro,[171] F. Barreiro,[96] J. Barreiro Guimarães da Costa,[15a] R. Bartoldus,[150] A. E. Barton,[87] P. Bartos,[28a] A. Basalaev,[134] A. Bassalat,[128] R. L. Bates,[55] S. J. Batista,[164] S. Batlamous,[34e] J. R. Batley,[31] M. Battaglia,[143] M. Bauce,[70a,70b] F. Bauer,[142] K. T. Bauer,[168] H. S. Bawa,[150,g] J. B. Beacham,[122] M. D. Beattie,[87] T. Beau,[132] P. H. Beauchemin,[167] P. Bechtle,[24] H. C. Beck,[51] H. P. Beck,[20,h] K. Becker,[50] M. Becker,[97] C. Becot,[44] A. Beddall,[12d] A. J. Beddall,[12a] V. A. Bednyakov,[77] M. Bedognetti,[118] C. P. Bee,[152] T. A. Beermann,[35] M. Begalli,[78b] M. Begel,[29] A. Behera,[152] J. K. Behr,[44] A. S. Bell,[92] G. Bella,[158] L. Bellagamba,[23b] A. Bellerive,[33] M. Bellomo,[157] P. Bellos,[9] K. Belotskiy,[110] N. L. Belyaev,[110] O. Benary,[158,a]

D. Benchekroun,[34a] M. Bender,[112] N. Benekos,[10] Y. Benhammou,[158] E. Benhar Noccioli,[180] J. Benitez,[75] D. P. Benjamin,[47] M. Benoit,[52] J. R. Bensinger,[26] S. Bentvelsen,[118] L. Beresford,[131] M. Beretta,[49] D. Berge,[44] E. Bergeaas Kuutmann,[169] N. Berger,[5] L. J. Bergsten,[26] J. Beringer,[18] S. Berlendis,[7] N. R. Bernard,[100] G. Bernardi,[132] C. Bernius,[150] F. U. Bernlochner,[24] T. Berry,[91] P. Berta,[97] C. Bertella,[15a] G. Bertoli,[43a,43b] I. A. Bertram,[87] G. J. Besjes,[39] O. Bessidskaia Bylund,[43a,43b] M. Bessner,[44] N. Besson,[142] A. Bethani,[98] S. Bethke,[113] A. Betti,[24] A. J. Bevan,[90] J. Beyer,[113] R. M. Bianchi,[135] O. Biebel,[112] D. Biedermann,[19] R. Bielski,[98] K. Bierwagen,[97] N. V. Biesuz,[69a,69b] M. Biglietti,[72a] T. R. V. Billoud,[107] M. Bindi,[51] A. Bingul,[12d] C. Bini,[70a,70b] S. Biondi,[23b,23a] T. Bisanz,[51] J. P. Biswal,[158] C. Bittrich,[46] D. M. Bjergaard,[47] J. E. Black,[150] K. M. Black,[25] R. E. Blair,[6] T. Blazek,[28a] I. Bloch,[44] C. Blocker,[26] A. Blue,[55] U. Blumenschein,[90] Dr. Blunier,[144a] G. J. Bobbink,[118] V. S. Bobrovnikov,[120b,120a] S. S. Bocchetta,[94] A. Bocci,[47] D. Boerner,[179] D. Bogavac,[112] A. G. Bogdanchikov,[120b,120a] C. Bohm,[43a] V. Boisvert,[91] P. Bokan,[169,i] T. Bold,[81a] A. S. Boldyrev,[111] A. E. Bolz,[59b] M. Bomben,[132] M. Bona,[90] J. S. Bonilla,[127] M. Boonekamp,[142] A. Borisov,[140] G. Borissov,[87] J. Bortfeldt,[35] D. Bortoletto,[131] V. Bortolotto,[71a,61b,61c,71b] D. Boscherini,[23b] M. Bosman,[14] J. D. Bossio Sola,[30] K. Bouaouda,[34a] J. Boudreau,[135] E. V. Bouhova-Thacker,[87] D. Boumediene,[37] C. Bourdarios,[128] S. K. Boutle,[55] A. Boveia,[122] J. Boyd,[35] I. R. Boyko,[77] A. J. Bozson,[91] J. Bracinik,[21] N. Brahimi,[99] A. Brandt,[8] G. Brandt,[179] O. Brandt,[59a] F. Braren,[44] U. Bratzler,[161] B. Brau,[100] J. E. Brau,[127] W. D. Breaden Madden,[55] K. Brendlinger,[44] A. J. Brennan,[102] L. Brenner,[44] R. Brenner,[169] S. Bressler,[177] B. Brickwedde,[97] D. L. Briglin,[21] D. Britton,[55] D. Britzger,[59b] I. Brock,[24] R. Brock,[104] G. Brooijmans,[38] T. Brooks,[91] W. K. Brooks,[144b] E. Brost,[119] J. H. Broughton,[21] P. A. Bruckman de Renstrom,[82] D. Bruncko,[28b] A. Bruni,[23b] G. Bruni,[23b] L. S. Bruni,[118] S. Bruno,[71a,71b] B. H. Brunt,[31] M. Bruschi,[23b] N. Bruscino,[135] P. Bryant,[36] L. Bryngemark,[44] T. Buanes,[17] Q. Buat,[35] P. Buchholz,[148] A. G. Buckley,[55] I. A. Budagov,[77] F. Buehrer,[50] M. K. Bugge,[130] O. Bulekov,[110] D. Bullock,[8] T. J. Burch,[119] S. Burdin,[88] C. D. Burgard,[118] A. M. Burger,[5] B. Burghgrave,[119] K. Burka,[82] S. Burke,[141] I. Burmeister,[45] J. T. P. Burr,[131] D. Büscher,[50] V. Büscher,[97] E. Buschmann,[51] P. Bussey,[55] J. M. Butler,[25] C. M. Buttar,[55] J. M. Butterworth,[92] P. Butti,[35] W. Buttinger,[35] A. Buzatu,[155] A. R. Buzykaev,[120b,120a] G. Cabras,[23b,23a] S. Cabrera Urbán,[171] D. Caforio,[138] H. Cai,[170] V. M. M. Cairo,[2] O. Cakir,[4a] N. Calace,[52] P. Calafiura,[18] A. Calandri,[99] G. Calderini,[132] P. Calfayan,[63] G. Callea,[40b,40a] L. P. Caloba,[78b] S. Calvente Lopez,[96] D. Calvet,[37] S. Calvet,[37] T. P. Calvet,[152] M. Calvetti,[69a,69b] R. Camacho Toro,[132] S. Camarda,[35] P. Camarri,[71a,71b] D. Cameron,[130] R. Caminal Armadans,[100] C. Camincher,[35] S. Campana,[35] M. Campanelli,[92] A. Camplani,[39] A. Campoverde,[148] V. Canale,[67a,67b] M. Cano Bret,[58c] J. Cantero,[125] T. Cao,[158] Y. Cao,[170] M. D. M. Capeans Garrido,[35] I. Caprini,[27b] M. Caprini,[27b] M. Capua,[40b,40a] R. M. Carbone,[38] R. Cardarelli,[71a] F. C. Cardillo,[50] I. Carli,[139] T. Carli,[35] G. Carlino,[67a] B. T. Carlson,[135] L. Carminati,[66a,66b] R. M. D. Carney,[43a,43b] S. Caron,[117] E. Carquin,[144b] S. Carrá,[66a,66b] G. D. Carrillo-Montoya,[35] D. Casadei,[32b] M. P. Casado,[14,j] A. F. Casha,[164] M. Casolino,[14] D. W. Casper,[168] R. Castelijn,[118] F. L. Castillo,[171] V. Castillo Gimenez,[171] N. F. Castro,[136a,136e] A. Catinaccio,[35] J. R. Catmore,[130] A. Cattai,[35] J. Caudron,[24] V. Cavaliere,[29] E. Cavallaro,[14] D. Cavalli,[66a] M. Cavalli-Sforza,[14] V. Cavasinni,[69a,69b] E. Celebi,[12b] F. Ceradini,[72a,72b] L. Cerda Alberich,[171] A. S. Cerqueira,[78a] A. Cerri,[153] L. Cerrito,[71a,71b] F. Cerutti,[18] A. Cervelli,[23b,23a] S. A. Cetin,[12b] A. Chafaq,[34a] D Chakraborty,[119] S. K. Chan,[57] W. S. Chan,[118] Y. L. Chan,[61a] P. Chang,[170] J. D. Chapman,[31] D. G. Charlton,[21] C. C. Chau,[33] C. A. Chavez Barajas,[153] S. Che,[122] A. Chegwidden,[104] S. Chekanov,[6] S. V. Chekulaev,[165a] G. A. Chelkov,[77,k] M. A. Chelstowska,[35] C. Chen,[58a] C. H. Chen,[76] H. Chen,[29] J. Chen,[58a] J. Chen,[38] S. Chen,[133] S. J. Chen,[15c] X. Chen,[15b,l] Y. Chen,[80] Y-H. Chen,[44] H. C. Cheng,[103] H. J. Cheng,[15d] A. Cheplakov,[77] E. Cheremushkina,[140] R. Cherkaoui El Moursli,[34e] E. Cheu,[7] K. Cheung,[62] L. Chevalier,[142] V. Chiarella,[49] G. Chiarelli,[69a] G. Chiodini,[65a] A. S. Chisholm,[35] A. Chitan,[27b] I. Chiu,[160] Y. H. Chiu,[173] M. V. Chizhov,[77] K. Choi,[63] A. R. Chomont,[128] S. Chouridou,[159] Y. S. Chow,[118] V. Christodoulou,[92] M. C. Chu,[61a] J. Chudoba,[137] A. J. Chuinard,[101] J. J. Chwastowski,[82] L. Chytka,[126] D. Cinca,[45] V. Cindro,[89] I. A. Cioară,[24] A. Ciocio,[18] F. Cirotto,[67a,67b] Z. H. Citron,[177] M. Citterio,[66a] A. Clark,[52] M. R. Clark,[38] P. J. Clark,[48] C. Clement,[43a,43b] Y. Coadou,[99] M. Cobal,[64a,64c] A. Coccaro,[53b,53a] J. Cochran,[76] A. E. C. Coimbra,[177] L. Colasurdo,[117] B. Cole,[38] A. P. Colijn,[118] J. Collot,[56] P. Conde Muiño,[136a,136b] E. Coniavitis,[50] S. H. Connell,[32b] I. A. Connelly,[98] S. Constantinescu,[27b] F. Conventi,[67a,m] A. M. Cooper-Sarkar,[131] F. Cormier,[172] K. J. R. Cormier,[164] M. Corradi,[70a,70b] E. E. Corrigan,[94] F. Corriveau,[101,n] A. Cortes-Gonzalez,[35] M. J. Costa,[171] D. Costanzo,[146] G. Cottin,[31] G. Cowan,[91] B. E. Cox,[98] J. Crane,[98] K. Cranmer,[121] S. J. Crawley,[55] R. A. Creager,[133] G. Cree,[33] S. Crépé-Renaudin,[56] F. Crescioli,[132] M. Cristinziani,[24] V. Croft,[121] G. Crosetti,[40b,40a] A. Cueto,[96] T. Cuhadar Donszelmann,[146] A. R. Cukierman,[150] M. Curatolo,[49] J. Cúth,[97] S. Czekierda,[82] P. Czodrowski,[35] M. J. Da Cunha Sargedas De Sousa,[58b,136b] C. Da Via,[98] W. Dabrowski,[81a] T. Dado,[28a,i] S. Dahbi,[34e] T. Dai,[103] F. Dallaire,[107] C. Dallapiccola,[100] M. Dam,[39]

G. D'amen,[23b,23a] J. Damp,[97] J. R. Dandoy,[133] M. F. Daneri,[30] N. P. Dang,[178,f] N.D Dann,[98] M. Danninger,[172] V. Dao,[35] G. Darbo,[53b] S. Darmora,[8] O. Dartsi,[5] A. Dattagupta,[127] T. Daubney,[44] S. D'Auria,[55] W. Davey,[24] C. David,[44] T. Davidek,[139] D. R. Davis,[47] E. Dawe,[102] I. Dawson,[146] K. De,[8] R. De Asmundis,[67a] A. De Benedetti,[124] S. De Castro,[23b,23a] S. De Cecco,[70a,70b] N. De Groot,[117] P. de Jong,[118] H. De la Torre,[104] F. De Lorenzi,[76] A. De Maria,[51,o] D. De Pedis,[70a] A. De Salvo,[70a] U. De Sanctis,[71a,71b] A. De Santo,[153] K. De Vasconcelos Corga,[99] J. B. De Vivie De Regie,[128] C. Debenedetti,[143] D. V. Dedovich,[77] N. Dehghanian,[3] M. Del Gaudio,[40b,40a] J. Del Peso,[96] D. Delgove,[128] F. Deliot,[142] C. M. Delitzsch,[7] M. Della Pietra,[67a,67b] D. Della Volpe,[52] A. Dell'Acqua,[35] L. Dell'Asta,[25] M. Delmastro,[5] C. Delporte,[128] P. A. Delsart,[56] D. A. DeMarco,[164] S. Demers,[180] M. Demichev,[77] S. P. Denisov,[140] D. Denysiuk,[118] L. D'Eramo,[132] D. Derendarz,[82] J. E. Derkaoui,[34d] F. Derue,[132] P. Dervan,[88] K. Desch,[24] C. Deterre,[44] K. Dette,[164] M. R. Devesa,[30] P. O. Deviveiros,[35] A. Dewhurst,[141] S. Dhaliwal,[26] F. A. Di Bello,[52] A. Di Ciaccio,[71a,71b] L. Di Ciaccio,[5] W. K. Di Clemente,[133] C. Di Donato,[67a,67b] A. Di Girolamo,[35] B. Di Micco,[72a,72b] R. Di Nardo,[35] K. F. Di Petrillo,[57] A. Di Simone,[50] R. Di Sipio,[164] D. Di Valentino,[33] C. Diaconu,[99] M. Diamond,[164] F. A. Dias,[39] T. Dias Do Vale,[136a] M. A. Diaz,[144a] J. Dickinson,[18] E. B. Diehl,[103] J. Dietrich,[19] S. Díez Cornell,[44] A. Dimitrievska,[18] J. Dingfelder,[24] F. Dittus,[35] F. Djama,[99] T. Djobava,[156b] J. I. Djuvsland,[59a] M. A. B. Do Vale,[78c] M. Dobre,[27b] D. Dodsworth,[26] C. Doglioni,[94] J. Dolejsi,[139] Z. Dolezal,[139] M. Donadelli,[78d] J. Donini,[37] A. D'onofrio,[90] M. D'Onofrio,[88] J. Dopke,[141] A. Doria,[67a] M. T. Dova,[86] A. T. Doyle,[55] E. Drechsler,[51] E. Dreyer,[149] T. Dreyer,[51] M. Dris,[10] Y. Du,[58b] J. Duarte-Campderros,[158] F. Dubinin,[108] M. Dubovsky,[28a] A. Dubreuil,[52] E. Duchovni,[177] G. Duckeck,[112] A. Ducourthial,[132] O. A. Ducu,[107,p] D. Duda,[113] A. Dudarev,[35] A. C. Dudder,[97] E. M. Duffield,[18] L. Duflot,[128] M. Dührssen,[35] C. Dülsen,[179] M. Dumancic,[177] A. E. Dumitriu,[27b,q] A. K. Duncan,[55] M. Dunford,[59a] A. Duperrin,[99] H. Duran Yildiz,[4a] M. Düren,[54] A. Durglishvili,[156b] D. Duschinger,[46] B. Dutta,[44] D. Duvnjak,[1] M. Dyndal,[44] S. Dysch,[98] B. S. Dziedzic,[82] C. Eckardt,[44] K. M. Ecker,[113] R. C. Edgar,[103] T. Eifert,[35] G. Eigen,[17] K. Einsweiler,[18] T. Ekelof,[169] M. El Kacimi,[34c] R. El Kosseifi,[99] V. Ellajosyula,[99] M. Ellert,[169] F. Ellinghaus,[179] A. A. Elliot,[90] N. Ellis,[35] J. Elmsheuser,[29] M. Elsing,[35] D. Emeliyanov,[141] Y. Enari,[160] J. S. Ennis,[175] M. B. Epland,[47] J. Erdmann,[45] A. Ereditato,[20] S. Errede,[170] M. Escalier,[128] C. Escobar,[171] B. Esposito,[49] O. Estrada Pastor,[171] A. I. Etienvre,[142] E. Etzion,[158] H. Evans,[63] A. Ezhilov,[134] M. Ezzi,[34e] F. Fabbri,[55] L. Fabbri,[23b,23a] V. Fabiani,[117] G. Facini,[92] R. M. Faisca Rodrigues Pereira,[136a] R. M. Fakhrutdinov,[140] S. Falciano,[70a] P. J. Falke,[5] S. Falke,[5] J. Faltova,[139] Y. Fang,[15a] M. Fanti,[66a,66b] A. Farbin,[8] A. Farilla,[72a] E. M. Farina,[68a,68b] T. Farooque,[104] S. Farrell,[18] S. M. Farrington,[175] P. Farthouat,[35] F. Fassi,[34e] P. Fassnacht,[35] D. Fassouliotis,[9] M. Faucci Giannelli,[48] A. Favareto,[53b,53a] W. J. Fawcett,[52] L. Fayard,[128] O. L. Fedin,[134,r] W. Fedorko,[172] M. Feickert,[41] S. Feigl,[130] L. Feligioni,[99] C. Feng,[58b] E. J. Feng,[35] M. Feng,[47] M. J. Fenton,[55] A. B. Fenyuk,[140] L. Feremenga,[8] J. Ferrando,[44] A. Ferrari,[169] P. Ferrari,[118] R. Ferrari,[68a] D. E. Ferreira de Lima,[59b] A. Ferrer,[171] D. Ferrere,[52] C. Ferretti,[103] F. Fiedler,[97] A. Filipčič,[89] F. Filthaut,[117] K. D. Finelli,[25] M. C. N. Fiolhais,[136a,136c,s] L. Fiorini,[171] C. Fischer,[14] W. C. Fisher,[104] N. Flaschel,[44] I. Fleck,[148] P. Fleischmann,[103] R. R. M. Fletcher,[133] T. Flick,[179] B. M. Flierl,[112] L. M. Flores,[133] L. R. Flores Castillo,[61a] N. Fomin,[17] G. T. Forcolin,[98] A. Formica,[142] F. A. Förster,[14] A. C. Forti,[98] A. G. Foster,[21] D. Fournier,[128] H. Fox,[87] S. Fracchia,[146] P. Francavilla,[69a,69b] M. Franchini,[23b,23a] S. Franchino,[59a] D. Francis,[35] L. Franconi,[130] M. Franklin,[57] M. Frate,[168] M. Fraternali,[68a,68b] D. Freeborn,[92] S. M. Fressard-Batraneanu,[35] B. Freund,[107] W. S. Freund,[78b] D. Froidevaux,[35] J. A. Frost,[131] C. Fukunaga,[161] T. Fusayasu,[114] J. Fuster,[171] O. Gabizon,[157] A. Gabrielli,[23b,23a] A. Gabrielli,[18] G. P. Gach,[81a] S. Gadatsch,[52] P. Gadow,[113] G. Gagliardi,[53b,53a] L. G. Gagnon,[107] C. Galea,[27b] B. Galhardo,[136a,136c] E. J. Gallas,[131] B. J. Gallop,[141] P. Gallus,[138] G. Galster,[39] R. Gamboa Goni,[90] K. K. Gan,[122] S. Ganguly,[177] Y. Gao,[88] Y. S. Gao,[150,g] C. García,[171] J. E. García Navarro,[171] J. A. García Pascual,[15a] M. Garcia-Sciveres,[18] R. W. Gardner,[36] N. Garelli,[150] V. Garonne,[130] K. Gasnikova,[44] A. Gaudiello,[53b,53a] G. Gaudio,[68a] I. L. Gavrilenko,[108] A. Gavrilyuk,[109] C. Gay,[172] G. Gaycken,[24] E. N. Gazis,[10] C. N. P. Gee,[141] J. Geisen,[51] M. Geisen,[97] M. P. Geisler,[59a] K. Gellerstedt,[43a,43b] C. Gemme,[53b] M. H. Genest,[56] C. Geng,[103] S. Gentile,[70a,70b] C. Gentsos,[159] S. George,[91] D. Gerbaudo,[14] G. Gessner,[45] S. Ghasemi,[148] M. Ghasemi Bostanabad,[173] M. Ghneimat,[24] B. Giacobbe,[23b] S. Giagu,[70a,70b] N. Giangiacomi,[23b,23a] P. Giannetti,[69a] S. M. Gibson,[91] M. Gignac,[143] D. Gillberg,[33] G. Gilles,[179] D. M. Gingrich,[3,e] M. P. Giordani,[64a,64c] F. M. Giorgi,[23b] P. F. Giraud,[142] P. Giromini,[57] G. Giugliarelli,[64a,64c] D. Giugni,[66a] F. Giuli,[131] M. Giulini,[59b] S. Gkaitatzis,[159] I. Gkialas,[9,t] E. L. Gkougkousis,[14] P. Gkountoumis,[10] L. K. Gladilin,[111] C. Glasman,[96] J. Glatzer,[14] P. C. F. Glaysher,[44] A. Glazov,[44] M. Goblirsch-Kolb,[26] J. Godlewski,[82] S. Goldfarb,[102] T. Golling,[52] D. Golubkov,[140] A. Gomes,[136a,136b,136d] R. Goncalves Gama,[78a] R. Gonçalo,[136a] G. Gonella,[50] L. Gonella,[21] A. Gongadze,[77] F. Gonnella,[21] J. L. Gonski,[57] S. González de la Hoz,[171] S. Gonzalez-Sevilla,[52] L. Goossens,[35] P. A. Gorbounov,[109] H. A. Gordon,[29] B. Gorini,[35]

E. Gorini,[65a,65b] A. Gorišek,[89] A. T. Goshaw,[47] C. Gössling,[45] M. I. Gostkin,[77] C. A. Gottardo,[24] C. R. Goudet,[128] D. Goujdami,[34c] A. G. Goussiou,[145] N. Govender,[32b,u] C. Goy,[5] E. Gozani,[157] I. Grabowska-Bold,[81a] P. O. J. Gradin,[169] E. C. Graham,[88] J. Gramling,[168] E. Gramstad,[130] S. Grancagnolo,[19] V. Gratchev,[134] P. M. Gravila,[27f] C. Gray,[55] H. M. Gray,[18] Z. D. Greenwood,[93,v] C. Grefe,[24] K. Gregersen,[92] I. M. Gregor,[44] P. Grenier,[150] K. Grevtsov,[44] J. Griffiths,[8] A. A. Grillo,[143] K. Grimm,[150] S. Grinstein,[14,w] Ph. Gris,[37] J.-F. Grivaz,[128] S. Groh,[97] E. Gross,[177] J. Grosse-Knetter,[51] G. C. Grossi,[93] Z. J. Grout,[92] C. Grud,[103] A. Grummer,[116] L. Guan,[103] W. Guan,[178] J. Guenther,[35] A. Guerguichon,[128] F. Guescini,[165a] D. Guest,[168] R. Gugel,[50] B. Gui,[122] T. Guillemin,[5] S. Guindon,[35] U. Gul,[55] C. Gumpert,[35] J. Guo,[58c] W. Guo,[103] Y. Guo,[58a,x] Z. Guo,[99] R. Gupta,[41] S. Gurbuz,[12c] G. Gustavino,[124] B. J. Gutelman,[157] P. Gutierrez,[124] C. Gutschow,[92] C. Guyot,[142] M. P. Guzik,[81a] C. Gwenlan,[131] C. B. Gwilliam,[88] A. Haas,[121] C. Haber,[18] H. K. Hadavand,[8] N. Haddad,[34e] A. Hadef,[58a] S. Hageböck,[24] M. Hagihara,[166] H. Hakobyan,[181,a] M. Haleem,[174] J. Haley,[125] G. Halladjian,[104] G. D. Hallewell,[99] K. Hamacher,[179] P. Hamal,[126] K. Hamano,[173] A. Hamilton,[32a] G. N. Hamity,[146] K. Han,[58a,y] L. Han,[58a] S. Han,[15d] K. Hanagaki,[79,z] M. Hance,[143] D. M. Handl,[112] B. Haney,[133] R. Hankache,[132] P. Hanke,[59a] E. Hansen,[94] J. B. Hansen,[39] J. D. Hansen,[39] M. C. Hansen,[24] P. H. Hansen,[39] K. Hara,[166] A. S. Hard,[178] T. Harenberg,[179] S. Harkusha,[105] P. F. Harrison,[175] N. M. Hartmann,[112] Y. Hasegawa,[147] A. Hasib,[48] S. Hassani,[142] S. Haug,[20] R. Hauser,[104] L. Hauswald,[46] L. B. Havener,[38] M. Havranek,[138] C. M. Hawkes,[21] R. J. Hawkings,[35] D. Hayden,[104] C. Hayes,[152] C. P. Hays,[131] J. M. Hays,[90] H. S. Hayward,[88] S. J. Haywood,[141] M. P. Heath,[48] V. Hedberg,[94] L. Heelan,[8] S. Heer,[24] K. K. Heidegger,[50] J. Heilman,[33] S. Heim,[44] T. Heim,[18] B. Heinemann,[44,aa] J. J. Heinrich,[112] L. Heinrich,[121] C. Heinz,[54] J. Hejbal,[137] L. Helary,[35] A. Held,[172] S. Hellesund,[130] S. Hellman,[43a,43b] C. Helsens,[35] R. C. W. Henderson,[87] Y. Heng,[178] S. Henkelmann,[172] A. M. Henriques Correia,[35] G. H. Herbert,[19] H. Herde,[26] V. Herget,[174] Y. Hernández Jiménez,[32c] H. Herr,[97] G. Herten,[50] R. Hertenberger,[112] L. Hervas,[35] T. C. Herwig,[133] G. G. Hesketh,[92] N. P. Hessey,[165a] J. W. Hetherly,[41] S. Higashino,[79] E. Higón-Rodriguez,[171] K. Hildebrand,[36] E. Hill,[173] J. C. Hill,[31] K. K. Hill,[29] K. H. Hiller,[44] S. J. Hillier,[21] M. Hils,[46] I. Hinchliffe,[18] M. Hirose,[129] D. Hirschbuehl,[179] B. Hiti,[89] O. Hladik,[137] D. R. Hlaluku,[32c] X. Hoad,[48] J. Hobbs,[152] N. Hod,[165a] M. C. Hodgkinson,[146] A. Hoecker,[35] M. R. Hoeferkamp,[116] F. Hoenig,[112] D. Hohn,[24] D. Hohov,[128] T. R. Holmes,[36] M. Holzbock,[112] M. Homann,[45] S. Honda,[166] T. Honda,[79] T. M. Hong,[135] A. Hönle,[113] B. H. Hooberman,[170] W. H. Hopkins,[127] Y. Horii,[115] P. Horn,[46] A. J. Horton,[149] L. A. Horyn,[36] J-Y. Hostachy,[56] A. Hostiuc,[145] S. Hou,[155] A. Hoummada,[34a] J. Howarth,[98] J. Hoya,[86] M. Hrabovsky,[126] J. Hrdinka,[35] I. Hristova,[19] J. Hrivnac,[128] A. Hrynevich,[106] T. Hryn'ova,[5] P. J. Hsu,[62] S.-C. Hsu,[145] Q. Hu,[29] S. Hu,[58c] Y. Huang,[15a] Z. Hubacek,[138] F. Hubaut,[99] M. Huebner,[24] F. Huegging,[24] T. B. Huffman,[131] E. W. Hughes,[38] M. Huhtinen,[35] R. F. H. Hunter,[33] P. Huo,[152] A. M. Hupe,[33] N. Huseynov,[77,d] J. Huston,[104] J. Huth,[57] R. Hyneman,[103] G. Iacobucci,[52] G. Iakovidis,[29] I. Ibragimov,[148] L. Iconomidou-Fayard,[128] Z. Idrissi,[34e] P. Iengo,[35] R. Ignazzi,[39] O. Igonkina,[118,bb] R. Iguchi,[160] T. Iizawa,[52] Y. Ikegami,[79] M. Ikeno,[79] D. Iliadis,[159] N. Ilic,[150] F. Iltzsche,[46] G. Introzzi,[68a,68b] M. Iodice,[72a] K. Iordanidou,[38] V. Ippolito,[70a,70b] M. F. Isacson,[169] N. Ishijima,[129] M. Ishino,[160] M. Ishitsuka,[162] W. Islam,[125] C. Issever,[131] S. Istin,[12c,cc] F. Ito,[166] J. M. Iturbe Ponce,[61a] R. Iuppa,[73a,73b] A. Ivina,[177] H. Iwasaki,[79] J. M. Izen,[42] V. Izzo,[67a] S. Jabbar,[3] P. Jacka,[137] P. Jackson,[1] R. M. Jacobs,[24] V. Jain,[2] G. Jäkel,[179] K. B. Jakobi,[97] K. Jakobs,[50] S. Jakobsen,[74] T. Jakoubek,[137] D. O. Jamin,[125] D. K. Jana,[93] R. Jansky,[52] J. Janssen,[24] M. Janus,[51] P. A. Janus,[81a] G. Jarlskog,[94] N. Javadov,[77,d] T. Javůrek,[50] M. Javurkova,[50] F. Jeanneau,[142] L. Jeanty,[18] J. Jejelava,[156a,dd] A. Jelinskas,[175] P. Jenni,[50,ee] J. Jeong,[44] C. Jeske,[175] S. Jézéquel,[5] H. Ji,[178] J. Jia,[152] H. Jiang,[76] Y. Jiang,[58a] Z. Jiang,[150,ff] S. Jiggins,[50] F. A. Jimenez Morales,[37] J. Jimenez Pena,[171] S. Jin,[15c] A. Jinaru,[27b] O. Jinnouchi,[162] H. Jivan,[32c] P. Johansson,[146] K. A. Johns,[7] C. A. Johnson,[63] W. J. Johnson,[145] K. Jon-And,[43a,43b] R. W. L. Jones,[87] S. D. Jones,[153] S. Jones,[7] T. J. Jones,[88] J. Jongmanns,[59a] P. M. Jorge,[136a,136b] J. Jovicevic,[165a] X. Ju,[178] J. J. Junggeburth,[113] A. Juste Rozas,[14,w] A. Kaczmarska,[82] M. Kado,[128] H. Kagan,[122] M. Kagan,[150] T. Kaji,[176] E. Kajomovitz,[157] C. W. Kalderon,[94] A. Kaluza,[97] S. Kama,[41] A. Kamenshchikov,[140] L. Kanjir,[89] Y. Kano,[160] V. A. Kantserov,[110] J. Kanzaki,[79] B. Kaplan,[121] L. S. Kaplan,[178] D. Kar,[32c] M. J. Kareem,[165b] E. Karentzos,[10] S. N. Karpov,[77] Z. M. Karpova,[77] V. Kartvelishvili,[87] A. N. Karyukhin,[140] K. Kasahara,[166] L. Kashif,[178] R. D. Kass,[122] A. Kastanas,[151] Y. Kataoka,[160] C. Kato,[160] J. Katzy,[44] K. Kawade,[80] K. Kawagoe,[85] T. Kawamoto,[160] G. Kawamura,[51] E. F. Kay,[88] V. F. Kazanin,[120b,120a] R. Keeler,[173] R. Kehoe,[41] J. S. Keller,[33] E. Kellermann,[94] J. J. Kempster,[21] J. Kendrick,[21] O. Kepka,[137] S. Kersten,[179] B. P. Kerševan,[89] R. A. Keyes,[101] M. Khader,[170] F. Khalil-Zada,[13] A. Khanov,[125] A. G. Kharlamov,[120b,120a] T. Kharlamova,[120b,120a] A. Khodinov,[163] T. J. Khoo,[52] E. Khramov,[77] J. Khubua,[156b] S. Kido,[80] M. Kiehn,[52] C. R. Kilby,[91] S. H. Kim,[166] Y. K. Kim,[36] N. Kimura,[64a,64c] O. M. Kind,[19] B. T. King,[88] D. Kirchmeier,[46] J. Kirk,[141] A. E. Kiryunin,[113] T. Kishimoto,[160] D. Kisielewska,[81a] V. Kitali,[44] O. Kivernyk,[5] E. Kladiva,[28b] T. Klapdor-Kleingrothaus,[50] M. H. Klein,[103]

M. Klein,[88] U. Klein,[88] K. Kleinknecht,[97] P. Klimek,[119] A. Klimentov,[29] R. Klingenberg,[45,a] T. Klingl,[24] T. Klioutchnikova,[35] F. F. Klitzner,[112] P. Kluit,[118] S. Kluth,[113] E. Kneringer,[74] E. B. F. G. Knoops,[99] A. Knue,[50] A. Kobayashi,[160] D. Kobayashi,[85] T. Kobayashi,[160] M. Kobel,[46] M. Kocian,[150] P. Kodys,[139] T. Koffas,[33] E. Koffeman,[118] N. M. Köhler,[113] T. Koi,[150] M. Kolb,[59b] I. Koletsou,[5] T. Kondo,[79] N. Kondrashova,[58c] K. Köneke,[50] A. C. König,[117] T. Kono,[79] R. Konoplich,[121,gg] V. Konstantinides,[92] N. Konstantinidis,[92] B. Konya,[94] R. Kopeliansky,[63] S. Koperny,[81a] K. Korcyl,[82] K. Kordas,[159] A. Korn,[92] I. Korolkov,[14] E. V. Korolkova,[146] O. Kortner,[113] S. Kortner,[113] T. Kosek,[139] V. V. Kostyukhin,[24] A. Kotwal,[47] A. Koulouris,[10] A. Kourkoumeli-Charalampidi,[68a,68b] C. Kourkoumelis,[9] E. Kourlitis,[146] V. Kouskoura,[29] A. B. Kowalewska,[82] R. Kowalewski,[173] T. Z. Kowalski,[81a] C. Kozakai,[160] W. Kozanecki,[142] A. S. Kozhin,[140] V. A. Kramarenko,[111] G. Kramberger,[89] D. Krasnopevtsev,[110] M. W. Krasny,[132] A. Krasznahorkay,[35] D. Krauss,[113] J. A. Kremer,[81a] J. Kretzschmar,[88] P. Krieger,[164] K. Krizka,[18] K. Kroeninger,[45] H. Kroha,[113] J. Kroll,[137] J. Kroll,[133] J. Krstic,[16] U. Kruchonak,[77] H. Krüger,[24] N. Krumnack,[76] M. C. Kruse,[47] T. Kubota,[102] S. Kuday,[4b] J. T. Kuechler,[179] S. Kuehn,[35] A. Kugel,[59a] F. Kuger,[174] T. Kuhl,[44] V. Kukhtin,[77] R. Kukla,[99] Y. Kulchitsky,[105] S. Kuleshov,[144b] Y. P. Kulinich,[170] M. Kuna,[56] T. Kunigo,[83] A. Kupco,[137] T. Kupfer,[45] O. Kuprash,[158] H. Kurashige,[80] L. L. Kurchaninov,[165a] Y. A. Kurochkin,[105] M. G. Kurth,[15d] E. S. Kuwertz,[173] M. Kuze,[162] J. Kvita,[126] T. Kwan,[101] A. La Rosa,[113] J. L. La Rosa Navarro,[78d] L. La Rotonda,[40b,40a] F. La Ruffa,[40b,40a] C. Lacasta,[171] F. Lacava,[70a,70b] J. Lacey,[44] D. P. J. Lack,[98] H. Lacker,[19] D. Lacour,[132] E. Ladygin,[77] R. Lafaye,[5] B. Laforge,[132] T. Lagouri,[32c] S. Lai,[51] S. Lammers,[63] W. Lampl,[7] E. Lançon,[29] U. Landgraf,[50] M. P. J. Landon,[90] M. C. Lanfermann,[52] V. S. Lang,[44] J. C. Lange,[14] R. J. Langenberg,[35] A. J. Lankford,[168] F. Lanni,[29] K. Lantzsch,[24] A. Lanza,[68a] A. Lapertosa,[53b,53a] S. Laplace,[132] J. F. Laporte,[142] T. Lari,[66a] F. Lasagni Manghi,[23b,23a] M. Lassnig,[35] T. S. Lau,[61a] A. Laudrain,[128] A. T. Law,[143] P. Laycock,[88] M. Lazzaroni,[66a,66b] B. Le,[102] O. Le Dortz,[132] E. Le Guirriec,[99] E. P. Le Quilleuc,[142] M. LeBlanc,[7] T. LeCompte,[6] F. Ledroit-Guillon,[56] C. A. Lee,[29] G. R. Lee,[144a] L. Lee,[57] S. C. Lee,[155] B. Lefebvre,[101] M. Lefebvre,[173] F. Legger,[112] C. Leggett,[18] N. Lehmann,[179] G. Lehmann Miotto,[35] W. A. Leight,[44] A. Leisos,[159,hh] M. A. L. Leite,[78d] R. Leitner,[139] D. Lellouch,[177] B. Lemmer,[51] K. J. C. Leney,[92] T. Lenz,[24] B. Lenzi,[35] R. Leone,[7] S. Leone,[69a] C. Leonidopoulos,[48] G. Lerner,[153] C. Leroy,[107] R. Les,[164] A. A. J. Lesage,[142] C. G. Lester,[31] M. Levchenko,[134] J. Levêque,[5] D. Levin,[103] L. J. Levinson,[177] D. Lewis,[90] B. Li,[103] C-Q. Li,[58a] H. Li,[58b] L. Li,[58c] Q. Li,[15d] Q. Y. Li,[58a] S. Li,[58d,58c] X. Li,[58c] Y. Li,[148] Z. Liang,[15a] B. Liberti,[71a] A. Liblong,[164] K. Lie,[61c] S. Liem,[118] A. Limosani,[154] C. Y. Lin,[31] K. Lin,[104] T. H. Lin,[97] R. A. Linck,[63] B. E. Lindquist,[152] A. L. Lionti,[52] E. Lipeles,[133] A. Lipniacka,[17] M. Lisovyi,[59b] T. M. Liss,[170,ii] A. Lister,[172] A. M. Litke,[143] J. D. Little,[8] B. Liu,[76] B.L Liu,[6] H. B. Liu,[29] H. Liu,[103] J. B. Liu,[58a] J. K. K. Liu,[131] K. Liu,[132] M. Liu,[58a] P. Liu,[18] Y. Liu,[15a] Y. L. Liu,[58a] Y. W. Liu,[58a] M. Livan,[68a,68b] A. Lleres,[56] J. Llorente Merino,[15a] S. L. Lloyd,[90] C. Y. Lo,[61b] F. Lo Sterzo,[41] E. M. Lobodzinska,[44] P. Loch,[7] F. K. Loebinger,[98] A. Loesle,[50] K. M. Loew,[26] T. Lohse,[19] K. Lohwasser,[146] M. Lokajicek,[137] B. A. Long,[25] J. D. Long,[170] R. E. Long,[87] L. Longo,[65a,65b] K. A. Looper,[122] J. A. Lopez,[144b] I. Lopez Paz,[14] A. Lopez Solis,[146] J. Lorenz,[112] N. Lorenzo Martinez,[5] M. Losada,[22] P. J. Lösel,[112] X. Lou,[44] X. Lou,[15a] A. Lounis,[128] J. Love,[6] P. A. Love,[87] J. J. Lozano Bahilo,[171] H. Lu,[61a] M. Lu,[58a] N. Lu,[103] Y. J. Lu,[62] H. J. Lubatti,[145] C. Luci,[70a,70b] A. Lucotte,[56] C. Luedtke,[50] F. Luehring,[63] I. Luise,[132] W. Lukas,[74] L. Luminari,[70a] B. Lund-Jensen,[151] M. S. Lutz,[100] P. M. Luzi,[132] D. Lynn,[29] R. Lysak,[137] E. Lytken,[94] F. Lyu,[15a] V. Lyubushkin,[77] H. Ma,[29] L. L. Ma,[58b] Y. Ma,[58b] G. Maccarrone,[49] A. Macchiolo,[113] C. M. Macdonald,[146] J. Machado Miguens,[133,136b] D. Madaffari,[171] R. Madar,[37] W. F. Mader,[46] A. Madsen,[44] N. Madysa,[46] J. Maeda,[80] K. Maekawa,[160] S. Maeland,[17] T. Maeno,[29] A. S. Maevskiy,[111] V. Magerl,[50] C. Maidantchik,[78b] T. Maier,[112] A. Maio,[136a,136b,136d] O. Majersky,[28a] S. Majewski,[127] Y. Makida,[79] N. Makovec,[128] B. Malaescu,[132] Pa. Malecki,[82] V. P. Maleev,[134] F. Malek,[56] U. Mallik,[75] D. Malon,[6] C. Malone,[31] S. Maltezos,[10] S. Malyukov,[35] J. Mamuzic,[171] G. Mancini,[49] I. Mandić,[89] J. Maneira,[136a] L. Manhaes de Andrade Filho,[78a] J. Manjarres Ramos,[46] K. H. Mankinen,[94] A. Mann,[112] A. Manousos,[74] B. Mansoulie,[142] J. D. Mansour,[15a] M. Mantoani,[51] S. Manzoni,[66a,66b] G. Marceca,[30] L. March,[52] L. Marchese,[131] G. Marchiori,[132] M. Marcisovsky,[137] C. A. Marin Tobon,[35] M. Marjanovic,[37] D. E. Marley,[103] F. Marroquim,[78b] Z. Marshall,[18] M. U. F. Martensson,[169] S. Marti-Garcia,[171] C. B. Martin,[122] T. A. Martin,[175] V. J. Martin,[48] B. Martin dit Latour,[17] M. Martinez,[14,w] V. I. Martinez Outschoorn,[100] S. Martin-Haugh,[141] V. S. Martoiu,[27b] A. C. Martyniuk,[92] A. Marzin,[35] L. Masetti,[97] T. Mashimo,[160] R. Mashinistov,[108] J. Masik,[98] A. L. Maslennikov,[120b,120a] L. H. Mason,[102] L. Massa,[71a,71b] P. Mastrandrea,[5] A. Mastroberardino,[40b,40a] T. Masubuchi,[160] P. Mättig,[179] J. Maurer,[27b] B. Maček,[89] S. J. Maxfield,[88] D. A. Maximov,[120b,120a] R. Mazini,[155] I. Maznas,[159] S. M. Mazza,[143] N. C. Mc Fadden,[116] G. Mc Goldrick,[164] S. P. Mc Kee,[103] A. McCarn,[103] T. G. McCarthy,[113] L. I. McClymont,[92] E. F. McDonald,[102] J. A. Mcfayden,[35] G. Mchedlidze,[51] M. A. McKay,[41] K. D. McLean,[173]

S. J. McMahon,[141] P. C. McNamara,[102] C. J. McNicol,[175] R. A. McPherson,[173,n] J. E. Mdhluli,[32c] Z. A. Meadows,[100] S. Meehan,[145] T. M. Megy,[50] S. Mehlhase,[112] A. Mehta,[88] T. Meideck,[56] B. Meirose,[42] D. Melini,[171,jj] B. R. Mellado Garcia,[32c] J. D. Mellenthin,[51] M. Melo,[28a] F. Meloni,[20] A. Melzer,[24] S. B. Menary,[98] E. D. Mendes Gouveia,[136a] L. Meng,[88] X. T. Meng,[103] A. Mengarelli,[23b,23a] S. Menke,[113] E. Meoni,[40b,40a] S. Mergelmeyer,[19] C. Merlassino,[20] P. Mermod,[52] L. Merola,[67a,67b] C. Meroni,[66a] F. S. Merritt,[36] A. Messina,[70a,70b] J. Metcalfe,[6] A. S. Mete,[168] C. Meyer,[133] J. Meyer,[157] J-P. Meyer,[142] H. Meyer Zu Theenhausen,[59a] F. Miano,[153] R. P. Middleton,[141] L. Mijović,[48] G. Mikenberg,[177] M. Mikestikova,[137] M. Mikuž,[89] M. Milesi,[102] A. Milic,[164] D. A. Millar,[90] D. W. Miller,[36] A. Milov,[177] D. A. Milstead,[43a,43b] A. A. Minaenko,[140] M. Miñano Moya,[171] I. A. Minashvili,[156b] A. I. Mincer,[121] B. Mindur,[81a] M. Mineev,[77] Y. Minegishi,[160] Y. Ming,[178] L. M. Mir,[14] A. Mirto,[65a,65b] K. P. Mistry,[133] T. Mitani,[176] J. Mitrevski,[112] V. A. Mitsou,[171] A. Miucci,[20] P. S. Miyagawa,[146] A. Mizukami,[79] J. U. Mjörnmark,[94] T. Mkrtchyan,[181] M. Mlynarikova,[139] T. Moa,[43a,43b] K. Mochizuki,[107] P. Mogg,[50] S. Mohapatra,[38] S. Molander,[43a,43b] R. Moles-Valls,[24] M. C. Mondragon,[104] K. Mönig,[44] J. Monk,[39] E. Monnier,[99] A. Montalbano,[149] J. Montejo Berlingen,[35] F. Monticelli,[86] S. Monzani,[66a] R. W. Moore,[3] N. Morange,[128] D. Moreno,[22] M. Moreno Llácer,[35] P. Morettini,[53b] M. Morgenstern,[118] S. Morgenstern,[35] D. Mori,[149] T. Mori,[160] M. Morii,[57] M. Morinaga,[176] V. Morisbak,[130] A. K. Morley,[35] G. Mornacchi,[35] A. P. Morris,[92] J. D. Morris,[90] L. Morvaj,[152] P. Moschovakos,[10] M. Mosidze,[156b] H. J. Moss,[146] J. Moss,[150,kk] K. Motohashi,[162] R. Mount,[150] E. Mountricha,[35] E. J. W. Moyse,[100] S. Muanza,[99] F. Mueller,[113] J. Mueller,[135] R. S. P. Mueller,[112] D. Muenstermann,[87] P. Mullen,[55] G. A. Mullier,[20] F. J. Munoz Sanchez,[98] P. Murin,[28b] W. J. Murray,[175,141] A. Murrone,[66a,66b] M. Muškinja,[89] C. Mwewa,[32a] A. G. Myagkov,[140,ll] J. Myers,[127] M. Myska,[138] B. P. Nachman,[18] O. Nackenhorst,[45] K. Nagai,[131] K. Nagano,[79] Y. Nagasaka,[60] K. Nagata,[166] M. Nagel,[50] E. Nagy,[99] A. M. Nairz,[35] Y. Nakahama,[115] K. Nakamura,[79] T. Nakamura,[160] I. Nakano,[123] H. Nanjo,[129] F. Napolitano,[59a] R. F. Naranjo Garcia,[44] R. Narayan,[11] D. I. Narrias Villar,[59a] I. Naryshkin,[134] T. Naumann,[44] G. Navarro,[22] R. Nayyar,[7] H. A. Neal,[103] P. Y. Nechaeva,[108] T. J. Neep,[142] A. Negri,[68a,68b] M. Negrini,[23b] S. Nektarijevic,[117] C. Nellist,[51] M. E. Nelson,[131] S. Nemecek,[137] P. Nemethy,[121] M. Nessi,[35,mm] M. S. Neubauer,[170] M. Neumann,[179] P. R. Newman,[21] T. Y. Ng,[61c] Y. S. Ng,[19] H. D. N. Nguyen,[99] T. Nguyen Manh,[107] E. Nibigira,[37] R. B. Nickerson,[131] R. Nicolaidou,[142] J. Nielsen,[143] N. Nikiforou,[11] V. Nikolaenko,[140,ll] I. Nikolic-Audit,[132] K. Nikolopoulos,[21] P. Nilsson,[29] Y. Ninomiya,[79] A. Nisati,[70a] N. Nishu,[58c] R. Nisius,[113] I. Nitsche,[45] T. Nitta,[176] T. Nobe,[160] Y. Noguchi,[83] M. Nomachi,[129] I. Nomidis,[132] M. A. Nomura,[29] T. Nooney,[90] M. Nordberg,[35] N. Norjoharuddeen,[131] T. Novak,[89] O. Novgorodova,[46] R. Novotny,[138] M. Nozaki,[79] L. Nozka,[126] K. Ntekas,[168] E. Nurse,[92] F. Nuti,[102] F. G. Oakham,[33,e] H. Oberlack,[113] T. Obermann,[24] J. Ocariz,[132] A. Ochi,[80] I. Ochoa,[38] J. P. Ochoa-Ricoux,[144a] K. O'Connor,[26] S. Oda,[85] S. Odaka,[79] A. Oh,[98] S. H. Oh,[47] C. C. Ohm,[151] H. Oide,[53b,53a] H. Okawa,[166] Y. Okazaki,[83] Y. Okumura,[160] T. Okuyama,[79] A. Olariu,[27b] L. F. Oleiro Seabra,[136a] S. A. Olivares Pino,[144a] D. Oliveira Damazio,[29] J. L. Oliver,[1] M. J. R. Olsson,[36] A. Olszewski,[82] J. Olszowska,[82] D. C. O'Neil,[149] A. Onofre,[136a,136e] K. Onogi,[115] P. U. E. Onyisi,[11] H. Oppen,[130] M. J. Oreglia,[36] Y. Oren,[158] D. Orestano,[72a,72b] E. C. Orgill,[98] N. Orlando,[61b] A. A. O'Rourke,[44] R. S. Orr,[164] B. Osculati,[53b,53a,a] V. O'Shea,[55] R. Ospanov,[58a] G. Otero y Garzon,[30] H. Otono,[85] M. Ouchrif,[34d] F. Ould-Saada,[130] A. Ouraou,[142] Q. Ouyang,[15a] M. Owen,[55] R. E. Owen,[21] V. E. Ozcan,[12c] N. Ozturk,[8] J. Pacalt,[126] H. A. Pacey,[31] K. Pachal,[149] A. Pacheco Pages,[14] L. Pacheco Rodriguez,[142] C. Padilla Aranda,[14] S. Pagan Griso,[18] M. Paganini,[180] G. Palacino,[63] S. Palazzo,[40b,40a] S. Palestini,[35] M. Palka,[81b] D. Pallin,[37] I. Panagoulias,[10] C. E. Pandini,[35] J. G. Panduro Vazquez,[91] P. Pani,[35] G. Panizzo,[64a,64c] L. Paolozzi,[52] T. D. Papadopoulou,[10] K. Papageorgiou,[9,t] A. Paramonov,[6] D. Paredes Hernandez,[61b] S. R. Paredes Saenz,[131] B. Parida,[58c] A. J. Parker,[87] K. A. Parker,[44] M. A. Parker,[31] F. Parodi,[53b,53a] J. A. Parsons,[38] U. Parzefall,[50] V. R. Pascuzzi,[164] J. M. P. Pasner,[143] E. Pasqualucci,[70a] S. Passaggio,[53b] F. Pastore,[91] P. Pasuwan,[43a,43b] S. Pataraia,[97] J. R. Pater,[98] A. Pathak,[178,f] T. Pauly,[35] B. Pearson,[113] M. Pedersen,[130] L. Pedraza Diaz,[117] S. Pedraza Lopez,[171] R. Pedro,[136a,136b] S. V. Peleganchuk,[120b,120a] O. Penc,[137] C. Peng,[15d] H. Peng,[58a] B. S. Peralva,[78a] M. M. Perego,[142] A. P. Pereira Peixoto,[136a] D. V. Perepelitsa,[29] F. Peri,[19] L. Perini,[66a,66b] H. Pernegger,[35] S. Perrella,[67a,67b] V. D. Peshekhonov,[77,a] K. Peters,[44] R. F. Y. Peters,[98] B. A. Petersen,[35] T. C. Petersen,[39] E. Petit,[56] A. Petridis,[1] C. Petridou,[159] P. Petroff,[128] E. Petrolo,[70a] M. Petrov,[131] F. Petrucci,[72a,72b] M. Pettee,[180] N. E. Pettersson,[100] A. Peyaud,[142] R. Pezoa,[144b] T. Pham,[102] F. H. Phillips,[104] P. W. Phillips,[141] G. Piacquadio,[152] E. Pianori,[18] A. Picazio,[100] M. A. Pickering,[131] R. Piegaia,[30] J. E. Pilcher,[36] A. D. Pilkington,[98] M. Pinamonti,[71a,71b] J. L. Pinfold,[3] M. Pitt,[177] M-A. Pleier,[29] V. Pleskot,[139] E. Plotnikova,[77] D. Pluth,[76] P. Podberezko,[120b,120a] R. Poettgen,[94] R. Poggi,[52] L. Poggioli,[128] I. Pogrebnyak,[104] D. Pohl,[24] I. Pokharel,[51] G. Polesello,[68a] A. Poley,[44] A. Policicchio,[40b,40a] R. Polifka,[35] A. Polini,[23b] C. S. Pollard,[44] V. Polychronakos,[29] D. Ponomarenko,[110] L. Pontecorvo,[70a]

G. A. Popeneciu,[27d] D. M. Portillo Quintero,[132] S. Pospisil,[138] K. Potamianos,[44] I. N. Potrap,[77] C. J. Potter,[31] H. Potti,[11] T. Poulsen,[94] J. Poveda,[35] T. D. Powell,[146] M. E. Pozo Astigarraga,[35] P. Pralavorio,[99] S. Prell,[76] D. Price,[98] M. Primavera,[65a] S. Prince,[101] N. Proklova,[110] K. Prokofiev,[61c] F. Prokoshin,[144b] S. Protopopescu,[29] J. Proudfoot,[6] M. Przybycien,[81a] A. Puri,[170] P. Puzo,[128] J. Qian,[103] Y. Qin,[98] A. Quadt,[51] M. Queitsch-Maitland,[44] A. Qureshi,[1] P. Rados,[102] F. Ragusa,[66a,66b] G. Rahal,[95] J. A. Raine,[98] S. Rajagopalan,[29] A. Ramirez Morales,[90] T. Rashid,[128] S. Raspopov,[5] M. G. Ratti,[66a,66b] D. M. Rauch,[44] F. Rauscher,[112] S. Rave,[97] B. Ravina,[146] I. Ravinovich,[177] J. H. Rawling,[98] M. Raymond,[35] A. L. Read,[130] N. P. Readioff,[56] M. Reale,[65a,65b] D. M. Rebuzzi,[68a,68b] A. Redelbach,[174] G. Redlinger,[29] R. Reece,[143] R. G. Reed,[32c] K. Reeves,[42] L. Rehnisch,[19] J. Reichert,[133] A. Reiss,[97] C. Rembser,[35] H. Ren,[15d] M. Rescigno,[70a] S. Resconi,[66a] E. D. Resseguie,[133] S. Rettie,[172] E. Reynolds,[21] O. L. Rezanova,[120b,120a] P. Reznicek,[139] R. Richter,[113] S. Richter,[92] E. Richter-Was,[81b] O. Ricken,[24] M. Ridel,[132] P. Rieck,[113] C. J. Riegel,[179] O. Rifki,[44] M. Rijssenbeek,[152] A. Rimoldi,[68a,68b] M. Rimoldi,[20] L. Rinaldi,[23b] G. Ripellino,[151] B. Ristić,[87] E. Ritsch,[35] I. Riu,[14] J. C. Rivera Vergara,[144a] F. Rizatdinova,[125] E. Rizvi,[90] C. Rizzi,[14] R. T. Roberts,[98] S. H. Robertson,[101,n] A. Robichaud-Veronneau,[101] D. Robinson,[31] J. E. M. Robinson,[44] A. Robson,[55] E. Rocco,[97] C. Roda,[69a,69b] Y. Rodina,[99] S. Rodriguez Bosca,[171] A. Rodriguez Perez,[14] D. Rodriguez Rodriguez,[171] A. M. Rodríguez Vera,[165b] S. Roe,[35] C. S. Rogan,[57] O. Røhne,[130] R. Röhrig,[113] C. P. A. Roland,[63] J. Roloff,[57] A. Romaniouk,[110] M. Romano,[23b,23a] N. Rompotis,[88] M. Ronzani,[121] L. Roos,[132] S. Rosati,[70a] K. Rosbach,[50] P. Rose,[143] N-A. Rosien,[51] E. Rossi,[67a,67b] L. P. Rossi,[53b] L. Rossini,[66a,66b] J. H. N. Rosten,[31] R. Rosten,[14] M. Rotaru,[27b] J. Rothberg,[145] D. Rousseau,[128] D. Roy,[32c] A. Rozanov,[99] Y. Rozen,[157] X. Ruan,[32c] F. Rubbo,[150] F. Rühr,[50] A. Ruiz-Martinez,[33] Z. Rurikova,[50] N. A. Rusakovich,[77] H. L. Russell,[101] J. P. Rutherfoord,[7] N. Ruthmann,[35] E. M. Rüttinger,[44,nn] Y. F. Ryabov,[134] M. Rybar,[170] G. Rybkin,[128] S. Ryu,[6] A. Ryzhov,[140] G. F. Rzehorz,[51] P. Sabatini,[51] G. Sabato,[118] S. Sacerdoti,[128] H. F-W. Sadrozinski,[143] R. Sadykov,[77] F. Safai Tehrani,[70a] P. Saha,[119] M. Sahinsoy,[59a] A. Sahu,[179] M. Saimpert,[44] M. Saito,[160] T. Saito,[160] H. Sakamoto,[160] A. Sakharov,[121,gg] D. Salamani,[52] G. Salamanna,[72a,72b] J. E. Salazar Loyola,[144b] D. Salek,[118] P. H. Sales De Bruin,[169] D. Salihagic,[113] A. Salnikov,[150] J. Salt,[171] D. Salvatore,[40b,40a] F. Salvatore,[153] A. Salvucci,[61a,61b,61c] A. Salzburger,[35] D. Sammel,[50] D. Sampsonidis,[159] D. Sampsonidou,[159] J. Sánchez,[171] A. Sanchez Pineda,[64a,64c] H. Sandaker,[130] C. O. Sander,[44] M. Sandhoff,[179] C. Sandoval,[22] D. P. C. Sankey,[141] M. Sannino,[53b,53a] Y. Sano,[115] A. Sansoni,[49] C. Santoni,[37] H. Santos,[136a] I. Santoyo Castillo,[153] A. Sapronov,[77] J. G. Saraiva,[136a,136d] O. Sasaki,[79] K. Sato,[166] E. Sauvan,[5] P. Savard,[164,e] N. Savic,[113] R. Sawada,[160] C. Sawyer,[141] L. Sawyer,[93,v] C. Sbarra,[23b] A. Sbrizzi,[23b,23a] T. Scanlon,[92] J. Schaarschmidt,[145] P. Schacht,[113] B. M. Schachtner,[112] D. Schaefer,[36] L. Schaefer,[133] J. Schaeffer,[97] S. Schaepe,[35] U. Schäfer,[97] A. C. Schaffer,[128] D. Schaile,[112] R. D. Schamberger,[152] N. Scharmberg,[98] V. A. Schegelsky,[134] D. Scheirich,[139] F. Schenck,[19] M. Schernau,[168] C. Schiavi,[53b,53a] S. Schier,[143] L. K. Schildgen,[24] Z. M. Schillaci,[26] E. J. Schioppa,[35] M. Schioppa,[40b,40a] K. E. Schleicher,[50] S. Schlenker,[35] K. R. Schmidt-Sommerfeld,[113] K. Schmieden,[35] C. Schmitt,[97] S. Schmitt,[44] S. Schmitz,[97] U. Schnoor,[50] L. Schoeffel,[142] A. Schoening,[59b] E. Schopf,[24] M. Schott,[97] J. F. P. Schouwenberg,[117] J. Schovancova,[35] S. Schramm,[52] A. Schulte,[97] H-C. Schultz-Coulon,[59a] M. Schumacher,[50] B. A. Schumm,[143] Ph. Schune,[142] A. Schwartzman,[150] T. A. Schwarz,[103] H. Schweiger,[98] Ph. Schwemling,[142] R. Schwienhorst,[104] A. Sciandra,[24] G. Sciolla,[26] M. Scornajenghi,[40b,40a] F. Scuri,[69a] F. Scutti,[102] L. M. Scyboz,[113] J. Searcy,[103] C. D. Sebastiani,[70a,70b] P. Seema,[24] S. C. Seidel,[116] A. Seiden,[143] T. Seiss,[36] J. M. Seixas,[78b] G. Sekhniaidze,[67a] K. Sekhon,[103] S. J. Sekula,[41] N. Semprini-Cesari,[23b,23a] S. Sen,[47] S. Senkin,[37] C. Serfon,[130] L. Serin,[128] L. Serkin,[64a,64b] M. Sessa,[72a,72b] H. Severini,[124] T. Šfiligoj,[89] F. Sforza,[167] A. Sfyrla,[52] E. Shabalina,[51] J. D. Shahinian,[143] N. W. Shaikh,[43a,43b] L. Y. Shan,[15a] R. Shang,[170] J. T. Shank,[25] M. Shapiro,[18] A. S. Sharma,[1] A. Sharma,[131] P. B. Shatalov,[109] K. Shaw,[153] S. M. Shaw,[98] A. Shcherbakova,[134] Y. Shen,[124] N. Sherafati,[33] A. D. Sherman,[25] P. Sherwood,[92] L. Shi,[155,oo] S. Shimizu,[80] C. O. Shimmin,[180] M. Shimojima,[114] I. P. J. Shipsey,[131] S. Shirabe,[85] M. Shiyakova,[77] J. Shlomi,[177] A. Shmeleva,[108] D. Shoaleh Saadi,[107] M. J. Shochet,[36] S. Shojaii,[102] D. R. Shope,[124] S. Shrestha,[122] E. Shulga,[110] P. Sicho,[137] A. M. Sickles,[170] P. E. Sidebo,[151] E. Sideras Haddad,[32c] O. Sidiropoulou,[174] A. Sidoti,[23b,23a] F. Siegert,[46] Dj. Sijacki,[16] J. Silva,[136a] M. Silva Jr.,[178] M. V. Silva Oliveira,[78a] S. B. Silverstein,[43a] L. Simic,[77] S. Simion,[128] E. Simioni,[97] M. Simon,[97] P. Sinervo,[164] N. B. Sinev,[127] M. Sioli,[23b,23a] G. Siragusa,[174] I. Siral,[103] S.Yu. Sivoklokov,[111] J. Sjölin,[43a,43b] M. B. Skinner,[87] P. Skubic,[124] M. Slater,[21] T. Slavicek,[138] M. Slawinska,[82] K. Sliwa,[167] R. Slovak,[139] V. Smakhtin,[177] B. H. Smart,[5] J. Smiesko,[28a] N. Smirnov,[110] S.Yu. Smirnov,[110] Y. Smirnov,[110] L. N. Smirnova,[111] O. Smirnova,[94] J. W. Smith,[51] M. N. K. Smith,[38] R. W. Smith,[38] M. Smizanska,[87] K. Smolek,[138] A. A. Snesarev,[108] I. M. Snyder,[127] S. Snyder,[29] R. Sobie,[173,n] A. M. Soffa,[168] A. Soffer,[158] A. Søgaard,[48] D. A. Soh,[155] G. Sokhrannyi,[89] C. A. Solans Sanchez,[35] M. Solar,[138] E. Yu. Soldatov,[110] U. Soldevila,[171]

A. A. Solodkov,[140] A. Soloshenko,[77] O. V. Solovyanov,[140] V. Solovyev,[134] P. Sommer,[146] H. Son,[167] W. Song,[141] A. Sopczak,[138] F. Sopkova,[28b] D. Sosa,[59b] C. L. Sotiropoulou,[69a,69b] S. Sottocornola,[68a,68b] R. Soualah,[64a,64c,pp] A. M. Soukharev,[120b,120a] D. South,[44] B. C. Sowden,[91] S. Spagnolo,[65a,65b] M. Spalla,[113] M. Spangenberg,[175] F. Spanò,[91] D. Sperlich,[19] F. Spettel,[113] T. M. Spieker,[59a] R. Spighi,[23b] G. Spigo,[35] L. A. Spiller,[102] D. P. Spiteri,[55] M. Spousta,[139] A. Stabile,[66a,66b] R. Stamen,[59a] S. Stamm,[19] E. Stanecka,[82] R. W. Stanek,[6] C. Stanescu,[72a] B. Stanislaus,[131] M. M. Stanitzki,[44] B. Stapf,[118] S. Stapnes,[130] E. A. Starchenko,[140] G. H. Stark,[36] J. Stark,[56] S.H Stark,[39] P. Staroba,[137] P. Starovoitov,[59a] S. Stärz,[35] R. Staszewski,[82] M. Stegler,[44] P. Steinberg,[29] B. Stelzer,[149] H. J. Stelzer,[35] O. Stelzer-Chilton,[165a] H. Stenzel,[54] T. J. Stevenson,[90] G. A. Stewart,[55] M. C. Stockton,[127] G. Stoicea,[27b] P. Stolte,[51] S. Stonjek,[113] A. Straessner,[46] J. Strandberg,[151] S. Strandberg,[43a,43b] M. Strauss,[124] P. Strizenec,[28b] R. Ströhmer,[174] D. M. Strom,[127] R. Stroynowski,[41] A. Strubig,[48] S. A. Stucci,[29] B. Stugu,[17] J. Stupak,[124] N. A. Styles,[44] D. Su,[150] J. Su,[135] S. Suchek,[59a] Y. Sugaya,[129] M. Suk,[138] V. V. Sulin,[108] D. M. S. Sultan,[52] S. Sultansoy,[4c] T. Sumida,[83] S. Sun,[103] X. Sun,[3] K. Suruliz,[153] C. J. E. Suster,[154] M. R. Sutton,[153] S. Suzuki,[79] M. Svatos,[137] M. Swiatlowski,[36] S. P. Swift,[2] A. Sydorenko,[97] I. Sykora,[28a] T. Sykora,[139] D. Ta,[97] K. Tackmann,[44,qq] J. Taenzer,[158] A. Taffard,[168] R. Tafirout,[165a] E. Tahirovic,[90] N. Taiblum,[158] H. Takai,[29] R. Takashima,[84] E. H. Takasugi,[113] K. Takeda,[80] T. Takeshita,[147] Y. Takubo,[79] M. Talby,[99] A. A. Talyshev,[120b,120a] J. Tanaka,[160] M. Tanaka,[162] R. Tanaka,[128] R. Tanioka,[80] B. B. Tannenwald,[122] S. Tapia Araya,[144b] S. Tapprogge,[97] A. Tarek Abouelfadl Mohamed,[132] S. Tarem,[157] G. Tarna,[27b,q] G. F. Tartarelli,[66a] P. Tas,[139] M. Tasevsky,[137] T. Tashiro,[83] E. Tassi,[40b,40a] A. Tavares Delgado,[136a,136b] Y. Tayalati,[34e] A. C. Taylor,[116] A. J. Taylor,[48] G. N. Taylor,[102] P. T. E. Taylor,[102] W. Taylor,[165b] A. S. Tee,[87] P. Teixeira-Dias,[91] H. Ten Kate,[35] P. K. Teng,[155] J. J. Teoh,[129] F. Tepel,[179] S. Terada,[79] K. Terashi,[160] J. Terron,[96] S. Terzo,[14] M. Testa,[49] R. J. Teuscher,[164,n] S. J. Thais,[180] T. Theveneaux-Pelzer,[44] F. Thiele,[39] J. P. Thomas,[21] A. S. Thompson,[55] P. D. Thompson,[21] L. A. Thomsen,[180] E. Thomson,[133] Y. Tian,[38] R. E. Ticse Torres,[51] V. O. Tikhomirov,[108,rr] Yu.A. Tikhonov,[120b,120a] S. Timoshenko,[110] P. Tipton,[180] S. Tisserant,[99] K. Todome,[162] S. Todorova-Nova,[5] S. Todt,[46] J. Tojo,[85] S. Tokár,[28a] K. Tokushuku,[79] E. Tolley,[122] K. G. Tomiwa,[32c] M. Tomoto,[115] L. Tompkins,[150,ff] K. Toms,[116] B. Tong,[57] P. Tornambe,[50] E. Torrence,[127] H. Torres,[46] E. Torró Pastor,[145] C. Tosciri,[131] J. Toth,[99,ss] F. Touchard,[99] D. R. Tovey,[146] C. J. Treado,[121] T. Trefzger,[174] F. Tresoldi,[153] A. Tricoli,[29] I. M. Trigger,[165a] S. Trincaz-Duvoid,[132] M. F. Tripiana,[14] W. Trischuk,[164] B. Trocmé,[56] A. Trofymov,[128] C. Troncon,[66a] M. Trovatelli,[173] F. Trovato,[153] L. Truong,[32b] M. Trzebinski,[82] A. Trzupek,[82] F. Tsai,[44] J.C-L. Tseng,[131] P. V. Tsiareshka,[105] N. Tsirintanis,[9] V. Tsiskaridze,[152] E. G. Tskhadadze,[156a] I. I. Tsukerman,[109] V. Tsulaia,[18] S. Tsuno,[79] D. Tsybychev,[152] Y. Tu,[61b] A. Tudorache,[27b] V. Tudorache,[27b] T. T. Tulbure,[27a] A. N. Tuna,[57] S. Turchikhin,[77] D. Turgeman,[177] I. Turk Cakir,[4b,tt] R. Turra,[66a] P. M. Tuts,[38] E. Tzovara,[97] G. Ucchielli,[23b,23a] I. Ueda,[79] M. Ughetto,[43a,43b] F. Ukegawa,[166] G. Unal,[35] A. Undrus,[29] G. Unel,[168] F. C. Ungaro,[102] Y. Unno,[79] K. Uno,[160] J. Urban,[28b] P. Urquijo,[102] P. Urrejola,[97] G. Usai,[8] J. Usui,[79] L. Vacavant,[99] V. Vacek,[138] B. Vachon,[101] K. O. H. Vadla,[130] A. Vaidya,[92] C. Valderanis,[112] E. Valdes Santurio,[43a,43b] M. Valente,[52] S. Valentinetti,[23b,23a] A. Valero,[171] L. Valéry,[44] R. A. Vallance,[21] A. Vallier,[5] J. A. Valls Ferrer,[171] T. R. Van Daalen,[14] W. Van Den Wollenberg,[118] H. Van der Graaf,[118] P. Van Gemmeren,[6] J. Van Nieuwkoop,[149] I. Van Vulpen,[118] M. C. van Woerden,[118] M. Vanadia,[71a,71b] W. Vandelli,[35] A. Vaniachine,[163] P. Vankov,[118] R. Vari,[70a] E. W. Varnes,[7] C. Varni,[53b,53a] T. Varol,[41] D. Varouchas,[128] A. Vartapetian,[8] K. E. Varvell,[154] G. A. Vasquez,[144b] J. G. Vasquez,[180] F. Vazeille,[37] D. Vazquez Furelos,[14] T. Vazquez Schroeder,[101] J. Veatch,[51] V. Vecchio,[72a,72b] L. M. Veloce,[164] F. Veloso,[136a,136c] S. Veneziano,[70a] A. Ventura,[65a,65b] M. Venturi,[173] N. Venturi,[35] V. Vercesi,[68a] M. Verducci,[72a,72b] C. M. Vergel Infante,[76] W. Verkerke,[118] A. T. Vermeulen,[118] J. C. Vermeulen,[118] M. C. Vetterli,[149,e] N. Viaux Maira,[144b] O. Viazlo,[94] I. Vichou,[170,a] T. Vickey,[146] O. E. Vickey Boeriu,[146] G. H. A. Viehhauser,[131] S. Viel,[18] L. Vigani,[131] M. Villa,[23b,23a] M. Villaplana Perez,[66a,66b] E. Vilucchi,[49] M. G. Vincter,[33] V. B. Vinogradov,[77] A. Vishwakarma,[44] C. Vittori,[23b,23a] I. Vivarelli,[153] S. Vlachos,[10] M. Vogel,[179] P. Vokac,[138] G. Volpi,[14] S. E. von Buddenbrock,[32c] E. Von Toerne,[24] V. Vorobel,[139] K. Vorobev,[110] M. Vos,[171] J. H. Vossebeld,[88] N. Vranjes,[16] M. Vranjes Milosavljevic,[16] V. Vrba,[138] M. Vreeswijk,[118] R. Vuillermet,[35] I. Vukotic,[36] P. Wagner,[24] W. Wagner,[179] J. Wagner-Kuhr,[112] H. Wahlberg,[86] S. Wahrmund,[46] K. Wakamiya,[80] V. M. Walbrecht,[113] J. Walder,[87] R. Walker,[112] W. Walkowiak,[148] V. Wallangen,[43a,43b] A. M. Wang,[57] C. Wang,[58b,q] F. Wang,[178] H. Wang,[18] H. Wang,[3] J. Wang,[154] J. Wang,[59b] P. Wang,[41] Q. Wang,[124] R.-J. Wang,[132] R. Wang,[58a] R. Wang,[6] S. M. Wang,[155] W. T. Wang,[58a] W. Wang,[155,uu] W. X. Wang,[58a,vv] Y. Wang,[58a] Z. Wang,[58c] C. Wanotayaroj,[44] A. Warburton,[101] C. P. Ward,[31] D. R. Wardrope,[92] A. Washbrook,[48] P. M. Watkins,[21] A. T. Watson,[21] M. F. Watson,[21] G. Watts,[145] S. Watts,[98] B. M. Waugh,[92] A. F. Webb,[11] S. Webb,[97] C. Weber,[180] M. S. Weber,[20] S. A. Weber,[33] S. M. Weber,[59a] J. S. Webster,[6] A. R. Weidberg,[131] B. Weinert,[63]

J. Weingarten,[51] M. Weirich,[97] C. Weiser,[50] P. S. Wells,[35] T. Wenaus,[29] T. Wengler,[35] S. Wenig,[35] N. Wermes,[24] M. D. Werner,[76] P. Werner,[35] M. Wessels,[59a] T. D. Weston,[20] K. Whalen,[127] N. L. Whallon,[145] A. M. Wharton,[87] A. S. White,[103] A. White,[8] M. J. White,[1] R. White,[144b] D. Whiteson,[168] B. W. Whitmore,[87] F. J. Wickens,[141] W. Wiedenmann,[178] M. Wielers,[141] C. Wiglesworth,[39] L. A. M. Wiik-Fuchs,[50] A. Wildauer,[113] F. Wilk,[98] H. G. Wilkens,[35] L. J. Wilkins,[91] H. H. Williams,[133] S. Williams,[31] C. Willis,[104] S. Willocq,[100] J. A. Wilson,[21] I. Wingerter-Seez,[5] E. Winkels,[153] F. Winklmeier,[127] O. J. Winston,[153] B. T. Winter,[24] M. Wittgen,[150] M. Wobisch,[93] A. Wolf,[97] T. M. H. Wolf,[118] R. Wolff,[99] M. W. Wolter,[82] H. Wolters,[136a,136c] V. W. S. Wong,[172] N. L. Woods,[143] S. D. Worm,[21] B. K. Wosiek,[82] K. W. Woźniak,[82] K. Wraight,[55] M. Wu,[36] S. L. Wu,[178] X. Wu,[52] Y. Wu,[58a] T. R. Wyatt,[98] B. M. Wynne,[48] S. Xella,[39] Z. Xi,[103] L. Xia,[175] D. Xu,[15a] H. Xu,[58a] L. Xu,[29] T. Xu,[142] W. Xu,[103] B. Yabsley,[154] S. Yacoob,[32a] K. Yajima,[129] D. P. Yallup,[92] D. Yamaguchi,[162] Y. Yamaguchi,[162] A. Yamamoto,[79] T. Yamanaka,[160] F. Yamane,[80] M. Yamatani,[160] T. Yamazaki,[160] Y. Yamazaki,[80] Z. Yan,[25] H. J. Yang,[58c,58d] H. T. Yang,[18] S. Yang,[75] Y. Yang,[160] Z. Yang,[17] W-M. Yao,[18] Y. C. Yap,[44] Y. Yasu,[79] E. Yatsenko,[58c,58d] J. Ye,[41] S. Ye,[29] I. Yeletskikh,[77] E. Yigitbasi,[25] E. Yildirim,[97] K. Yorita,[176] K. Yoshihara,[133] C. J. S. Young,[35] C. Young,[150] J. Yu,[8] J. Yu,[76] X. Yue,[59a] S. P. Y. Yuen,[24] I. Yusuff,[31,ww] B. Zabinski,[82] G. Zacharis,[10] E. Zaffaroni,[52] R. Zaidan,[14] A. M. Zaitsev,[140,ll] N. Zakharchuk,[44] J. Zalieckas,[17] S. Zambito,[57] D. Zanzi,[35] D. R. Zaripovas,[55] S. V. Zeißner,[45] C. Zeitnitz,[179] G. Zemaityte,[131] J. C. Zeng,[170] Q. Zeng,[150] O. Zenin,[140] T. Ženiš,[28a] D. Zerwas,[128] M. Zgubič,[131] D. F. Zhang,[58b] D. Zhang,[103] F. Zhang,[178] G. Zhang,[58a,vv] H. Zhang,[15c] J. Zhang,[6] L. Zhang,[50] L. Zhang,[58a] M. Zhang,[170] P. Zhang,[15c] R. Zhang,[58a,q] R. Zhang,[24] X. Zhang,[58b] Y. Zhang,[15d] Z. Zhang,[128] P. Zhao,[47] X. Zhao,[41] Y. Zhao,[58b,128,y] Z. Zhao,[58a] A. Zhemchugov,[77] B. Zhou,[103] C. Zhou,[178] L. Zhou,[41] M. S. Zhou,[15d] M. Zhou,[152] N. Zhou,[58c] Y. Zhou,[7] C. G. Zhu,[58b] H. L. Zhu,[58a] H. Zhu,[15a] J. Zhu,[103] Y. Zhu,[58a] X. Zhuang,[15a] K. Zhukov,[108] V. Zhulanov,[120b,120a] A. Zibell,[174] D. Zieminska,[63] N. I. Zimine,[77] S. Zimmermann,[50] Z. Zinonos,[113] M. Zinser,[97] M. Ziolkowski,[148] L. Živković,[16] G. Zobernig,[178] A. Zoccoli,[23b,23a] K. Zoch,[51] T. G. Zorbas,[146] R. Zou,[36] M. Zur Nedden,[19] and L. Zwalinski[35]

(ATLAS Collaboration)

[1]*Department of Physics, University of Adelaide, Adelaide, Australia*
[2]*Physics Department, SUNY Albany, Albany, New York, USA*
[3]*Department of Physics, University of Alberta, Edmonton, Alberta, Canada*
[4a]*Department of Physics, Ankara University, Ankara, Turkey*
[4b]*Istanbul Aydin University, Istanbul, Turkey*
[4c]*Division of Physics, TOBB University of Economics and Technology, Ankara, Turkey*
[5]*LAPP, Université Grenoble Alpes, Université Savoie Mont Blanc, CNRS/IN2P3, Annecy, France*
[6]*High Energy Physics Division, Argonne National Laboratory, Argonne, Illinois, USA*
[7]*Department of Physics, University of Arizona, Tucson, Arizona, USA*
[8]*Department of Physics, University of Texas at Arlington, Arlington, Texas, USA*
[9]*Physics Department, National and Kapodistrian University of Athens, Athens, Greece*
[10]*Physics Department, National Technical University of Athens, Zografou, Greece*
[11]*Department of Physics, University of Texas at Austin, Austin, Texas, USA*
[12a]*Bahcesehir University, Faculty of Engineering and Natural Sciences, Istanbul, Turkey*
[12b]*Istanbul Bilgi University, Faculty of Engineering and Natural Sciences, Istanbul, Turkey*
[12c]*Department of Physics, Bogazici University, Istanbul, Turkey*
[12d]*Department of Physics Engineering, Gaziantep University, Gaziantep, Turkey*
[13]*Institute of Physics, Azerbaijan Academy of Sciences, Baku, Azerbaijan*
[14]*Institut de Física d'Altes Energies (IFAE), Barcelona Institute of Science and Technology, Barcelona, Spain*
[15a]*Institute of High Energy Physics, Chinese Academy of Sciences, Beijing, China*
[15b]*Physics Department, Tsinghua University, Beijing, China*
[15c]*Department of Physics, Nanjing University, Nanjing, China*
[15d]*University of Chinese Academy of Science (UCAS), Beijing, China*
[16]*Institute of Physics, University of Belgrade, Belgrade, Serbia*
[17]*Department for Physics and Technology, University of Bergen, Bergen, Norway*
[18]*Physics Division, Lawrence Berkeley National Laboratory and University of California, Berkeley, California, USA*
[19]*Institut für Physik, Humboldt Universität zu Berlin, Berlin, Germany*
[20]*Albert Einstein Center for Fundamental Physics and Laboratory for High Energy Physics, University of Bern, Bern, Switzerland*

[21]*School of Physics and Astronomy, University of Birmingham, Birmingham, United Kingdom*
[22]*Centro de Investigaciónes, Universidad Antonio Nariño, Bogota, Colombia*
[23a]*Dipartimento di Fisica e Astronomia, Università di Bologna, Bologna, Italy*
[23b]*INFN Sezione di Bologna, Italy*
[24]*Physikalisches Institut, Universität Bonn, Bonn, Germany*
[25]*Department of Physics, Boston University, Boston, Massachusetts, USA*
[26]*Department of Physics, Brandeis University, Waltham, Massachusetts, USA*
[27a]*Transilvania University of Brasov, Brasov, Romania*
[27b]*Horia Hulubei National Institute of Physics and Nuclear Engineering, Bucharest, Romania*
[27c]*Department of Physics, Alexandru Ioan Cuza University of Iasi, Iasi, Romania*
[27d]*National Institute for Research and Development of Isotopic and Molecular Technologies, Physics Department, Cluj-Napoca, Romania*
[27e]*University Politehnica Bucharest, Bucharest, Romania*
[27f]*West University in Timisoara, Timisoara, Romania*
[28a]*Faculty of Mathematics, Physics and Informatics, Comenius University, Bratislava, Slovak Republic*
[28b]*Department of Subnuclear Physics, Institute of Experimental Physics of the Slovak Academy of Sciences, Kosice, Slovak Republic*
[29]*Physics Department, Brookhaven National Laboratory, Upton, New York, USA*
[30]*Departamento de Física, Universidad de Buenos Aires, Buenos Aires, Argentina*
[31]*Cavendish Laboratory, University of Cambridge, Cambridge, United Kingdom*
[32a]*Department of Physics, University of Cape Town, Cape Town, South Africa*
[32b]*Department of Mechanical Engineering Science, University of Johannesburg, Johannesburg, South Africa*
[32c]*School of Physics, University of the Witwatersrand, Johannesburg, South Africa*
[33]*Department of Physics, Carleton University, Ottawa, Ontario, Canada*
[34a]*Faculté des Sciences Ain Chock, Réseau Universitaire de Physique des Hautes Energies - Université Hassan II, Casablanca, Morocco*
[34b]*Centre National de l'Energie des Sciences Techniques Nucleaires (CNESTEN), Rabat, Morocco*
[34c]*Faculté des Sciences Semlalia, Université Cadi Ayyad, LPHEA-Marrakech, Morocco*
[34d]*Faculté des Sciences, Université Mohamed Premier and LPTPM, Oujda, Morocco*
[34e]*Faculté des sciences, Université Mohammed V, Rabat, Morocco*
[35]*CERN, Geneva, Switzerland*
[36]*Enrico Fermi Institute, University of Chicago, Chicago, Illinois, USA*
[37]*LPC, Université Clermont Auvergne, CNRS/IN2P3, Clermont-Ferrand, France*
[38]*Nevis Laboratory, Columbia University, Irvington, New York, USA*
[39]*Niels Bohr Institute, University of Copenhagen, Copenhagen, Denmark*
[40a]*Dipartimento di Fisica, Università della Calabria, Rende, Italy*
[40b]*INFN Gruppo Collegato di Cosenza, Laboratori Nazionali di Frascati, Italy*
[41]*Physics Department, Southern Methodist University, Dallas, Texas, USA*
[42]*Physics Department, University of Texas at Dallas, Richardson, Texas, USA*
[43a]*Department of Physics, Stockholm University, Sweden*
[43b]*Oskar Klein Centre, Stockholm, Sweden*
[44]*Deutsches Elektronen-Synchrotron DESY, Hamburg and Zeuthen, Germany*
[45]*Lehrstuhl für Experimentelle Physik IV, Technische Universität Dortmund, Dortmund, Germany*
[46]*Institut für Kern- und Teilchenphysik, Technische Universität Dresden, Dresden, Germany*
[47]*Department of Physics, Duke University, Durham, North Carolina, USA*
[48]*SUPA - School of Physics and Astronomy, University of Edinburgh, Edinburgh, United Kingdom*
[49]*INFN e Laboratori Nazionali di Frascati, Frascati, Italy*
[50]*Physikalisches Institut, Albert-Ludwigs-Universität Freiburg, Freiburg, Germany*
[51]*II. Physikalisches Institut, Georg-August-Universität Göttingen, Göttingen, Germany*
[52]*Département de Physique Nucléaire et Corpusculaire, Université de Genève, Genève, Switzerland*
[53a]*Dipartimento di Fisica, Università di Genova, Genova, Italy*
[53b]*INFN Sezione di Genova, Italy*
[54]*II. Physikalisches Institut, Justus-Liebig-Universität Giessen, Giessen, Germany*
[55]*SUPA - School of Physics and Astronomy, University of Glasgow, Glasgow, United Kingdom*
[56]*LPSC, Université Grenoble Alpes, CNRS/IN2P3, Grenoble INP, Grenoble, France*
[57]*Laboratory for Particle Physics and Cosmology, Harvard University, Cambridge, Massachusetts, USA*
[58a]*Department of Modern Physics and State Key Laboratory of Particle Detection and Electronics, University of Science and Technology of China, Hefei, China*

[58b]Institute of Frontier and Interdisciplinary Science and Key Laboratory of Particle Physics and Particle Irradiation (MOE), Shandong University, Qingdao, China
[58c]School of Physics and Astronomy, Shanghai Jiao Tong University, KLPPAC-MoE, SKLPPC, Shanghai, China
[58d]Tsung-Dao Lee Institute, Shanghai, China
[59a]Kirchhoff-Institut für Physik, Ruprecht-Karls-Universität Heidelberg, Heidelberg, Germany
[59b]Physikalisches Institut, Ruprecht-Karls-Universität Heidelberg, Heidelberg, Germany
[60]Faculty of Applied Information Science, Hiroshima Institute of Technology, Hiroshima, Japan
[61a]Department of Physics, Chinese University of Hong Kong, Shatin, N.T., Hong Kong, China
[61b]Department of Physics, University of Hong Kong, Hong Kong, China
[61c]Department of Physics and Institute for Advanced Study, Hong Kong University of Science and Technology, Clear Water Bay, Kowloon, Hong Kong, China
[62]Department of Physics, National Tsing Hua University, Hsinchu, Taiwan
[63]Department of Physics, Indiana University, Bloomington, Indiana, USA
[64a]INFN Gruppo Collegato di Udine, Sezione di Trieste, Udine, Italy
[64b]ICTP, Trieste, Italy
[64c]Dipartimento di Chimica, Fisica e Ambiente, Università di Udine, Udine, Italy
[65a]INFN Sezione di Lecce, Italy
[65b]Dipartimento di Matematica e Fisica, Università del Salento, Lecce, Italy
[66a]INFN Sezione di Milano, Italy
[66b]Dipartimento di Fisica, Università di Milano, Milano, Italy
[67a]INFN Sezione di Napoli, Italy
[67b]Dipartimento di Fisica, Università di Napoli, Napoli, Italy
[68a]INFN Sezione di Pavia, Italy
[68b]Dipartimento di Fisica, Università di Pavia, Pavia, Italy
[69a]INFN Sezione di Pisa, Italy
[69b]Dipartimento di Fisica E. Fermi, Università di Pisa, Pisa, Italy
[70a]INFN Sezione di Roma, Italy
[70b]Dipartimento di Fisica, Sapienza Università di Roma, Roma, Italy
[71a]INFN Sezione di Roma Tor Vergata, Italy
[71b]Dipartimento di Fisica, Università di Roma Tor Vergata, Roma, Italy
[72a]INFN Sezione di Roma Tre, Italy
[72b]Dipartimento di Matematica e Fisica, Università Roma Tre, Roma, Italy
[73a]INFN-TIFPA, Italy
[73b]Università degli Studi di Trento, Trento, Italy
[74]Institut für Astro- und Teilchenphysik, Leopold-Franzens-Universität, Innsbruck, Austria
[75]University of Iowa, Iowa City, Iowa, USA
[76]Department of Physics and Astronomy, Iowa State University, Ames, Iowa, USA
[77]Joint Institute for Nuclear Research, Dubna, Russia
[78a]Departamento de Engenharia Elétrica, Universidade Federal de Juiz de Fora (UFJF), Juiz de Fora, Brazil
[78b]Universidade Federal do Rio De Janeiro COPPE/EE/IF, Rio de Janeiro, Brazil
[78c]Universidade Federal de São João del Rei (UFSJ), São João del Rei, Brazil
[78d]Instituto de Física, Universidade de São Paulo, São Paulo, Brazil
[79]KEK, High Energy Accelerator Research Organization, Tsukuba, Japan
[80]Graduate School of Science, Kobe University, Kobe, Japan
[81a]AGH University of Science and Technology, Faculty of Physics and Applied Computer Science, Krakow, Poland
[81b]Marian Smoluchowski Institute of Physics, Jagiellonian University, Krakow, Poland
[82]Institute of Nuclear Physics Polish Academy of Sciences, Krakow, Poland
[83]Faculty of Science, Kyoto University, Kyoto, Japan
[84]Kyoto University of Education, Kyoto, Japan
[85]Research Center for Advanced Particle Physics and Department of Physics, Kyushu University, Fukuoka, Japan
[86]Instituto de Física La Plata, Universidad Nacional de La Plata and CONICET, La Plata, Argentina
[87]Physics Department, Lancaster University, Lancaster, United Kingdom
[88]Oliver Lodge Laboratory, University of Liverpool, Liverpool, United Kingdom
[89]Department of Experimental Particle Physics, Jožef Stefan Institute and Department of Physics, University of Ljubljana, Ljubljana, Slovenia
[90]School of Physics and Astronomy, Queen Mary University of London, London, United Kingdom

[91]*Department of Physics, Royal Holloway University of London, Egham, United Kingdom*
[92]*Department of Physics and Astronomy, University College London, London, United Kingdom*
[93]*Louisiana Tech University, Ruston, Louisiana, USA*
[94]*Fysiska institutionen, Lunds universitet, Lund, Sweden*
[95]*Centre de Calcul de l'Institut National de Physique Nucléaire et de Physique des Particules (IN2P3), Villeurbanne, France*
[96]*Departamento de Física Teorica C-15 and CIAFF, Universidad Autónoma de Madrid, Madrid, Spain*
[97]*Institut für Physik, Universität Mainz, Mainz, Germany*
[98]*School of Physics and Astronomy, University of Manchester, Manchester, United Kingdom*
[99]*CPPM, Aix-Marseille Université, CNRS/IN2P3, Marseille, France*
[100]*Department of Physics, University of Massachusetts, Amherst, Massachusetts, USA*
[101]*Department of Physics, McGill University, Montreal, Quebec, Canada*
[102]*School of Physics, University of Melbourne, Victoria, Australia*
[103]*Department of Physics, University of Michigan, Ann Arbor, Michigan, USA*
[104]*Department of Physics and Astronomy, Michigan State University, East Lansing, Michigan, USA*
[105]*B.I. Stepanov Institute of Physics, National Academy of Sciences of Belarus, Minsk, Belarus*
[106]*Research Institute for Nuclear Problems of Byelorussian State University, Minsk, Belarus*
[107]*Group of Particle Physics, University of Montreal, Montreal, Quebec, Canada*
[108]*P.N. Lebedev Physical Institute of the Russian Academy of Sciences, Moscow, Russia*
[109]*Institute for Theoretical and Experimental Physics (ITEP), Moscow, Russia*
[110]*National Research Nuclear University MEPhI, Moscow, Russia*
[111]*D.V. Skobeltsyn Institute of Nuclear Physics, M.V. Lomonosov Moscow State University, Moscow, Russia*
[112]*Fakultät für Physik, Ludwig-Maximilians-Universität München, München, Germany*
[113]*Max-Planck-Institut für Physik (Werner-Heisenberg-Institut), München, Germany*
[114]*Nagasaki Institute of Applied Science, Nagasaki, Japan*
[115]*Graduate School of Science and Kobayashi-Maskawa Institute, Nagoya University, Nagoya, Japan*
[116]*Department of Physics and Astronomy, University of New Mexico, Albuquerque, New Mexico, USA*
[117]*Institute for Mathematics, Astrophysics and Particle Physics, Radboud University Nijmegen/Nikhef, Nijmegen, Netherlands*
[118]*Nikhef National Institute for Subatomic Physics and University of Amsterdam, Amsterdam, Netherlands*
[119]*Department of Physics, Northern Illinois University, DeKalb, Illinois, USA*
[120a]*Budker Institute of Nuclear Physics, SB RAS, Novosibirsk, Russia*
[120b]*Novosibirsk State University Novosibirsk, Russia*
[121]*Department of Physics, New York University, New York, New York, USA*
[122]*The Ohio State University, Columbus, Ohio, USA*
[123]*Faculty of Science, Okayama University, Okayama, Japan*
[124]*Homer L. Dodge Department of Physics and Astronomy, University of Oklahoma, Norman, Oklahoma, USA*
[125]*Department of Physics, Oklahoma State University, Stillwater, Oklahoma, USA*
[126]*Palacký University, RCPTM, Joint Laboratory of Optics, Olomouc, Czech Republic*
[127]*Center for High Energy Physics, University of Oregon, Eugene, Oregon, USA*
[128]*LAL, Université Paris-Sud, CNRS/IN2P3, Université Paris-Saclay, Orsay, France*
[129]*Graduate School of Science, Osaka University, Osaka, Japan*
[130]*Department of Physics, University of Oslo, Oslo, Norway*
[131]*Department of Physics, Oxford University, Oxford, United Kingdom*
[132]*LPNHE, Sorbonne Université, Paris Diderot Sorbonne Paris Cité, CNRS/IN2P3, Paris, France*
[133]*Department of Physics, University of Pennsylvania, Philadelphia, Pennsylvania, USA*
[134]*Konstantinov Nuclear Physics Institute of National Research Centre "Kurchatov Institute", PNPI, St. Petersburg, Russia*
[135]*Department of Physics and Astronomy, University of Pittsburgh, Pittsburgh, Pennsylvania, USA*
[136a]*Laboratório de Instrumentação e Física Experimental de Partículas - LIP, Portugal*
[136b]*Departamento de Física, Faculdade de Ciências, Universidade de Lisboa, Lisboa, Portugal*
[136c]*Departamento de Física, Universidade de Coimbra, Coimbra, Portugal*
[136d]*Centro de Física Nuclear da Universidade de Lisboa, Lisboa, Portugal*
[136e]*Departamento de Física, Universidade do Minho, Braga, Portugal*
[136f]*Departamento de Física Teorica y del Cosmos, Universidad de Granada, Granada (Spain), Spain*
[136g]*Dep Física and CEFITEC of Faculdade de Ciências e Tecnologia, Universidade Nova de Lisboa, Caparica, Portugal*
[137]*Institute of Physics, Academy of Sciences of the Czech Republic, Prague, Czech Republic*

[138]Czech Technical University in Prague, Prague, Czech Republic
[139]Charles University, Faculty of Mathematics and Physics, Prague, Czech Republic
[140]State Research Center Institute for High Energy Physics, NRC KI, Protvino, Russia
[141]Particle Physics Department, Rutherford Appleton Laboratory, Didcot, United Kingdom
[142]IRFU, CEA, Université Paris-Saclay, Gif-sur-Yvette, France
[143]Santa Cruz Institute for Particle Physics, University of California Santa Cruz, Santa Cruz, California, USA
[144a]Departamento de Física, Pontificia Universidad Católica de Chile, Santiago, Chile
[144b]Departamento de Física, Universidad Técnica Federico Santa María, Valparaíso, Chile
[145]Department of Physics, University of Washington, Seattle, Washington, USA
[146]Department of Physics and Astronomy, University of Sheffield, Sheffield, United Kingdom
[147]Department of Physics, Shinshu University, Nagano, Japan
[148]Department Physik, Universität Siegen, Siegen, Germany
[149]Department of Physics, Simon Fraser University, Burnaby, British Columbia, Canada
[150]SLAC National Accelerator Laboratory, Stanford, California, USA
[151]Physics Department, Royal Institute of Technology, Stockholm, Sweden
[152]Departments of Physics and Astronomy, Stony Brook University, Stony Brook, New York, USA
[153]Department of Physics and Astronomy, University of Sussex, Brighton, United Kingdom
[154]School of Physics, University of Sydney, Sydney, Australia
[155]Institute of Physics, Academia Sinica, Taipei, Taiwan
[156a]E. Andronikashvili Institute of Physics, Iv. Javakhishvili Tbilisi State University, Tbilisi, Georgia
[156b]High Energy Physics Institute, Tbilisi State University, Tbilisi, Georgia
[157]Department of Physics, Technion, Israel Institute of Technology, Haifa, Israel
[158]Raymond and Beverly Sackler School of Physics and Astronomy, Tel Aviv University, Tel Aviv, Israel
[159]Department of Physics, Aristotle University of Thessaloniki, Thessaloniki, Greece
[160]International Center for Elementary Particle Physics and Department of Physics, University of Tokyo, Tokyo, Japan
[161]Graduate School of Science and Technology, Tokyo Metropolitan University, Tokyo, Japan
[162]Department of Physics, Tokyo Institute of Technology, Tokyo, Japan
[163]Tomsk State University, Tomsk, Russia
[164]Department of Physics, University of Toronto, Toronto, Ontario, Canada
[165a]TRIUMF, Vancouver, British Columbia, Canada
[165b]Department of Physics and Astronomy, York University, Toronto, Ontario, Canada
[166]Division of Physics and Tomonaga Center for the History of the Universe, Faculty of Pure and Applied Sciences, University of Tsukuba, Tsukuba, Japan
[167]Department of Physics and Astronomy, Tufts University, Medford, Massachusetts, USA
[168]Department of Physics and Astronomy, University of California Irvine, Irvine, California, USA
[169]Department of Physics and Astronomy, University of Uppsala, Uppsala, Sweden
[170]Department of Physics, University of Illinois, Urbana, Illinois, USA
[171]Instituto de Física Corpuscular (IFIC), Centro Mixto Universidad de Valencia - CSIC, Valencia, Spain
[172]Department of Physics, University of British Columbia, Vancouver, British Columbia, Canada
[173]Department of Physics and Astronomy, University of Victoria, Victoria, British Columbia, Canada
[174]Fakultät für Physik und Astronomie, Julius-Maximilians-Universität Würzburg, Würzburg, Germany
[175]Department of Physics, University of Warwick, Coventry, United Kingdom
[176]Waseda University, Tokyo, Japan
[177]Department of Particle Physics, Weizmann Institute of Science, Rehovot, Israel
[178]Department of Physics, University of Wisconsin, Madison, Wisconsin, USA
[179]Fakultät für Mathematik und Naturwissenschaften, Fachgruppe Physik, Bergische Universität Wuppertal, Wuppertal, Germany
[180]Department of Physics, Yale University, New Haven, Connecticut, USA
[181]Yerevan Physics Institute, Yerevan, Armenia

[a]Deceased.
[b]Also at Department of Physics, King's College London, London, United Kingdom.
[c]Also at Istanbul University, Department of Physics, Istanbul, Turkey.
[d]Also at Institute of Physics, Azerbaijan Academy of Sciences, Baku, Azerbaijan.
[e]Also at TRIUMF, Vancouver, British Columbia, Canada.
[f]Also at Department of Physics and Astronomy, University of Louisville, Louisville, Kentucky, USA.
[g]Also at Department of Physics, California State University, Fresno, Stanford, California, USA.
[h]Also at Department of Physics, University of Fribourg, Fribourg, Switzerland.

[i]Also at II. Physikalisches Institut, Georg-August-Universität Göttingen, Göttingen, Germany.
[j]Also at Departament de Fisica de la Universitat Autonoma de Barcelona, Barcelona, Spain.
[k]Also at Tomsk State University, Tomsk, and Moscow Institute of Physics and Technology State University, Dolgoprudny, Russia.
[l]Also at The Collaborative Innovation Center of Quantum Matter (CICQM), Beijing, China.
[m]Also at Universita di Napoli Parthenope, Napoli, Italy.
[n]Also at Institute of Particle Physics (IPP), Canada.
[o]Also at Dipartimento di Fisica E. Fermi, Università di Pisa, Pisa, Italy.
[p]Also at Horia Hulubei National Institute of Physics and Nuclear Engineering, Bucharest, Romania.
[q]Also at CPPM, Aix-Marseille Université, CNRS/IN2P3, Marseille, France.
[r]Also at Department of Physics, St. Petersburg State Polytechnical University, St. Petersburg, Russia.
[s]Also at Borough of Manhattan Community College, City University of New York, New York, USA.
[t]Also at Department of Financial and Management Engineering, University of the Aegean, Chios, Greece.
[u]Also at Centre for High Performance Computing, CSIR Campus, Rosebank, Cape Town, South Africa.
[v]Also at Louisiana Tech University, Ruston, Louisiana, USA.
[w]Also at Institucio Catalana de Recerca i Estudis Avancats, ICREA, Barcelona, Spain.
[x]Also at Department of Physics, University of Michigan, Ann Arbor, Michigan, USA.
[y]Also at LAL, Université Paris-Sud, CNRS/IN2P3, Université Paris-Saclay, Orsay, France.
[z]Also at Graduate School of Science, Osaka University, Osaka, Japan.
[aa]Also at Physikalisches Institut, Albert-Ludwigs-Universität Freiburg, Freiburg, Germany.
[bb]Also at Institute for Mathematics, Astrophysics and Particle Physics, Radboud University Nijmegen/Nikhef, Nijmegen, Netherlands.
[cc]Also at Near East University, Nicosia, North Cyprus, Mersin, Turkey.
[dd]Also at Institute of Theoretical Physics, Ilia State University, Tbilisi, Georgia.
[ee]Also at CERN, Geneva, Switzerland.
[ff]Also at Department of Physics, Stanford University, USA.
[gg]Also at Manhattan College, New York, New York, USA.
[hh]Also at Hellenic Open University, Patras, Greece.
[ii]Also at The City College of New York, New York, New York, USA.
[jj]Also at Departamento de Física Teorica y del Cosmos, Universidad de Granada, Granada (Spain), Spain.
[kk]Also at Department of Physics, California State University, Sacramento, Stanford, California, USA.
[ll]Also at Moscow Institute of Physics and Technology State University, Dolgoprudny, Russia.
[mm]Also at Département de Physique Nucléaire et Corpusculaire, Université de Genève, Genève, Switzerland.
[nn]Also at Department of Physics and Astronomy, University of Sheffield, Sheffield, United Kingdom.
[oo]Also at School of Physics, Sun Yat-sen University, Guangzhou, China.
[pp]Also at Department of Applied Physics and Astronomy, University of Sharjah, Sharjah, United Arab Emirates.
[qq]Also at Institut für Experimentalphysik, Universität Hamburg, Hamburg, Germany.
[rr]Also at National Research Nuclear University MEPhI, Moscow, Russia.
[ss]Also at Institute for Particle and Nuclear Physics, Wigner Research Centre for Physics, Budapest, Hungary.
[tt]Also at Giresun University, Faculty of Engineering, Giresun, Turkey.
[uu]Also at Department of Physics, Nanjing University, Nanjing, China.
[vv]Also at Institute of Physics, Academia Sinica, Taipei, Taiwan.
[ww]Also at Department of Physics, University of Malaya, Kuala Lumpur, Malaysia.